Title

Regulation of Germinal Center Antibody Responses by TLR Signaling in Dendritic Cells and B Cells

Author
Rookhuizen, Derek Carl

Publication Date
2012

Regulation of Germinal Center Antibody Responses by TLR signaling in Dendritic Cells and B cells

By

Derek Carl Rookhuizen

A dissertation submitted in partial satisfaction of the

requirements for the degree of

Doctor of Philosophy

in

Molecular and Cell Biology

in the

Graduate Division

of the

University of California, Berkeley

Committee in charge:

Professor Anthony L. DeFranco (Co-chair)
Professor Greg M. Barton (Co-chair)
Professor Laurent Coscoy
Professor Eva Harris
Professor Ellen Robey

Fall 2012

Abstract

Regulation of Germinal Center Antibody Responses by TLR Signaling in Dendritic Cells and B Cells

by

Derek Carl Rookhuizen

Doctor of Philosophy in Molecular and Cell Biology

University of California, Berkeley

Professor Anthony L. DeFranco (UCSF), Co-chair

Professor Greg M. Barton (UC Berkeley), Co-chair

The ultimate goal of the immune system is to eliminate pathogens and establish an immunological memory for rapid response upon reinfection. It can be broadly divided into innate and adaptive compartments. Immediately or shortly after infection occurs, the innate immune system uses pattern recognition receptors (PRRs) to identify ancient conserved features of pathogens, for example, DNA, RNA and carbohydrate, termed pathogen associated molecular patters (PAMPs). Stimulation of PRRs by PAMPs triggers signaling events that both limit the spread of infection as well as inform the adaptive immune system to generate the appropriate type of immunological memory. For example, the adaptive system uses *cellular immunity* to eliminate pathogens such as *Mycobacterium tuberculosis* that reside within cells while it generates antibodies (*humoral immunity*) to neutralize and remove extracellular pathogens such as the bacteria *Pseudomonas aeruginosa* that causes pneumonia. Thus, innate responses provide the first wave of defense by containing infection while the slower acting adaptive response eliminates pathogens and programs the ability to respond more efficiently upon subsequent exposures.

How innate signals sculpt adaptive responses is not well understood, and therefore, this thesis focuses on the ability of innate signaling by a family of PRRs known as toll-like receptors (TLRs) to program antibody responses. Ten and twelve TLRs have been identified in humans and mice, respectively, and they recognize a variety of PAMPs expressed by bacteria, viruses, fungi, and parasites including lipopolysaccharide (TLR4), flagellin (TLR5 and TLR11), and unmethylated CpG motifs in DNA (TLR9). Briefly, antibody responses may be broadly divided into those that require T cell help (T-dependent) and those that are independent of T cell help (T-independent). T-dependent antibody responses can occur either outside the B cell follicle (extrafollicular) or within the follicle in specialized transient structures termed germinal centers (GCs) that generate high affinity, long-lived humoral memory. To dissect how TLR signaling impacts GC antibody responses, I immunized mice with an oligovalent T-dependent protein antigen that was linked to either oligonucleotides containing (CpG) or lacking (nonCpG) a TLR9

ligand. In chapter two, I focus on the cellular contribution of TLR signaling to GC magnitude and quality by using a Cre recombinase system to selectively delete the TLR signaling adaptor MyD88 in either dendritic cells or B cells. This series of experiments revealed a division of labor for TLR signaling in DCs and B cells that controls GC magnitude and quality, respectively. In chapter three, I address the role of costimulation by the inducible costimulator (ICOS) on T cells and ICOS ligand (ICOSL) on B cells to direct the GC response against antigen linked to a TLR9 ligand. These experiments revealed that ICOSL acted B cell-extrinsically to impact GC quality and also unveiled a surprising B cell-intrinsic role for TLR9 signaling in affinity maturation. Collectively, these studies suggest that innate signals imprint the quality of T cell help that subsequently defines the antibody response and that they also act on B cells receiving TLR9 stimuli to directly enhance their affinity maturation. These results have implications in both human disease and rational vaccine design.

Table of Contents

List of Figures

ACKNOWLEDGEMENTS

This thesis was possible because of the support that others generously provided. It has been what most would consider a long stint, six years, yet it does not seem as long to me. It is more a collection of intense and great experiences strung together with a common thread, the thesis. Something that I did not anticipate from graduate school was a fertile grounds for personal growth, and among many things I take with me, is a valuable new focus on a life without fear of challenge. Berkeley is a magical and sensuous place, and I have tried consciously to cherish every drop of it.

To Tony, You are an incredible mentor, a generous spirit and a great scientist. Thank you for taking a chance and bringing me into your lab. You've done a lot for me. It has truly been an exhilarating experience working with you at UCSF.

To Greg Barton, Laurent Coscoy, Eva Harris, and Ellen Robey, you helped me turn things around. Truthfully, I was scared to switch tracks, but your reassurance made it possible. Thank you!

To Robert Beatty, thank you for your mentorship and for taking the time to relate your experiences when you were a graduate student that needed to make a leap as well. This really helped me.

To Tanya Grimes, Berta Parra, Christina Bianchi, and Eric Buhlis in the GAO, and to James Berger, chair of the GAC, I owe you many thank you's for helping me accomplish this Ph.D.

To my comrades in the DeFranco Lab, Matt, Irina, Linda and little Matt, you're great, and you made me look forward to long days in the laboratory. Thank you for making it fun. I look forward to seeing what each of you does next.

I would also like to thank everyone in Jason Cyster's lab, including Jason, for their generous provision of advice, ideas, resources, and humor.

To Dina, Sonia, Kevin and Eric, here's to completing this thesis. Dina, I'm so glad that we shared a sense of the absurd. Thank you for helping me laugh.

Mom, thank you for always encouraging me to explore and follow my heart. It means a lot.

Dad, you were great. Among many things, you were always able to provide two key ingredients, a listening ear and humor.

Raymond, thank you not only for all of the encouragement and laughter, but also for sharing your wisdom. You have changed my life.

To my little bruder Darin, the great chef, thank you for the absurd adventures and all of those beautiful meals we shared. I really loved our home of teas, cats, and laughter. Good luck with Holly.

Thank you Seong-Ji for your stalwart support. It was important to know that I could count on you. I hope that I can return the favor.

To Toby and Sophie, some of my most treasured and intensely joyful times were with and because of you. I look forward to more. See you in Paris or Japan or perhaps even at my apartment in Berkeley.

Dima, thank you for spontaneity, music, and for dancing wildly.

To my classmates Jess Lyons and Mark Gurling, and to all of those at La Mesa, some of my warmest memories in Berkeley are with and because of you.

To Catalan and Roommate Annie, you've been two of my most ardent supporters these six years, and it has meant more than I'm going to write. I'm so happy that you are in my life.

Lenka, who could have guessed our magical meeting? I'm so thankful for your enduring spirit and appreciation of devotion and accomplishment.

Keith, all of our cerebral talks and your interest in the world of ideas and imagination has inspired me to keep going more than you know. Here's to absurdity!

Marc and Nicole, without you, I wouldn't have been able to come here and do what I've done. I am happily indebted to you.

Osa, thank you for your spontaneity and excitement for life.

Stefanie, I've waited a long time to thank you, and I owe you so much more. Undoubtedly, you're one of the reasons that I'm here. I miss you.

Brian, thank you for helping me rearrange my thoughts through long conversation, vast amounts of coffee, and a shared appreciation for exploring the autonomy of the individual in this world, the key to magic.

Thank you Heidi, for the most brilliant and random non sequiturs, insight, and understanding that, ipso facto, have forged new pathways in my brain and led it to exciting new conclusions. May we write more theses together. Here's to Ignatius and Mr. Merde!

Also, thank you Mariusz and Stacey, you helped me start this path, and I miss you.

To Matt Silverman, thank you for encouraging me to go to graduate school. It made a difference.

To Mr. and Mrs. Rangan, thank you for the warmth and the dinners that you shared in your beautiful home. They made me feel much better.

Thank you Geraldine for always being intersested in what I'm doing, and thank you Reece for your spark and imagination. Just let it all go, go, go!

Also, I would like to thank my first mentor at Berkeley, Bill Sha. Bill, I learned a lot from you and always appreciated your uniqueness of thought. Thank you.

Finally, thank you to the University of California, Berkeley and to the department of Molecular and Cell Biology for bringing me here, providing me with an amazing opportunity to work and think for six years, and for going beyond to support me to the completion of this work. My life is different now.

Chapter One

Introduction

Informing adaptive immunity with innate signaling pathways

INTRODUCTION

The ultimate goal of the immune response is to clear pathogens from the host and to program immunological memory. The innate immune system recognizes and responds to general features inherent to pathogenic bacteria, viruses, fungi, and parasites and then informs the adaptive immune system to produce high affinity antibodies for the elimination of extracellular pathogens (humoral immunity) and/or to activate subsets of T lymphocytes that instruct the elimination of intracellular pathogens through direct cell-mediated mechanisms (cellular immunity), and finally to develop an immunological memory of these pathogens (**Fig. 1.1**). Briefly, professional antigen presenting cells (APCs) such as dendritic cells, B cells and macrophage sense pathogen associated molecular patterns (PAMPS), cardinal features of microbes, through pattern receptors (PRRs, discussed below) and respond by producing inflammatory cytokines and by upregulating costimulatory molecules that instruct effector T cells to propel the adaptive immune response. Understanding how innate stimuli are translated into adaptive responses and memory is an area of intense effort because of its implications for human diseases as well as for rational vaccine design and consequently, serves as the main focus of this thesis.

Innate immunity

Recognition of PAMPS by APCs through pattern recognition receptors (PRRs) provides the first line of defense against infection. So far, five classes of PRRs have been characterized: Toll-like receptors (TLRs) that respond to a wide variety of PAMPs, C-type lectin receptors (CLRs) which recognize carbohydrates, nucleotide-binding domain-leucine-rich repeat-containing receptors (NLRs) that respond to bacterial peptidoglycans, RNA helicase RIG-I-like receptors (RLRs) that detect cytosolic viral RNA, and cytoplasmic DNA receptor AIM2-like receptors (ALRs)[1-4]. TLRs were the first PRRs to be identified, and their discovery stems from genetic and biochemical studies in the fruit fly *Drosophila melanogaster*. That *Drosophila* could produce antimicrobial peptides[5-7] (Samakovlis 1990; Kylsten 1990; Wicker 1990) in response to bacterial and fungal infections began the chain of scientific inquiry that eventually revealed their regulation by a signaling pathway that could be initiated by the transmembrane receptor, Toll[8,9]. The observation that Toll and the human interleukin-1 receptor (IL-R) shared homology in their Toll/IL1-R (TIR) domains and were transmembrane receptors that activated the NF-κB pathway[10-12] gave momentum to Charles Janeway's Pattern Recognition Hypothesis[13]. Janeway realized that immunizations worked best in combination with adjuvants which contain bacteria or their components, "immunology's dirty little secret," leading to the hypothesis that receptors in the mammalian immune system could recognize cardinal features of pathogens and signal to alarm effector T and B lymphocytes of the adaptive immune system, thus forming a bridge between innate and adaptive immunity[14]. In 1997, the first human TLR[15] was cloned and since that time at least 10 and 12 have been identified in humans and mice, respectively[3].

TLR structure and function

TLRs are germline-encoded type I transmembrane receptors with an ectodomain that interacts with PAMPs through leucine-rich repeats, a transmembrane region and intracellular TIR domain that interacts with various adaptor molecules to initiate downstream signaling events[16]. Each TLR or combination of TLRs recognizes unique PAMPs from a variety of pathogens including bacteria, viruses, fungi and parasites. TLR2 recognizes triacyl and diacyl lipoproteins from bacteria and mycobacteria, by forming distinct heterodimers with TLR1 and TLR6, respectively, to induce proinflammatory cytokines[17]. In contrast, TLR2 homodimers signal in response to viral infection in inflammatory monocytes to stimulate type I interferon production[18]. Thus, the cell type might control the specific PAMP recognized by TLR2 and its downstream signaling outcome. TLR4 recognizes lipopolysaccharide (LPS) expressed on the surface of gram-negative bacteria and stimulates production of inflammatory cytokines. TLR5 recognizes bacterial flagellin and is especially active at mucosal surfaces in lung and gut[17, 19]. Recognition of dsRNA by TLR3 stimulates inflammatory cytokines and type I interferon, and, along with TLRs 7 and 9, TLR3 is endosomally restricted, most likely to prevent exposure to and activation by self-antigens[20, 21]. TLR7 recognizes single-stranded RNA from viruses and bacteria while TLR9 apparently responds to a variety of PAMPs including unmethylated CpG motifs in viral, fungal, and bacterial DNA, the sugar backbone of 2' deoxyribose, and more recently, it was demonstrated that hemozoin, a hemoglobin metabolic by-product from malaria parasites, also binds to TLR9[17, 22], although this remains somewhat controversial. Finally, TLR11 was demonstrated to be important for detecting profilin-like molecules expressed by protozoa such as *Toxoplasma gondii*, and just recently, it was demonstrated that recognition of *Salmonella typhi* flagellin by TLR11 on gut epithelium protected mice against infection[23].

TLRs bind to a variety of adaptor molecules, generating specificity in response to diverse stimuli. Upon binding PAMPs, TIRs in the cytosolic region of most TLRs, with the exception of TLR3, associate with the TIR-containing adaptor molecule MyD88, either directly (TLRs 5, 7, 9) or through TIRAP (TLRs 1, 2, 4, 6). While TLR3 associates exclusively with the adaptor TRIF, TLR4 can also utilize TRIF indirectly through another adaptor molecule, TRAM. Distinct adaptor combinations result in activation of unique signaling pathways. Most notably, MyD88 recruits members of the IRAK (IL-1 receptor-associated kinase) family of serine/threonine kinases through its death domain to initiate downstream signals that culminate in the activation of nuclear factor (NF)-κB and the production of inflammatory cytokines such as IL-6, IL-12 and TNFα[24]. The interaction of MyD88 with IRAK family members has been termed the Myddosome and has diverse function in the innate response since, in addition to TLRs, the IL-1, IL-18, and IL-33 cytokine signaling pathways that are involved in inflammation also use it[25, 26]. Additionally, TLRs 2, 3, 4, 7 and 9 can all initiate distinct signaling pathways that result in translocation of interferon regulatory factors (IRFs) to the nucleus where they stimulate type I interferon to combat viral replication[3].

TLRs in disease

MyD88-deficient mice are highly susceptible to infection with gram-positive and gram-negative bacteria, emphasizing the absolute requirement for these pathways in the host's first line of defense against infection[27]. In humans, multiple defects in TLR signaling pathways have been linked with disease. Briefly, mutations that compromise interaction between MyD88 and IRAK4 result in primary immunodeficiency early in life and manifest a variety of symptoms caused by pyogenic bacteria: meningitis, sepsis, arthritis ostomyelitis, cellulitis, furunculosis and foliculitis[28]. Interestingly, patients with autosomal dominant mutations affecting the TLR3 pathway have a selective susceptibility to recurrent herpes encephalitis for reasons that are not understood at this time [26]. Additionally, TLR7 and TLR8 have been linked to celiac disease[29]. Thus, studies involving the regulation/dysregulation of innate signaling pathways have clear relevance to human disease.

Adaptive immunity

In order for the adaptive immune system to respond to infection and program long-lived memory, the innate system needs a way to communicate with T lymphocytes that ultimately directs the course of the adaptive immune response. Briefly, exposure of antigen activates professional antigen presenting cells—dendritic cells (DCs), B cells, and macrophages—that translate information from innate signaling pathways and deliver it to T cells through costimulatory receptor/ligand interactions as well as through production and dissemination of cytokines and chemokines. Thus, innate signaling in APCs sculpts adaptive responses.

T cell activation requires two signals: 1) engagement of the T cell receptor (TCR) with peptide-loaded major histocompatibility complexes, and 2) costimulation by costimulatory ligand-receptor pairs[30, 31]. Initial priming of T cells by DCs instructs the development of the particular T cell signature that will dominate the immune response. Distinct helper $CD4^+$T cell subsets with unique transcriptional programs develop depending on the particular cytokine milieu. For example, the IL-12 cytokine stimulates naive $CD4^+$ T cells to adopt a Th1 signature characterized by the transcription factor T-bet and production of IFNγ. Conversely, exposure to IL-4 turns on the transcription factor GATA3 to polarize a Th2 response that produces more IL-4 and supports humoral immunity. Additional T cell subsets with distinct properties appropriate for a given immune response also exist. Upregulation of retinoic acid-related orphan receptor gamma-t (RORγt) in response to the combination of TGFβ and IL-6 cytokines drives development of inflammatory Th17 cells while TGFβ alone induces a $FoxP^+$T regulatory (T_{REG}) cell program. Finally, the combination of IL-6 and IL-21 induces a specialized subset of T cells that express CXCR5, the B cell follicle-homing chemokine receptor, and are particularly well equipped to support B cell responses through provision of cytokines and robust expression of costimulatory molecules[32]. Different cytokines induce specific immunoglobulin class switching in B cells. For example, IL-4 triggers class switch to IgG1 and IgE; IFNγ, IgG2a; TGFβ, IgA. Thus, regulation of costimulatory receptor/ligand pairs and cytokine production by the innate immune system, for example by TLR signaling, can manipulate distinct parameters to specify a particular T cell response[33-36].

Costimulation

CD28 on T cells and its ligands CD80 (B7.1) and CD86 (B7.2) were the first costimulatory receptor/ligand pairs belonging to the CD28/B7 family to be identified and are essential for T cell activation[37]. Subsequently, the inducible costimulator (ICOS) and its ligand ICOSL (also called B7h, B7RP-1, GL50) were also identified[38, 39] and were found to have a non-redundant role in T cell activation. Regulation of the CD28 and ICOS pathways differ in several aspects: 1) CD28 is constitutively expressed on T cells while ICOS is upregulated by T cell activation, 2) dendritic cells (DC) and B cells constitutively express ICOSL while activation of APCs induces CD80 and CD86 expression, and 3) activated T cells upregulate CTLA-4 to quench CD28 signaling whereas ICOS signaling is negatively regulated by at least two pathways. First, the ubiquitn-ligase roquin limits ICOS expression on T cells by limiting its mRNA[40, 41], and second, binding of ICOSL to ICOS induces ICOSL shedding from the antigen presenting cell surface, suggesting a novel mechanism to rapidly extinguish ICOS signaling[42]. CD28 and ICOS show uniqueness in their downstream signaling cascades as CD28 induces robust activation of extracellular signal regulated kinase (ERK) but only moderate activation of phosphoinositide-3 kinase (PI3K). In contrast ICOS primarily stimulates PI3K activity, and these signaling differences affect the resulting production of cytokines[43]. While CD28 and ICOS are positive regulators of T cell responses, PD-1 and its ligands, PD-L1 and PD-L2 can attenuate T cells responses, and high PD-1 expression on effector $CD4^+$T cells during chronic viral infection leads to T cell exhaustion[37].

In addition to the CD28/B7 family of costimulatory molecules, receptor/ligand pairs belonging to the tumor necrosis factor (TNF) and TNF receptor superfamilies are also critical mediators of T cell activation and function. Costimulatory signaling by the TNFR superfamily is distinct from CD28 and ICOS in that it recruits TNF receptor-associated factor (TRAF) adapter proteins and activates NF-kB[44]. CD40 on B cells and CD40L on T cells belong to the TNFR and TNF superfamilies, respectively, and are critical for T-dependent immune responses such as germinal center formation. In addition the OX40/OX40L receptor ligand pair are also critical for T-dependent responses and can critically skew the $CD4^+$T effector to T_{REG} ratio[45]. In contrast to CD40/CD40L and OX40/OX40L, other TNF family members such as BAFF (B cell-activating factor of the TNF family) and APRIL (a proliferation-inducing ligand) promote T-independent B cell activation by acting as soluble factors to stimulate both B cells in the splenic marginal zone as well as follicular B cells through engagement of either transmembrane activator and cyclophilin-ligand interactor (TACI) (BAFF and APRIL) or BAFF receptor (BAFF)[46]. Importantly, TLR signaling can cooperate with APRIL and BAFF to promote T cell-independent immunity and IgA class switch[46]. The diverse repertoire of costimulatory receptor/ligand pairs and the complexity of their signaling outcomes introduce the possibility to refine T-dependent and T-independent antibody responses by regulating their expression.

Germinal centers

Following activation by encounter with antigen, B cells may initiate either an extrafollicular antibody response characterized by short-lived Blimp1$^+$ plasmablasts and the generation of low-affinity antibody[47] or upregulate the transcription factor Bcl6 and migrate to the center of the B cell follicle to seed a germinal center (GC) reaction where affinity maturation, the process by which B cells accrue mutations in IgH and IgL genes and undergo selection for higher affinity variants, and selection for memory B cells occurs[48, 49]. First identified by Flemming in 1884 as the "Mutterform der kleine Elemente," meaning that he suspected the GC to be the source of all lymphocytes[50], more than a century of investigation has revealed that GCs are transient reactions where B cells compete for survival and selection cues in the form of cytokines and costimulatory signals from the transcriptionally distinct Bcl-6$^+$CXCR5$^+$ T cell subset termed follicular helper T cells (T_{FH}).

GCs are anatomically divided into dark and light zones in which proliferation and selection occur, respectively, and whose polarization is maintained by regulation of chemokine receptors CXCR4 and CXCR5, respectively, on GC B cells and T_{FH} cells[51-55]. It is postulated that BCR affinity drives competition for selection and survival cues from T_{FH} cells. This model predicts that B cells expressing a higher affinity BCR will capture more antigen retained on follicular dendritic cells in structures referred to as iccosomes[56] than lower affinity BCR-bearing competitors, leading to greater presentation of antigenic peptide-loaded MHC II, and therefore increasing the likelihood of encountering T_{FH} cells expressing cognate T cell receptors[49].

Considerable progress has been made in the elucidation of selection events during affinity maturation[57]. Indeed, several groups have used elegant microscopy and cell-based techniques to generate data both in vivo and in vitro demonstrating that BCR affinity determines the amount of antigen captured[58], that GC T_{FH} cell help is selectively limited compared with access to antigen[59], and that eliminating B cell competition by delivering antigen to all GC B cells boosted T_{FH} cell numbers and equalized affinity maturation across GC B cell clones[60]. Thus, better affinity maturation translates to increased T cell help.

While these data support an incremental affinity maturation process during the GC response, precursor affinity may determine extrafollicular versus GC B cell fate decisions at the beginning of the response. Early experiments showed that low affinity precursors preferentially adopted the GC B cell fate while high affinity BCRs drove the extrafollicular antibody response[61]; however, a growing collection of observations supports the opposite, that B cells bearing relatively higher affinity BCRs are selected into the GC pathway[62-64]. These apparently contradictory observations may reflect differences between the transgenic MD4 BCR that recognizes hen egg lysozyme (HEL)[61] and the B1-8 and quasimonoclonal (QM) transgenic systems that recognize nitrophenol-haptenated antigen[62, 64].

Early studies suggested that affinity of BCRs for antigen might drive selection of B cells within the GC to seed the memory B cell compartment for rapid recall upon secondary Ag exposure or to become long lived plasma cells that reside in bone marrow and continuously proved antibody[65]. However it now appears that while high affinity clones are preferentially selected within the GC to build B cell memory, a GC-independent pathway also exists for the production of low affinity unswitched memory B cells[66, 67]. These low affinity memory B cells are postulated to serve as a recall reservoir for the rapid induction of GCs and new rounds of affinity maturation upon secondary antigenic challenge[68].

Follicular helper T cells (T_{FH})

As previously mentioned, T_{FH} cells are well-equipped to provide B cell help by localization to the GC light zone through upregulation of CXCR5, expression of costimulatory molecules such as ICOS, BTLA (B and T lymphocyte attenuator), and CD40L[32], and through ample provision of cytokines such as IL-4 and IL-21 that propel GC B and T_{FH} cell survival and also promote affinity maturation and B cell memory[69, 70]. Although T_{FH} cells possess a distinct transcriptional program characterized by high Bcl6 expression[71, 72], they can also adopt additional characteristics normally associated with other T cell subsets such as IL-17[73] and IFNγ[74] production[32]. In mouse models, nematode infection stimulated the development of Th2-like IL-4-producing T_{FH} cells[75] while viral infection stimulated a majority of $IFN\gamma^{+}T_{FH}$ cells and only a minority of $IL\text{-}4^{+}T_{FH}$ cells[76]. Thus, these observations suggest that the uniqueness of an innate stimulus will be reflected in the quality of the T_{FH} cell compartment and hence, in the ensuing antibody response. Reinhardt et al.[77], elegantly demonstrated this principle using Il-4 and IFNγ reporter mice to show that B cells from doublets containing $IL\text{-}4^{+}T_{FH}$ cells expressed IgG1 rearrangements while doublets containing $IFN\gamma^{+}T_{FH}$ cells expressed IgG2a transcripts. These data combined with other observations demonstrating that TLR signaling, for example, can boost the number of T_{FH} cells[78] start to provide a framework for the rational design of vaccines that can precisely define a particular T_{FH} cell phenotype to direct a desired antibody response.

TLRs and B cell responses

Although TLRs affect B cell proliferation and class switch recombination in a cell-intrinsic manner, their ability to impact T-dependent antibody responses remained controversial as two groups arrived at completely opposite conclusions [79, 80]. These differences may stem from the use of distinct antigens, ovalbumin versus haptenated proteins, and a subsequent publication demonstrated the MyD88-independent adjuvanticity of haptenated antigens[81]. Nevertheless, multiple groups using different approaches have now confirmed the ability of TLR signaling to enhance T-dependent antibody responses. Using mice that were specifically deleted for MyD88 in B cells, Hou et al.[82] clearly showed that TLR signaling in B cells boosted the antibody and GC response to a multivalent antigen containing a TLR ligand. These findings were corroborated by a separate group that used antigen and TLR ligands absorbed to separate nanoparticles to demonstrate that B cell-intrinsic TLR signaling expanded the overall antibody response, boosted GC persistence and increased affinity maturation[83]. Finally, in a live infection model, B cell-intrinsic TLR7 signaling was required for B cell participation in the GC response against lymphocytic choriomeningitis virus (LCMV) infection[84].

Thesis overview

How TLR signaling impacts qualitative aspects of the GC reaction such as affinity maturation, immunoglobulin class switch, and memory B cell formation is not well understood. In order to unearth these mechanisms, I conjugated the T-dependent antigen nitrophenol-haptenated chicken gamma globulin (NP-CGG) to oligonucleotides containing (CpG) or lacking (nonCpG) a TLR9 ligand and used it to address these questions at two levels:

1. First, I used mice that were *Myd88*-deficient in either DCs or B cells to dissect the cellular contribution of TLR signaling to GC quality. This revealed that TLR signaling in DCs primarily regulated GC magnitude by boosting the number of T_{FH} cells with robust ICOS expression and consequently increased the number of antigen-specific GC B cells. Separately, TLR signaling in B cells controlled GC quality by enhancing affinity maturation, producing more IgG2c, and making more memory B cells. Both cell types affected T_{FH} quality by modulating the expression of costimulatory receptors such as ICOS and PD-1 and also by regulating the ratio of T_{FH} to FoxP3$^+$T follicular regulatory (T_{FR}) cells which likely affected GC selection.

2. Second, since ICOS levels were significantly boosted in response to NP-CGG linked to a TLR ligand, I investigated the cellular requirements for ICOS/ICOSL costimulation in TLR9-enhanced T-dependent GC responses. Using ICOSL-deficient mice as well as a series of mixed bone marrow chimeras, we demonstrated that deletion of ICOSL on B cells compromised the expansion of diverse affinity IgG and that this could be rescued by the presence of approximately 50% *Icosl*$^{+/+}$ B cells, indicating that ICOSL acted B cell-extrinisically to boost the antibody response. Extrinsic effects of ICOSL expression were also evident in the T_{FH} compartment as the presence of 50% *Icosl*$^{-/-}$ B cells halved the number of T_{FH} cells. Surprisingly, the presence of 50% *Icosl*$^{+/+}$ B cells only partially restored affinity maturation in *Icosl*$^{-/-}$ B cells, revealing that ICOSL also had B cell-intrinsic effects and demonstrating that TLR9 specifically required ICOSL on the responding B cell to enhance affinity maturation.

Figure 1.1 Innate immunity informs adaptive responses. Soon after infection occurs, pathogen associated molecular patterns (PAMPS) bind pattern recognition receptors (PRRs) expressed by both hematopoietic and non-hematopoietic cells to stimulate inflammatory or anti-viral signaling events such as the release of signaling molecules termed cytokines. These signals ultimately direct T cells and B cells to establish a memory of the invading pathogen, a process that requires days to weeks. Immunological memory allows a more rapid adaptive response to occur upon reinfection, and thus, establishment of memory is the ultimate goal of vaccines.

Figure 1.2 TLR signaling in DCs and B cells can augment the germinal center response. It was previously shown that TLR signaling in DCs and B cells could augment the size of a GC response depending on both the physical nature of the antigen as well as the solubility of the TLR ligand. Coadministration of a TLR ligand either attached or unattached to a soluble protein antigen augmented GC formation by signaling in DCs[85]. Similarly, immunization with a particulate antigen such as a virus-like particle (VLP) and soluble TLR ligand also required DCs to enhance the antibody response; however, inclusion of a TLR ligand within a VLP or infection with LCMV was shown to trigger robust GC formation by stimulating B cells[82-84].

Figure 1.1

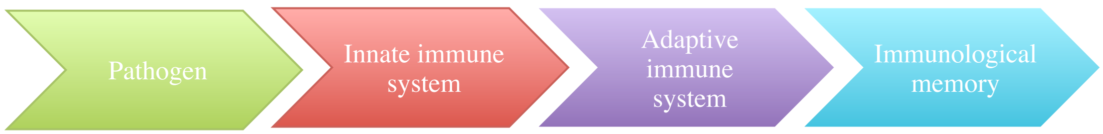

Figure 1.2

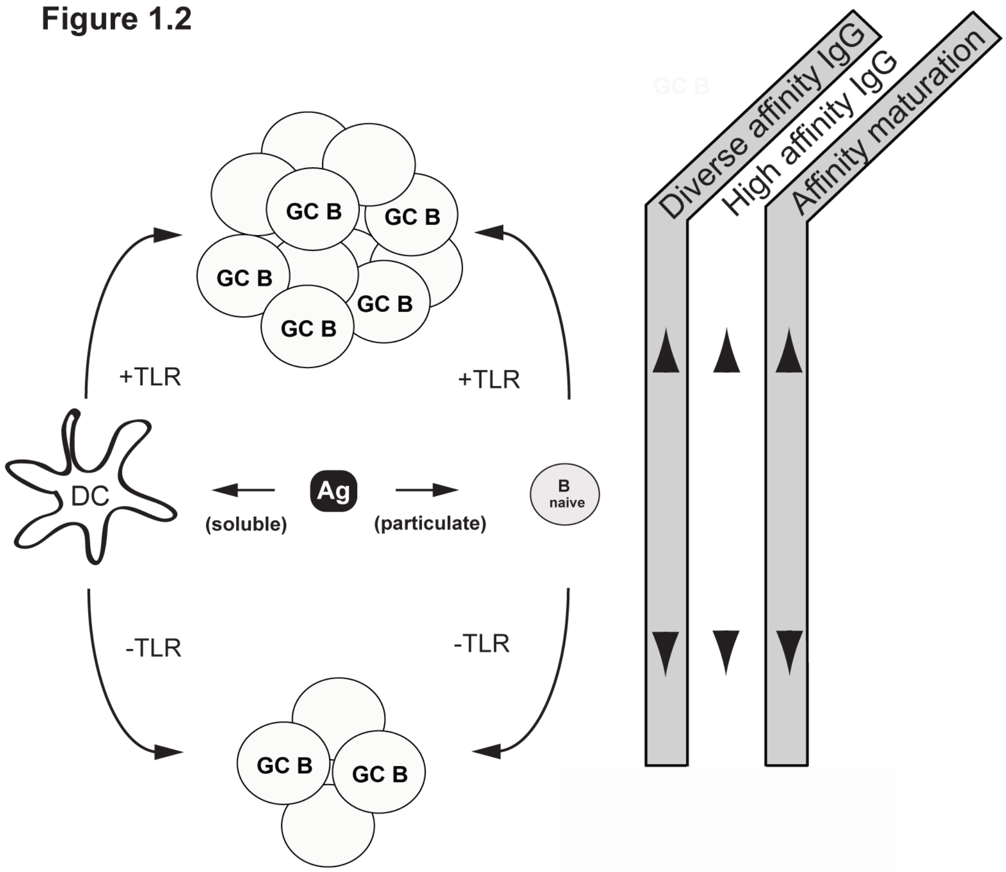

Chapter Two

Enhancement of germinal center magnitude and quality by TLR/MyD88 signaling in dendritic cells and B cells

Modulation of T_{FH} cell quality and B cell selection

ABSTRACT

To dissect how recognition of pathogen associated molecular patterns by toll-like receptors (TLR) enhances germinal center (GC) responses, mice selectively deleted for MyD88 in B cells or dendritic cells (DCs) were immunized with antigen bound to a TLR9 ligand. TLR9 signaling in DCs boosted GC magnitude by expanding follicular helper T cells (T_{FH}) and GC B cells, while in B cells, it improved GC quality through affinity maturation, class switch to IgG2a, and enhanced B cell memory. Qualitative changes resulted from B cell-intrinsic and -extrinsic effects, paralleling changes in T_{FH} and FoxP3$^+$ follicular regulatory CD4$^+$T cells (T_{FR}). Combined with recent reports, our data indicate a pervasive role for TLR/MyD88 signaling in specifying antibody responses through coordinated regulation of multiple cell types.

INTRODUCTION

The ability of the innate immune system to survey infection relies on pattern recognition receptors (PRRs) such as TLRs that signal through myeloid differentiation primary-response protein 88 (MyD88) upon recognition of PAMPs. By directing DCs to activate naive T cells [85-87] or by promoting B cell activation and terminal differentiation to antibody secreting plasma cells[82, 88], TLRs shape adaptive immunity. Following infection or vaccination, antibody responses generally proceed in two phases, an initial extrafollicular response, which rapidly generates short-lived plasmablasts that secrete low affinity IgM and isotoype-switched antibodies[47] and a slower germinal center (GC) response where B cells switch Ig isotype and increase affinity for antigen through somatic mutation of IgH and IgL genes and stringent selection processes[49]. Importantly, the GC builds humoral memory and protection from reinfection by selecting long-lived plasma cells and memory B cells from cells expressing isotype-switched affinity-matured BCRs. Initially, it was proposed that TLR signaling selectively favored the extrafollicular component of serological immunity[89] but subsequently it was shown that in B cells it could greatly augment the GC response to virus-like particles, nanoparticles, or virions[82, 83, 90].

T_{FH} cells govern GC maintenance and selection for GC B cells with increased affinity for antigen[32]. The transcriptional repressor Bcl-6 is essential for T_{FH} cell development and for the upregulation of CXCR5 expression that allows T_{FH} cells to migrate to GCs where they interact with GC B cells through costimulatory ligand-receptor pairs and provide survival and selection cues[32, 48]. Recently it has become clear that some follicular $CXCR5^+CD4^+$T cells are typically-derived $FoxP3^+$ regulatory T cells, referred to as T_{FR} cells[91-96]. Although their function is poorly understood at this point, T_{FR} cells appear to limit the size of the GC response[91-94].

Recent studies have shown that physical linkage of a TLR7 or TLR9 ligand to a particulate antigen can substantially boost the GC response and lead to greater production of high affinity antibody; however, the mechanisms underlying these effects are poorly understood[82, 83, 90]. Moreover, previous studies were limited in their ability to compare pathogen infection or VLP immunization to an immune response lacking PAMPs. To understand the mechanisms by which TLRs promote GC antibody responses, we created conjugates between a model protein antigen (nitrophenol-haptenated chicken gamma globulin, NP-CGG) and oligonucleotides that either contained or lacked a TLR9 ligand consensus CpG motif. Both antigens induced robust GC responses, but the CpG-containing antigen induced more anti-NP IgG early in the response, better affinity maturation, and more memory B cells. Immunization of mice with DC- and B cell-specific deletion of MyD88 unveiled separate roles for TLR9 control of the GC reaction, illuminating multiple checkpoints by which TLR recognition promotes GC output. In DCs, TLR9 signaling augmented the scale of the GC by increasing T_{FH} cell and antigen-specific B cell numbers. In contrast, TLR9 signaling in B cells did not affect GC magnitude but enhanced selection for high affinity antibody, class switch to IgG2a, and memory B cell formation. Some of these changes required TLR/MyD88 signaling in the responding B cells whereas others may have been mediated through effects on T_{FH} and T_{FR} cell populations. Our data, take together with several recent reports demonstrating that TLR signaling can greatly enhance antibody responses, indicate a widespread role for TLR signaling in the control and refinement of antibody responses through careful regulation of GC reactions.

RESULTS

TLR9 signaling enhances the germinal center response

To characterize the contribution of TLR9 signaling to the GC response, we established an immunization strategy that allowed us to compare the quality of GCs reacting to antigen that either contained or lacked a TLR9 ligand. I used streptavidin to link a biotinylated form of the T cell-dependent antigen NP-CGG to either a biotinylated CpG-containing oligonucleotide (CpG-NP-CGG) or to a control oligonucleotide lacking a CpG motif (nonCpG-NP-CGG). Immunization of C57BL/6 mice with either form of the antigen induced a robust GC response as detected by enumeration of GC B cells ($B220^{hi}IgD^{lo}Fas^{+}$) by flow cytometry (**Fig. 2.1A, B**). The numbers of GC B cells or of NP-specific GC B cells were increased on day 14 after immunization with either antigen, but the numbers were about 2-fold greater with the CpG oligonucleotide-containing antigen (**Fig. 2.1B**). Similarly, inclusion of a TLR9 ligand within the antigen boosted the total anti-NP IgG response by 2-3 fold on day 14 (**Fig. 2.1C**), although by day 21 both responses were of similar magnitude when diverse affinities were measured (e.g., ELISA with NP_{15}-BSA) (**Fig. 2.1C, D**). In contrast, when high affinity anti-NP IgG was selectively measured (e.g., ELISA with NP_{1}-BSA), it was evident that there was substantially increased production of high affinity antibodies in the response to the CpG-containing antigen (**Fig. 2.1C, D**). In addition, CpG-NP-CGG enhanced class switch to the highly inflammatory $IgG2a^{b}$ (IgG2c) isotype (**Fig. 2.1E**). Thus, inclusion of a TLR9 ligand in the antigen promoted the early production of IgG, whereas at later times, it enhanced affinity maturation and class switch to $IgG2a^{b}$, but did not affect overall IgG titers.

As expected from increased titers of anti-NP IgG at day 14 in mice immunized with CpG-NP-CGG, these mice also increased production of NIP-specific plasmablasts 14 days after immunization (**Fig. 2.2A, B**). To see if TLR9 stimulation also promoted the memory B cell component of the GC reaction, I immunized mice with nonCpG- and CpG-NP-CGG and boosted both groups of mice with NP-CGG in saline 7.5 weeks (53 days) later (**Fig. 2.1C, left**). The secondary IgG response was significantly elevated in mice that were initially immunized with CpG-NP-CGG, as demonstrated by the fold increase from day 53 to day 60 (day 7 post secondary challenge) of diverse affinity anti-NP IgG (**Fig. 2.1D, left**). The enhanced IgG recall response was dominated by high affinity antibody (**Fig. 2.1C, right; D**), which is consistent with memory B cells that are generated from a GC response undergoing selection for increased affinity[65]. Thus, in addition to boosting anti-NP IgG affinity and class switch to $IgG2a^{b}$, inclusion of a TLR9 ligand linked to a protein-based antigen also promoted GC quality through generation of more high affinity memory B cells.

TLR9 signaling increases the number and alters the phenotype of follicular T cells

The GC response is highly dependent on T_{FH} cells that localize to the GC and provide selection signals for GC B cell survival, affinity maturation, and fate decisions[32,

[48]. Immunization with CpG-NP-CGG significantly boosted the total number of T_{FH} ($CXCR5^{+}PD\text{-}1^{+}CD44^{hi}CD62L^{lo}CD4^{+}$) per LN, and also increased the percentage of activated ($CD44^{hi}CD62L^{lo}$) $CD4^{+}$ T cells that were T_{FH} cells as defined by $CXCR5^{+}PD\text{-}1^{+}$ expression (**Fig. 2.3A, B**). Expression of the T_{FH} cell-lineage transcription factor Bcl-6, confirmed the identity of these cells (**Fig. 2.3C,** and **Fig. 2.4A**). TLR9 stimulation also enhanced the frequency of T_{FH} cells relative to the number of GC B cells in the draining lymph node by approximately 2-fold (**Fig. 2.3D**). Immunofluorescent labeling of frozen LN sections confirmed the presence of a $CD4^{+}$ T_{FH} cell population in GCs following immunization with nonCpG- as well as CpG-NP-CGG conjugates (**Fig. 2.4A**). The increased numbers of T_{FH} cells relative to GC B cells may have contributed to the enhanced affinity maturation and memory B cell generation in mice immunized with CpG-NP-CGG.

CpG-NP-CGG immunization also produced striking effects on the cell surface expression of the costimulatory family molecules ICOS and PD-1 by T_{FH} cells. Surface expression of ICOS was enhanced on T_{FH} cells by 3-4 fold on average in mice immunized with CpG-NP-CGG compared to those immunized with nonCpG-NP-CGG (**Fig. 2.3E**), and furthermore, this was selective for the T_{FH} population as T_{EFF} cells only modestly increased their expression of ICOS (**Fig. 2.3E**). As ICOS is required for the GC reaction[97-99], enhanced ICOS expression on T_{FH} cells may contribute to enhanced GC responses. In contrast to the relatively homogenous expression of ICOS on T_{FH} cells, PD-1 expression was heterogeneous, and an increased proportion of these cells had low expression of PD-1 after immunization with antigen containing a TLR9 ligand (**Fig. 2.3F, G**). PD-1 is an inhibitory receptor in the context of effector T cell responses[100], and its blockade is associated with T_{FH} expansion[101, 102], consistent with an inhibitory role for PD-1 on T_{FH} cells as well.

To further characterize the quality of follicular helper $CD4^{+}$T cells induced by the two different immunizations, I amplified mRNAs encoding hallmark helper cytokines from sorted T_{FH} cells and measured their levels by quantitative RT-PCR. The sorted cells were phenotypically T_{FH} cells, showing high *Bcl-6* and *c-Maf*, and low *Prdm1* mRNA expression (data not shown). IL-21, which affects T_{FH} cell maintenance, affinity maturation and GC B cell fate decisions[69, 70], exhibited a modest but significant increase in its mRNA in T_{FH} cells from mice immunized with CpG-NP-CGG compared to nonCpG-NP-CGG (**Fig. 2.3H**). Interestingly, inclusion of a TLR9 ligand in the antigen resulted in substantially decreased IL-4 mRNA and increased IFNγ mRNA (**Fig. 2.3H**), which is consistent with the observed increase in isotype switching to $IgG2a^{b}$ [103]. These data indicate that TLR9 stimulation promoted increased numbers of T_{FH} cells within the GC and also affected them in qualitative ways that are consistent with the observed effects on affinity maturation and class switch to $IgG2a^{b}$.

TLR9 signaling in dendritic cells and B cells regulates the magnitude and quality of the GC reaction, respectively

To investigate how TLR9 signaling impacts the quality of the GC reaction, I employed mice that are defective in the key TLR signaling adaptor MyD88 selectively in either DCs or B cells. *CD11c-Cre Myd88$^{fl/fl}$* mice delete the Myd88 gene in approximately 98% of conventional DCs and in about 80% of plasmacytoid DCs, whereas *Mb1-Cre Myd88$^{fl/fl}$* mice delete *Myd88* in 98% of B cells[82]. As seen previously, immunization of WT mice with CpG-NP-CGG induced a 2-3-fold greater accumulation of total and NP-binding GC B cells, compared to mice immunized with nonCpG-NP-CGG. Deletion of TLR9 signaling in DCs ($DC^{-/-}$) selectively blocked this increase, whereas its deletion in B cells ($B^{-/-}$) did not have a clear effect on GC B cell numbers (**Fig. 2.5A and data not shown**).

Next, I examined anti-NP IgG affinity maturation as the ratio of the amount of high affinity anti-NP IgG to that of diverse affinity anti-NP IgG 14 days after immunization. In WT mice, inclusion of CpG-containing oligonucleotides in the antigen boosted affinity maturation, increasing the anti-NP_1/NP_{15} IgG ratio approximately 4-5 fold (**Fig. 2.5B**). In mice lacking MyD88 in DCs, the titers of anti-NP_{15} IgG at day 14 were not boosted by the presence of a TLR9 ligand in the antigen complex; however, the anti-NP_1/NP_{15} IgG ratio remained similar to WT (**Fig. 2.5B and Fig. 2.6A, B**), demonstrating that affinity maturation in these mice remained intact despite reduced GC B cell numbers. Likewise the reduction in diverse affinity anti-NP IgG titers reflected trends in the generation of NIP-binding $B220^{lo}CD138^{+}$ plasma cells on day 14 (**Supplementary Fig. 2.2A, B**).

Although mice lacking MyD88 only in B cells still exhibited an increase in the number of NP^{+}GC B cells (**Fig. 2.5A**) and NIP-binding plasma cells (**Fig. 2.2A, B)** following immunization with CpG-NP-CGG, there was a selective impairment of class switch to $IgG2a^{b}$ (**Fig. 2.5C**) and of affinity maturation as evidenced by a reduction in high affinity anti-NP IgG production and therefore a diminished anti-NP_1/NP_{15} ratio (**Fig. 2.5B and Fig. 2.6A, B**). These mice also did not exhibit an increase in the number of NP-specific memory B cells, as assessed by boosting with NP-CGG in saline 53 days after the initial immunization with a CpG-containing complex of NP-CGG and measuring the magnitude of the secondary response 7 and 14 days later (**Fig. 2.5D**). In contrast, MyD88 signaling in DCs only minimally influenced class switch to $IgG2a^{b}$—both total IgG and $IgG2a^{b}$ titers were reduced by deletion of *Myd88* in DCs—and was not required for the generation of robust anti-NP memory B cells (**Fig. 2.5C, D**). Thus, TLR9 signaling in DCs boosted the magnitude of the GC reaction, whereas in B cells it promoted the qualitative aspects of the GC, including improved affinity maturation, more class switch to $IgG2a^{b}$, and generation of more memory B cells, without affecting accumulation of NP-specific GC B cells. Thus, the ability of a TLR9 ligand complexed with NP-CGG to enhance IgG production reflected a stimulation of both DCs and B cells, which were able to enhance the GC response in distinct ways.

I also generated mice deficient for MyD88 in both DCs and B cells ($DC^{-/-}B^{-/-}$) by inclusion of both *CD11c-Cre* and *Mb1-Cre* transgenes together with *Myd88$^{fl/fl}$*. When these mice were immunized with CpG-NP-CGG, they had compromised NP-specific GC

B cell numbers similar to what was observed in $DC^{-/-}$ mice (**Fig. 2.5A**). Furthermore, affinity maturation in these mice was comparable to those of mice deficient for MyD88 in B cells (**Fig. 2.5B, Supplementary Fig. 2.6A, B**). These data corroborated data obtained from individual knockouts.

Effects of TLR9-Stimulated DCs and B cells on Follicular Helper T cells

We next examined how TLR9/MyD88 signaling in DCs and B cells affected the expansion and phenotypic properties of T_{FH} cells. MyD88 deletion in DCs compromised the burst in T_{FH} cell expansion in response to CpG-NP-CGG (**Fig. 2.7A**) and reduced the number of activated $CD4^+$ T cells in the draining lymph node (**Fig. 2.8A**), thereby leaving unaltered the frequency of T_{FH} cells relative to the number of activated T cells (**Fig. 2.7B**). The expansion of GC B cells was also compromised in these mice as described above, possibly as a secondary consequence of decreased numbers of T_{FH} cells[104, 105], and therefore, the ratio of T_{FH} to GC B cells was not affected (**Fig. 2.8C**). Thus, TLR9/MyD88 signaling in DCs boosted GC magnitude, at least in part, by promoting antigen-specific activation and proliferation of CD4 T cells which commit to the T_{FH} cell fate. MyD88/TLR9 signaling in DCs also impacted T_{FH} cell quality, as sorted T_{FH} cells from $DC^{-/-}$ mice expressed less IL-21 mRNA (**Fig. 2.8B**).

MyD88 deletion in B cells did not decrease the expansion of T_{FH} cells following CpG-NP-CGG immunization (**Fig. 2.7A**), although there was a statistically non-significant trend toward reduction in the frequency of T_{FH} cells relative to the pool of activated $CD4^+$ T cells (**Fig. 2.7B**). These results suggest that TLR9/MyD88 signaling in B cells promotes stabilization of activated T cells as T_{FH}, and/or their proliferation or survival. In line with the first hypothesis, IL-21 mRNA expression in sorted T_{FH} from $B^{-/-}$ mice was reduced compared to WT littermate controls (**Fig. 2.8B**).

I also examined the requirements for MyD88 in DCs and B cells for the changes in ICOS and PD-1 expression on the surface of T_{FH} cells in response to immunization with an antigen containing a TLR9 ligand. While increased levels of ICOS on T_{FH} cells were partially abrogated by deletion of Myd88 in either DCs or B cells (**Fig. 2.7D**), the effect of TLR9 signaling on T_{FH} cell expression of PD-1was primarily due to TLR9/MyD88 signaling in DCs (**Fig. 2.7E**).

Role of cell-intrinsic MyD88 signaling in B cells for the germinal center response

The qualitative effects on the GC reaction mediated by TLR9/MyD88 signaling in B cells could result from enhanced stimulation of antigen-specific T_{FH} cells, which in turn could affect selective processes of the GC reaction generally, or they could result from direct effects on B cells receiving stimulation via TLR9/MyD88 signaling. To address this mechanistic question, I generated mixed bone marrow chimeras that included B cells expressing MyD88 and those that did not, and expressed distinct IgH allotypes, making it possible to distinguish the cellular source of antigen-specific IgG. Lethally irradiated mice were reconstituted with equal portions of either $B^{-/-}$ (*Mb1-cre* $MyD88^{f/f}$, IgH^b) and

WT (IgH^a) bone marrows or with a mixture of WT (IgH^b) and WT (IgH^a) bone marrows as a control. Myd88 deficiency did not affect representation of B cells within the mature population of the LNs (**Fig. 2.10A**). At day 14 post-immunization, CpG-NP-CGG induced an elevated level of diverse affinity anti-NP IgG2a of both allotypes and this occurred similarly in both chimeras (**Fig. 2.9A**), whereas there was a selective defect in production of high affinity anti-NP IgG2a^b by MyD88-deficient B cells even in the presence of roughly 50% *Myd88*$^{+/+}$ B cells (**Fig. 2.9A)**. The affinity maturation of *Myd88*$^{+/+}$ B cells was apparently not adversely affected by the presence of *Myd88*$^{-/-}$ B cells. Thus, TLR9 regulated affinity maturation in a B cell-intrinsic fashion. Since *Myd88*$^{-/-}$ B cells in these mixed bone marrow chimeras made as much diverse affinity (high and low affinity) IgG2a anti-NP antibody as did the *Myd88*$^{+/+}$ B cells, they did not have a defect in class switch to IgG2a (**Fig. 2.9A**). Thus, the failure of MyD88$^{-/-}$ B cells to make high affinity anti-NP IgG2a^{b+} was due to a cell-intrinsic impairment in affinity maturation. The decreased production of high affinity IgG2a^{b+} antibody by MyD88$^{-/-}$ B cells was paralleled by a reduction in the number of IgG2a^{b+} GC B cells in the draining lymph node on day 14 (**Fig. 2.9B**), and a correspondingly diminished frequency of IgG2a^{b+} B cells among the NP$^+$ GC B cell population (**Fig. 2.10B**). To confirm that reduced numbers of IgG2a^{b+}*Myd88*$^{-/-}$ GC B cells did not reflect a class switch defect, I adopted a second mixed bone marrow chimera approach using equivalent portions of bone marrows expressing different allotypic forms of Ly5 (**Fig. 2.10C**) to distinguish *Myd88*$^{-/-}$ and *Myd88*$^{+/+}$ GC B cells. Following immunization of these mice with CpG-NP-CGG, I observed a similar disadvantage of *Myd88*$^{-/-}$ B cells in GCs from draining iLNs (**Fig. 2.9C**). Interestingly, the same trend was evident in GCs from mesenteric LNs (mLNs), where there is likely to be a high exposure to TLR ligands (**Fig. 2.9D**). Importantly, in both chimeric settings Fas$^+$IgD$^+$B220$^+$ GC precursor B cells were generated similarly (**Fig. 2.10D, E**), suggesting that TLR/MyD88 signaling in B cells acted later during the GC reaction to enhance selection rather than earlier at the time of GC formation.

These data indicate that much of the ability of TLR9/MyD88 signaling in B cells to enhance affinity maturation in the GC response was a cell intrinsic effect requiring signaling in the responding B cell. Nonetheless, in these experiments defective TLR9/MyD88 signaling in a fraction of the GC B cells clearly impacted T_{FH} cells in the GC and also the neighboring *Myd88*$^{+/+}$ B cells. The number of T_{FH} cells per lymph node trended lower in the mixed BM chimeras that had 50% *Myd88*$^{-/-}$ B cells compared to those that were 100% *Myd88*$^{+/+}$ (**Fig. 2.9D**). Correspondingly, expansion of *Myd88*$^{+/+}$B cells trended lower in the chimeras containing 50% *Myd88*$^{-/-}$B cells compared to the control chimeras that had 100% *Myd88*$^{+/+}$ B cells (**Fig. 2.9B**).

TLR9 signaling in DCs and B cells suppresses FoxP3$^+$$T_{FR}$ accumulation

Recent studies have revealed that follicular CD4$^+$ T cells are comprised of both T_{FH} cells as well as CXCR5$^+$ FoxP3$^+$ T_{FR} cells, the function of which is not fully understood but may include negative regulation of both T_{FH} and B cells during a GC response[91-94, 96]. Five days after immunization of WT and MyD88 conditional knockout mice with nonCpG- and CpG-NP-CGG, the T_{FR} cell frequency was similar among all groups (**Fig. 2.12A**). However, by day 14 the T_{FR} cell frequency relative to T_{FH} cells was decreased by 3-fold in WT mice that were immunized with CpG-NP-CGG conjugates compared to the nonCpG conjugates (**Fig. 2.11A, B**), and these changes were paralleled by diminished FoxP3 mRNA in follicular $CD4^+$ T cells (**Fig. 2.12B**). At day 14, $FoxP3^+CD3^+$ T_{FR} cells were visible in the follicles and GCs of draining iLNs (**Fig. 2.4C**) and their total numbers per lymph node increased in mice immunized with CpG-containing antigen (**Fig. 2.11C**). This expansion was balanced by an even greater increase in the number of T_{FH} cells (**Fig. 2.7A**). Interestingly, there was no effect of inclusion of a TLR9 ligand bound to the antigen on the number of T_{REG} cells as a frequency of activated $CD4^+$T cells in the non-follicular component of the $CD4^+$T cell response (**Supplementary Fig. 2.12C**). Thus, the presence of a TLR9 ligand conjugated to protein antigen selectively modulated the composition of follicular $CD4^+$T cells.

Deletion of MyD88 signaling in DCs compromised the expansion of T_{FH} cells (**Fig. 2.7A**), but it did not change the magnitude of the T_{FR} cell compartment induced by immunization with CpG-NP-CGG, and therefore the number of T_{FR} cells as a percentage of follicular $CD4^+$T cells was positively impacted by loss of MyD88 signaling in DCs (**Fig. 2.11A, B**). Thus, TLR9/MyD88 signaling in DCs selectively favored T_{FH} expansion over T_{FR} cell expansion. When *Myd88* was deleted in B cells, total T_{FR} cell numbers per lymph node increased (**Fig. 2.12C**) without significantly affecting T_{FH} cell numbers (**Fig. 2.7A**), again increasing the frequency of T_{FR} cells in the follicular $CD4^+$T cell pool (**Fig. 2.11A, B**). Deletion of *Myd88* in both B cells and DCs in the same mice significantly boosted the number of T_{FR} cells per LN compared to mice with MyD88 deletion in DCs alone but did not surpass the number observed in $B^{-/-}$ mice, consistent with a distinct role for TLR9/MyD88 signaling in B cells limiting the number of T_{FR} cells (**Fig. 2.11C**). Thus, MyD88 signaling in B cells and in DCs had different influences on the expansion of T_{FH} and T_{FR} cell populations, in both cases favoring T_{FH} cells over T_{FR} cells.

DISCUSSION

While a number of studies have indicated that TLRs promote rapid production of low affinity immunoglobulin through extrafollicular antibody responses, several recent reports have shown that TLRs can also promote GC responses[82-84, 106]. To analyze the mechanisms by which TLR signaling contributes to GC processes, I turned to an oligovalent haptenated protein antigen (NP-CGG) complexed with an oligonucleotide either containing or lacking CpG motifs. In agreement with earlier results indicating that haptenated soluble proteins are strongly immunogenic and do not require MyD88 signaling to induce vigorous antibody production[81], immunization with the nonCpG-NP-CGG induced a robust GC response. When the TLR9 ligand was included, however, more IgG was produced at early stages of the response, prior to day 21, and in addition, features associated with the quality of the GC reaction were substantially boosted. These changes were separately controlled by TLR9 signaling in DCs and B cells. TLR9/MyD88 signaling in DCs increased the magnitude of anti-NP IgG produced by promoting the expansion of T_{FH} and GC B cells, whereas in B cells, it primarily affected the quality of the GC response, resulting in better selection for high affinity antibody, more class switching to IgG2a^{b} and generation of more memory B cells.

A variety of studies have indicated that the initial activation of naive T cells by DCs induces some of them to become T_{FH} cells, and that in many circumstances, this is followed by a second checkpoint where interaction with antigen-presenting B cells induces T_{FH} cells to acquire a full GC T_{FH} cell phenotype, allowing them to enter GCs and contribute to selection[107-111]. Our data are consistent with this sequential model, as TLR9 signaling in DCs increased numbers of T_{FH} cells, while in B cells it affected T_{FH} cell expression of ICOS, which is critical for T_{FH} cell development, longevity and, ultimately, GC persistence[97-99, 108, 112]. ICOS expression by T_{FH} cells was also boosted by TLR9/MyD88 signaling in DCs. Importantly, a mutation of a negative regulator of ICOS mRNA, Roquin, leads to autoimmunity that has been attributed to overly active T_{FH} cells[40, 41]. Thus, elevated levels of cell-surface ICOS likely enhances T_{FH} cell function and contributes to the elevated GC response that resulted from linkage of a TLR9 agonist to the antigen.

Our findings complement emerging evidence showing that unique properties of different pathogens and immunization strategies imprint on T_{FH} cells to uniquely define their cytokine and costimulatory profile and ultimately specify the antibody response[48, 113 75, 114]. A possible distinguishing feature among pathogens is differential expression of TLR ligands, which may stimulate DCs to influence their cytokine profile and ability to promote T_{FH} cell expansion. Importantly, a previous study demonstrated that unlinked CpG oligonucleotide could enhance T_{FH} cell development in vivo[115], which may reflect an effect of TLR stimulation on DCs.

Stimulation of TLR9 in B cells by inclusion of a TLR9 ligand in the oligonucleotide-NP-CGG antigen enhanced the quality but not the overall magnitude at later times of the GC reaction. Compared to the response to nonCpG-NP-CGG, the anti-

NP response to CpG-NP-CGG included higher affinity IgG, more IgG2a, and greater production of anti-NP memory B cells. Surprisingly, each of these features was lost in mice selectively deleted for *Myd88* in B cells, resulting from a combination of effects on the follicular $CD4^+$ T cell population and direct effects within the responding B cells. With regard to the former mechanism, I observed both quantitative and qualitative differences in the follicular T cell compartment of mice lacking MyD88 selectively in B cells. First, there was a downward trend in the representation of T_{FH} cells as a fraction of activated $CD4^+$T cells (**Fig. 2.7A, B**), and secondly, their expression of ICOS was also reduced, suggesting that TLR9-stimulated B cells were better able to provide signals that maintain T_{FH} cell identity, promote their survival, and/or stimulate their proliferation. In line with this, previous reports have demonstrated that antigen presentation by GC B cells to T_{FH} cells resulted in higher expression by these cells of CXCR5 and costimulatory molecules such as ICOS[32, 108].

In addition to positive regulation of GCs by T_{FH} cells, T_{FR} cells function at least in part to restrict the GC reaction[93, 116-120]. I found that TLR9/MyD88 signaling in both DCs and B cells affected the relative balance between T_{FH} and T_{FR} cells in the GC. When *Myd88* was deleted selectively in B cells, the numbers of T_{FR} cells were increased whereas the numbers of T_{FH} cells were unchanged. In contrast, when *Myd88* was selectively deleted from DCs, there were fewer T_{FH} cells, but the numbers of T_{FR} cells were largely unaffected. Thus, TLR/MyD88 signaling in both DC and B cells acted to increase the number of T_{FH} cells relative to the number T_{FR} cells, but in complementary ways. The relative balance between T_{FH} and T_{FR} cells is likely to have important functional consequences, as several studies have indicated that T_{FR} cells can inhibit both T_{FH} cells and B cells to control different elements of GCs[92-94]; however, further investigation will be needed in this system to determine whether some portion of the effects of MyD88 signaling in DCs or B cells is mediated by decreasing the proportion of T_{FR} cells among the follicular $CD4^+$ T cell population.

While some of the effects of TLR9/MyD88 signaling in B cells appeared to be mediated by their modulation of the phenotype of T_{FH} cells and/or of the relative fraction of T_{FR} cells, the more prominent effects were intrinsic to $MyD88^{+/+}$ B cells when they were combined with $MyD88^{-/-}$ B cells in mixed bone marrow chimeric mice. In this experimental system, any effects of TLR signaling in B cells on T_{FH} cell function would likely be reflected equally by both types of B cells, since it is known that cognate interactions between T_{FH} cells and GC B cells are short-lived relative to the time frame of the GC responses being analyzed[121-123]. When different alleles of the cell surface molecule Ly5 were used to distinguish separate genotypes of B cells in response to CpG-NP-CGG, it was evident that *Myd88*$^{-/-}$ B cells in the GC were underrepresented relative to *Myd88*$^{+/+}$ B cells (**Fig. 2.9C**). Thus, B cell-intrinsic TLR9 signaling improved selection of antigen-specific B cells into the GC compartment, boosted their expansion, and/or enhanced their survival. Since GC precursor B cell frequency was similar between both genotypes, it suggests that TLR9/MyD88 signaling acted during the GC reaction rather than at the time of GC formation in order to modulate selection. These results agree with a recent study showing that TLR7 signaling in B cells was required for full participation in the GC response to LCMV infection[84]. Interestingly, the same discrimination against *Myd88*$^{-/-}$ cells was seen in GC B cells from the mesenteric LNs of Ly5.1/Ly5.2 chimeric animals (**Fig. 2.9C**), indicating that B cell-intrinsic MyD88 signaling contributes importantly to GC responses to gut microbiota-derived antigens. This function of MyD88 could contribute to the great susceptibility to encapsulated pathogenic bacteria seen in individuals deficient in MyD88 or IRAK4[28]. Similarly, when I used IgH allotype markers and focused on GC B cells that had isotype switched to IgG2a, we observed a decreased representation of *Myd88*$^{-/-}$IgG2a^{b+}GC B cells compared to *Myd88*$^{+/+}$IgG2a^{a+} GC B cells (**Fig. 2.9B and Fig. 2.10B**). Interestingly, B cell-intrinsic MyD88 signaling enhanced the amount of high affinity IgG2a^{b} secreted but did not affect the titer of diverse affinity IgG2a^{b} (**Fig. 2.9A**). Thus, B cell-intrinsic TLR9/MyD88 signaling conferred an advantage to B cells for GC development and/or survival that translated to increased production of high affinity IgG. In contrast, class switch to IgG2a was similar in both *Myd88*$^{-/-}$ and *Myd88*$^{+/+}$ B cells in mixed bone marrow chimeras, whereas it was defective if all B cells were *Myd88*$^{-/-}$. Therefore, I hypothesize that *Myd88*$^{+/+}$ B cells in the GC of mixed bone marrow chimeric mice were able to promote the ability of T_{FH} cells to induce B cells of either genotype to class switch to IgG2a (**Fig. 2.9A**), for example by production of IFNγ. Previous studies have demonstrated that in some immunizations class switch to IgG2a can be a B cell-intrinsic function of TLR9 signaling[88, 124], but it is also well established that IFNγ promotes class switch to IgG2a[103, 125]. Thus, there appear to be two distinct mechanisms by which TLR signaling promotes class switch to IgG2a in vivo.

The experiments presented here largely agree with a recent report by Pulendran and colleagues[83], which showed that co-administration of TLR ligands and antigen adsorbed separately to nanoparticles stimulated a vigorous GC response characterized by secretion of a large amount of high affinity antibody and robust B cell memory. In our experiments, a robust response was obtained by direct linkage of a haptenated protein antigen to a TLR9 ligand in oligomeric soluble complexes. In both systems, TLR signaling in DCs and in B cells was important for the enhanced IgG response achieved with this type of adjuvant. I have extended these findings by characterizing how TLR signaling in DCs and B cells differentially informs follicular CD4^{+} T cell populations, composed of both T_{FH} and T_{FR} cells. In addition, I identified B cell-intrinsic requirements for TLR signaling that enhance affinity maturation and increase the number of antigen-specific memory B cells. The results from the two systems were not entirely identical as nanoparticle immunization was similar to that observed with virus-like particles containing TLR7 or TLR9 ligands[82] where selective deficiency of MyD88 from B cells decreased the overall IgG response. This difference could reflect the particulate nature of these immunogens. Collectively these reports indicate that delivery of TLR ligands to B cells can result in significantly improved production of high affinity antibody and improved B cell memory, both of which are desirable goals of vaccination.

Materials and Methods

Mice. Mice carrying a floxed *Myd88* allele (*Myd88*$^{fl/fl}$, CBy.129P2(B6)-*Myd88*^{tm1Defr}/J) were generated as described previously[82, 85] and backcrossed to the C57BL/6 background for at least 10 generations. C57BL/6 backcrossed Mb1-Cre[126] and CD11c-Cre[127] mice were crossed to *Myd88*$^{fl/fl}$ mice to generate mice deleted for *Myd88* selectively in B cells or in dendritic cells, respectively. The following mice were obtained from Jackson Laboratory: C57BL/6 (B6), B6.*Cg-Igh*^{a} *Thy1*^{a} *Gpi1*^{a}*/J*, B6 CD45.1 (Ly5.1^{+}BoyJ, from Jackson or NCI). Male or female cohorts between 8 and 12 weeks were age matched within two weeks. Mice were housed in a specific pathogen-free animal facility at the University of California San Francisco. All procedures involving mice were preformed with institutional animal care and use committee (IACUC) approval and in accord with National Institutes of Health guidelines.

Generation of CpG- and nonCpG-NPCGG conjugates and mouse immunizations. 10mg of lyophilized 4-Hydroxy-3-nitrophenyl-haptenated chicken gamma globulin (NP_{15-17}CGG, Biomol) was reconstituted in 1mL 0.1M sodium bicarbonate buffer (pH 8.3) and biotinylated by adding dropwise 112mL of a solution containing biotin-sulfosuccinimidyl ester (Invitrogen, B6352) dissolved in dimethylformamide (10mg/mL) with constant stirring at 25°C. The reaction was allowed to proceed for 3hrs in the dark followed by three washes in Dulbecco's PBS by 30-fold dilution and centrifugation in an Amicon Ultra Centrifugal Filter (Millipore) with a 50kD molecular weight cut-off according to manufacturer's guidelines. Biotin-CpG1826 (TCCATGACGTTCCTGACGTT) or biotin–nonCpG1982 (TCCAGGACTTCTCTCAGGTT) (Integrative DNA Technologies) containing a phosphorothioate backbone in PBS was mixed with biotin-NP-CGG at a molar ratio of 2.6 to 1, followed by the addition of 4 moles of streptavidin monomer for each mole of NP-CGG in an equivalent volume of PBS. The mixture was incubated on a rocker for 3 h at 4°C, washed as described for biotinylated NP-CGG, and the final concentration adjusted to 0.5-0.66 mg of NP-CGG/ml in PBS. Mice were injected subcutaneously with 50 μl in the hind flanks, sacrificed at days 14 or 21-post immunization, and the draining inguinal lymph nodes harvested for analysis by flow cytometry or frozen in OTC for histological examination. For antibody titers, blood was collected by submandibular lance using Goldenrod lancets, in most cases on days 7, 14, 21 and every two weeks thereafter for time courses.

Flow Cytometry and Cell Sorting. Lymphocytes were harvested from inguinal lymph nodes by passage through a 40mm mesh filter (Fisher Scientific) and labeled in flow cytometry buffer HBSS (Cellgro) supplemented with 1mM EDTA, 2% heat-inactivated FBS, and 0.02% sodium azide) with antibodies to the following antigens: CXCR5-biotin, IgG2a^{a}-biotin, IgG2a^{b}-biotin, CD45.1-biotin, CD4-PECy7, PD-1-PE, IgD-FITC, CD44-FITC, CD44-APC, B220-PacBlu, B220-Alexa647, CD25-APC (BD Biosciences), IgD-PerCPCy-5.5, ICOS-PerCPCy-5.5, ICOS-PECy7, B220-APC-Cy7, CD62L-APC-Cy7, CD45.1 PercPCy5.5, CD45.2-PacBlu, CD45.2-Alexa700 (Biolegend) IgD-APC, and GL7-APC (eBioscience). Biotinylated antibodies were detected with streptavidin-

Qdot605 (Invitrogen). Lymphocyte nuclei were stained with anti-FoxP3-eFlour450 (eBioscience) using the BrdU Flow Kit from BD Biosciences. Antigen-binding cells were detected with NP (4-Hydroxy-3-nitrophenyl)- or NIP (4-Hydroxy-3-iodo-5-nitrophenyl)-labeled (Biosearch Technologies) R-phycoerythrin (P801, Invitrogen) and allophycocyanin (A803, Invitrogen), which were prepared as previously described[128]. All flow cytometry data were generated on an LSRII (Becton Dickinson) and analyzed with FlowJo (TreeStar) software, version 9.5. For sorting T_{FH}, $CD4^{+}$T cells were enriched by negative selection using Dynal Mouse CD4 Negative Isolation Kit (Invitrogen, Cat. No. 114.15D) before labeling $15x10^6$ cells with antibody in a one ml volume of HBSS buffer containing 2%BSA and 1mM EDTA. Cells were sorted on a MoFlo cell sorter (Dako Cytomation) into cold complete RPMI1640 medium containing 20% heat-inactivated FBS, pelleted in a microcentrofuge and stored at -80°C until RNA extraction.

Bone marrow chimeras. To generate *Mb1-cre/Myd88$^{fl/fl}$*:WT mixed bone marrow chimeras with different IgH allotypes, Ly5.1^{+}BoyJ mice (Jackson) were lethally-irradiated and reconstituted with 3 x 10^6 bone marrow cells composed of equal portions of bone marrows from *Mb-1cre/Myd88$^{fl/fl}$*(IgH^{b}) and B6.*Cg-Igh^{a}Thy1^{a}Gpi1^{a}/J* WT (IgH^{a}) or from C57BL/6 WT (IgH^{b}) and B6.*Cg-Igh^{a}Thy1^{a}Gpi1^{a}/J* WT (IgH^{a}) as a control. The same protocol was used to generate *Mb1-cre/Myd88$^{fl/fl}$*:WT mixed bone marrow chimeras expressing different Ly5 allotypes using either *Mb-1cre/Myd88$^{fl/fl}$*(Ly5.2^{+}) and BoyJ (Ly5.1^{+}) or C57BL/6 (Ly5.2^{+}) and BoyJ (Ly5.1^{+}) as a control. Chimeric mice were allowed to reconstitute for 10 weeks before immunization.

Immunohistochemistry. Draining lymph nodes were embedded in optimal cutting temperature compound (OCT) (Sakura Finetek), frozen on dry ice and liquid N_2 and sectioned into 7mm slices using a Leica CM3050S cryomicrotome. Fresh sections were allowed to dry o.n. at room temperature before acetone-dehydration and storage at -80ºC. Thawed sections were incubated in Tris-buffered saline (TBS), pH 8.5 containing 5%BSA and 1% normal mouse serum for 1hr at room temperature, rinsed in TBS, and endogenous streptavidin and biotin sites blocked using a Streptavidin and Biotin Blocking Kit (Vector Labs). GCs, T_{FH} and T_{FR} were visualized by labeling blocked sections with IgD-APC (Biolegend), CD3-FITC (BD Biosciences), followed by FoxP3 nuclear staining with biotin-FoxP3 (eBioscience) and streptavidin-Cy3 (Jackson) using the eBioscience FoxP3 staining kit. All images were captured with an Axio Observer Z1 microscope (Carl Zeiss) using Axiovision software version 4.8. All kits were used according to the manufacturers' protocols.

mRNA isolation, cDNA, and real-time PCR analysis. Frozen cell pellets were harvested in RLT lysis buffer (Quiagen) containing 0.1% 2−mercaptoethanol and RNA isolated using the RNeasy Micro Kit (Quiagen, Cat. No. 74004) with on-column DNA digestion. cDNA was reverse transcribed from total RNA using the iScript cDNA Synthesis Kit (Bio-Rad, Cat. No. 170-8890). A Sybr Green (Roche) assay was used to detect amplification of cDNA by quantitative PCR on an ABI 7700 sequence detection system (Taqman; PE Applied Biosystems) with the following primers: IL-21 forward, 5'-

GCTCCACAAGATGTAAAGGG-3'; reverse, 5'-TTATTGTTTCCAGGGTTTGA-3'; IL-4 forward, 5'-AGATCATCGGCATTTTGAACG-3'; reverse, 5'-TTTGGCACAT - CCATCTCCG-3'; IFNγ forward, 5'-AACATAAGCGTCA-TTGAATCA-3'; reverse 5'-GCTGGACCTGTGGGTTGT-3', FoxP3 forward, 5'-TCCAGGTTGCTCAAAGTC-TTCTTG-3'; reverse, 5'-AGGCTGCTGTTACGGGA- ATAGG-3'; glyceraldehyde-3-phosphate dehydrogenase (GAPDH) forward, 5'-GGTCTACATGTTCCAGTATG - ACTCCA-3'; reverse, 5'-GGGTCTCGCTCCTGGA- AGAT-3'. Sequence Detection software version 1.2.2 was used to calculate cross-threshold (Ct) values. mRNA expression was calculated relative to GAPDH.

ELISA. 96-half-well high binding polystyrene plates (Costar 3690) were coated overnight at 4ºC or for one hour at 37ºC with NP_{15}-BSA to capture diverse affinity anti-NP antibodies, or with NP_1-BSA for high affinity anti-NP IgG. Briefly, antigen-coated ELISA plates were blocked with 2% heat-inactivated FBS in PBS for 1hr at room temperature, incubated with serum overnight at 4°C for diverse and high affinity ELISAs followed by 4 washes in PBS (pH 7.4) supplemented with 0.02% Tween-20. Plates were then coated with horseradish peroxidase-conjugated detection antibodies (Southern Biotechnologies)—anti-total IgG (1/5000), -IgG1 (1/5000), and -IgG2c (1/5000)—for one hour at room temperature and then washed four times. For quantification of distinct IgH allotypes, biotinylated antibodies against $IgG1^{a}$(1/100), $IgG1^{b}$ (1/200), $IgG2a^{a}$(1/100), and $IgG2a^{b}$(1/200) (BD Biosciences) were incubated with serum-coated plates for one hour at room temperature, washed four times and then labeled with streptavidin-HRP (1/5000) for an additional hour and then washed as before. ELISA plates were then developed with 3,3',5,5'-tetramethylbenzidine (TMB) substrate (Vector Labs) and the reaction quenched with 2N sulfuric acid. The optical densities at 450 and 570 were measured on a VERSAmax microplate reader (Molecular Devices), and the difference in optical densities (O.D.450-570) was plotted for comparison of the slopes and calculation of relative titers.

Statistical analyses. One-way analysis of variance (ANOVA), Bonferroni's correction for multiple groups and Student's *t*-tests were performed with a 95% confidence interval using GraphPad software from Prism.

Figure 2.1 Attachment of a TLR9 ligand enhances the GC response to NP-CGG. (**A**) Gating strategy for flow cytometric identification of NP-specific GC B cells ($B220^{+}NP^{+}IgD^{lo}Fas^{hi}$) in the draining inguinal lymph nodes (iLN) after subcutaneous (s.c.) immunization of C57BL/6 mice with CpG-NP-CGG (CpG) or nonCpG-NP-CGG (non) conjugates. (**B**) Enumeration of total GC B cells ($B220^{+}IgD^{lo}Fas^{hi}$, open) and NP-specific GC B cells ($B220^{+}NP^{+}IgD^{lo}Fas^{hi}$, filled). Each symbol represents the value obtained for a single mouse. (**C**) Kinetics of primary and secondary diverse affinity anti-NP IgG (left) and high affinity anti-NP IgG (right) antibody levels following immunizations as in ***a***. and boosted s.c. on day 53 with NP-CGG in saline. (**D**) Diverse affinity (anti-NP_{15}, left), high affinity (anti-NP_{1}, center), and affinity maturation (ratio of anti-NP_{1} to anti-NP_{15} IgG, right) of anti-NP IgG measured by ELISA at day 21 following immunization of WT mice as in ***A***. (**E**) Total anti-NP $IgG2a^{b}$ measured by ELISA at day 21 following immunization as in a. (**F**) Effect of CpG inclusion in the antigen on generation of memory anti-NP B cells. Shown is fold increase in diverse affinity anti-NP IgG titers from day 53 to day 60 (day 7 post-secondary challenge), left, and in high affinity anti-NP IgG titers from day 53 to day 67 (day 14 post-secondary challenge) following secondary immunization with NP-CGG in saline: Black, CpG-NP-CGG; grey, nonCpG-NP-CGG. Data in ***A, B, D,*** and ***E*** are representative of at least 6 experiments and in ***C*** and ***F***, of two experiments. *$p<0.05$, **$p<0.005$, ***$p<0.0001$ (*t*-test). CpG, CpG-NP-CGG; non, nonCpG-NP-CGG. *dpi*, days post immunization.

Figure 2.2 Total numbers of NIP-binding plasma cells ($B220^{lo}CD138^{+}NIP^{+}IgD^{lo}$) per LN 14 days post-immunization. NIP (4-Hydroxy-3-iodo-5-nitrophenyl) is an iodinated form of the hapten NP (4-Hydroxy-3-nitrophenyl) which binds with higher affinity than NP to BCRs of the same specificity. (**A**) Representative flow cytometry plots for detection of $B220^{lo}CD138^{+}NIP^{+}IgD^{lo}$ plasma cells. (**B**) Enumeration of the total number of NIP-binding plasma cells per draining iLN.

Figure 2.3 A TLR9 ligand increases the numbers of T_{FH} and alters their phenotype. (**A**) Representative flow cytometry plots of $CD4^{+}$ T cells depicting T_{FH} gating scheme ($CD62L^{lo}B220^{lo}FoxP3^{-}CD44^{hi}PD\text{-}1^{+}CXCR5^{+}$). (**B**) Frequencies and numbers of T_{FH} 14 days after immunization with CpG-containing or non-CpG-containing NP-CGG conjugates. Upper, frequency of T_{FH} determined as shown in ***a*** and displayed as percent of activated ($CD44^{+}CD62L^{lo}$) CD4+ T cells. Lower, total number of T_{FH} per lymph node (LN). (**C**) Cells identified as T_{FH} in ***A*** were Bcl-6^{+} as shown by flow cytometry histograms comparing Bcl-6 expression in T_{FH}, T_{eff}, and naive $CD4^{+}$T cells. (**D**) Relative abundance of follicular helper T cells calculated as the ratio of the number of T_{FH} to the number of GC B cells per draining lymph node. (**E-G**) Effect of TLR9 ligand on T_{FH} cell expression of ICOS and PD-1. (**E**) Left, flow cytometry histogram of ICOS expression on $CD4^{+}$T cells ($B220^{lo}CXCR5^{-}$, filled grey), and T_{FH} cells from lymph nodes of nonCpG- (open grey) and CpG-NP-CGG-immunized mice (open black). Right, ICOS expression represented as median fluorescence intensity (MFI) of T_{FH} cells (filled) and effector $CD4^{+}$T (T_{EFF})cells ($CD62L^{lo}B220^{lo}CD44^{hi}CXCR5^{-}FoxP3^{-}$, open). (**F**) Flow cytometry histograms of PD-1 expression of all T_{FH} cells gated as $CD4^{+}CD62L^{lo}CD44^{hi}CXCR5^{+}$.

Right, PD-1 expression represented as median fluorescence intensity (MFI) of all T_{FH} and T_{eff}. (**G**) As PD-1 expression on T_{FH} was heterogeneous, the fraction of T_{FH} expressing PD-1 at a higher level is also shown. Left, flow cytometry plots showing the percentage of T_{FH} cells gated as $CD62L^{lo}CD44^{hi}FoxP3^{-}CXCR5^{+}CD4^{+}$ that are $PD\text{-}1^{hi}$. Right, summarized data from flow cytometry analysis depicted in left panel. (**H**) Cytokine-encoding mRNA expression by T_{FH} cells defined as in panel ***A*** and isolated by sorting cells from draining lymph nodes of mice immunized with nonCpG- and CpG-NP-CGG 14 days prior**.** (**B, D, G**) Open circles, nonCpG-NP-CGG; filled circles, CpG-NP-CGG. (**E, F**) Open circles, T_{EFF}; closed, T_{FH}. (**C-G**) statistical significance is indicated as follows: **p*<0.05*,* ***p*<0.005, ****p*<0.0001 (student's *t*-test) and **H,** **p*<0.05 (paired *t*-test).

Figure 2.4 Bcl-6 expression in mLN T_{FH} and iLN GC B cells and localization of T_{FH} and T_{FR} cells in the GC. (**A**) flow cytometry histogram of nuclear Bcl-6 staining in naive T cells ($CD4^{+}CD62L^{+}CD44^{-}$, filled grey histogram), effector T cells ($CXCR5^{-}CD62L^{-}CD44^{+}CD4^{+}$, open grey histogram), and follicular helper T cells ($CD62L^{-}CD44^{+}PD\text{-}1^{+}CXCR5^{+}CD4^{+}$, open black histogram) from mesenteric LNs of WT C57BL/6 mice. (**B**) Flow cytometry histogram of nuclear Bcl-6 staining in naive $IgD^{+}Fas^{-}B220^{+}$ B cells (filled grey histogram) and $IgD^{lo}Fas^{+}B220^{+}$GC B cells from inguinal LNs as a negative and positive control, respectively, for Bcl-6 staining in follicular helper $CD4^{+}$T cell depicted in ***A.*** (**C**) Immunofluorescent staining of with anti-CD3 for T cells (green), anti-FoxP3 (red) for regulatory T cells (red and green) and anti-IgD-APC to delimit the B cell follicles (blue) and T cell zone in LN sections sections from WT mice immunized with nonCpG- or CpG-NP-CGG 14 days prior. T_{FH} (green) and T_{FR} (green and red) cells can be seen inside germinal centers located within the IgD^{-} area at the centers of IgD^{+} (blue) follicles, top panel. Bottom, digitally magnified insets correspond to numbered white boxes, showing red $FoxP3^{+}$ nuclear staining with surrounding $CD3^{+}$ (green) surface staining: 1, extrafollicular region; 2-5, germinal center. White arrows indicate $FoxP3^{+}CD4^{+}$ cells.

Figure 2.5 TLR9 signaling in DCs and B cells control magnitude and quality of the GC response, respectively. (**A**) Wild type, *CD11c-cre/MyD88*$^{fl/fl}$ ($DC^{-/-}$), *Mb1-cre/MyD88*$^{fl/fl}$ ($B^{-/-}$), and *CD11c-cre x Mb1-cre/MyD88*$^{fl/fl}$ ($DC^{-/-}B^{-/-}$) mice were immunized with nonCpG- (white bars) or CpG-NP-CGG (dark bars) and the total number of NP^{+}GC B cells per LN were determined 14 days after immunization as described in Fig. 1. Preimmune numbers of GC B cells are also shown (gray bar). (**B**) Ratio of high affinity anti-NP IgG to diverse affinity anti-NP IgG as in **Fig 2.1D**. (**C**) Levels of class switched $IgG2a^{b}$ (IgG2c, left) and IgG1 (right) anti-NP antibodies present in the serum of $DC^{-/-}$ and $B^{-/-}$ mice 14 days after immunization with CpG-NP-CGG. (**D**) The cell-type specific requirements for TLR9 signaling to promote formation of memory B cells were assessed by measuring the fold-increase in diverse (left) and high affinity (right) IgG anti-NP antibody 7 or 14 days, respectively, following secondary immunization with NP-CGG in saline 53 days after the primary immunization. Statistical significance between different genotypes of mice was measured by one-way analysis of variance (ANOVA) and

Bonferonni's *post hoc* analysis for comparison of individual groups immunized with CpG-NP-CGG (**A-D**). For comparison between WT (+/+) mice immunized with non-CpG and CpG-NP-CGG, a Student's *t*-test was performed. $*p<0.05$, $**p<0.005$, $***p<0.0001$. ***A-C*** represent one of four replicate experiments and ***D*** represents one of two.

Figure 2.6 Production of diverse and high affinity anti-NP IgG in WT, $DC^{-/-}$, $B^{-/-}$, and $DC^{-/-}B^{-/-}$ mice. (**A**) Relative concentrations of diverse affinity anti-NP IgG from mice with cell type-specific deletion of MyD88 were determined by ELISA 14 days after immunization with non-CpG (white bars) or CpG-NP-CGG (black bars). (**B**) Relative concentrations of high affinity anti-NP IgG from mice with cell type-specific deletion of MyD88 were determined by ELISA 14 days after immunization as in ***B***. ***A,*** WT, $DC^{-/-}$, $B^{-/-}$, one of four experiments where similar results were obtained; $DC^{-/-}B^{-/-}$, one of two where similar results were obtained. ***B,*** experimental averages of anti-NP_1 IgG titers. ***A*** and ***B,*** white bars, nonCpG-NP-CGG; black bars, CpG-NP-CGG.

Figure 2.7 TLR9 signaling in DCs and B cells determines T_{FH} number and phenotype. WT mice (+/+) or mice deleted for *Myd88* selectively in DCs or B cells or both DCs and B cells were immunized with non-CpG- (white bars) or CpG-NP-CGG (black bars) as in **Fig. 2.1** and were analyzed by flow cytometry on day 14. Preimmune ("unimmunized") numbers of T_{FH} cells are also shown (gray bar). (**A**) Total numbers of T_{FH} per LN. (**B**) Pooled data showing frequency of T_{FH} ($PD\text{-}1^+CXCR5^+$) from WT, $DC^{-/-}$, and $B^{-/-}$ and $DC^{-/-}B^{-/-}$ mice as a percentage of activated $CD4^+$T cells ($CD62L^{lo}CD44^{hi}$). (**C**) Ratio of T_{FH} to GC B cells in draining lymph nodes of individual mice, normalized to WT mice immunized with nonCpG-NP-CGG. (**D**) Cell surface expression of ICOS (median fluorescence intensity, MFI) of T_{FH} from the draining lymph nodes, displayed as the fold increase relative to WT mice immunized with nonCpG-NP-CGG. (**E**) Percentage of PD-1^{hi} T_{FH}, gated as in **Fig. 2.3G** in WT and MyD88 conditional knockout mice. (***A-E***) $*p<0.05$, $**p<0.005$, $***p<0.0001$ (one-way ANOVA and Bonferonni's *post hoc* correction for multiple group analysis of different genotypes immunized with CpG-NP-CGG; student's *t*-test for comparison of two-different types of antigen for wild type mice as in **Fig. 2.5**. ***A-C,*** pooled data from two of two replicate experiments; ***D***, WT, $DC^{-/-}$ and $B^{-/-}$ data are from three experiments; $DC^{-/-}B^{-/-}$ data are from two; ***E***, WT, $DC^{-/-}$ and $B^{-/-}$ data are from four experiments; $DC^{-/-}B^{-/-}$ data are from two.

Figure 2.8 Expansion of T_{EFF} cells in response to CpG-linked antigen and cytokine expression in sorted T_{FH} from WT, $DC^{-/-}$, $B^{-/-}$, and $DC^{-/-}B^{-/-}$ mice. (**A**) Comparison of the total number of $CD4^+CD62L^{lo}CD44^{hi}FoxP3^-$ T_{EFF} cells per LN at day 14 post immunization with nonCpG- or CpG-NP-CGG in WT littermate control, *CD11c-Cre Myd88*$^{fl/fl}$ ($DC^{-/-}$), *Mb1-Cre Myd88*$^{fl/fl}$($B^{-/-}$), and *CD11c+Mb1-Cre Myd88*$^{fl/fl}$ ($DC^{-/-}B^{-/-}$) mice. Circles: open, nonCpG-NP-CGG; black, CpG-NP-CGG; grey, unimmunized. (**B**) Cytokine mRNA expression in sorted T cell subsets. T_{EFF} (black), T_{FH} (grey), and naive $CD4^+$T cells (light grey) from WT *Myd88*$^{fl/fl}$, *CD11c-Cre Myd88*$^{fl/fl}$ ($DC^{-/-}$), and *Mb1-Cre Myd88*$^{fl/fl}$($B^{-/-}$) mice were sorted by flow cytometry according to surface expression of proteins defined for each subset in **Fig. 2.4**. IFNγ, IL-21, and IL-4 cDNA were amplified using a qPCR SYBR Green assay and normalized to expression levels of GAPDH as described in materials and methods.

Figure 2.9 B cell-intrinsic TLR9 signaling promotes affinity maturation in the GC. Mixed bone marrow (BM) chimeras were generated by reconstituting lethally-irradiated $Ly5.1^+$ BoyJ mice with equal parts of $B^{-/-}$*(Mb1-cre)/MyD88*$^{f/f}$ (IgH^b) and WT(IgH^a) bone marrows or control WT (IgH^b) and WT(IgH^a) bone marrow. After reconstitution for 10 weeks, mice were immunized with nonCpG (open circles) or CpG-NP-CGG (closed circles). (**A**) 14 days post immunization, the relative amounts of diverse affinity (anti-NP_{15}, right) and high affinity (anti-NP_1, left) $IgG2a^b$ (top) and $IgG2a^a$ (bottom) were determined by ELISA as in **Fig. 2.1**. (**B**) Numbers from individual draining lymph nodes of allotyope-specific ($IgG2a^b$, top or $IgG2a^a$, bottom) NP-binding GC B cells obtained from mixed BM chimeric mice 14 days after immunization. (**C**) Left, flow cytometry gating logic for distinguishing $Ly5.1^+$ and $Ly5.2^+$ follicular B cells (IgD^+) and GC B cells ($B220^{hi}IgD^{lo}Fas^{hi}$) from draining inguinal LNs or from mesenteric LNs (mLNs) of a $B^{-/-}$ (*Mb1-cre Myd88*$^{fl/fl}$) ($Ly5.2^+$): WT ($Ly5.1^+$) chimeric mouse. Right, percentage of $NP^+Ly5.1^+$ or $NP^+Ly5.2^+$ GC B cells per total GC B cells from draining inguinal LNs (upper) or mLNs (lower) 14 days after immunization with CpG-NP-CGG. (**D**) Total T_{FH} cells in individual lymph nodes, enumerated on day 14 as in **Fig. 2.5B**. One-way ANOVA and Bonferonni's *post hoc* correction for multiple group analysis; Student's *t*-test for comparison of two-different types of antigen for wild type mice as in Fig. 3, $*p<0.05$, $**p<0.005$, $***p<0.0001$. Data are from two of two replicate experiments in which similar results were obtained.

Figure 2.10 B cell-intrinsic and -extrinsic MyD88 signaling promotes selection in the germinal center. (**A**) Lethally irradiated $Ly5.1^+$BoyJ mice were reconstituted with mixed bone marrow carrying allotypically distinct IgH^a and IgH^b alleles as in Fig. 5. The percentage of $IgD^+Fas^-B220^+$ B cells expressing either IgD^a (open circles) or IgD^b (closed circles) is shown. (**B**) Representative 2-dimensional flow cytometry plots displaying gating strategy to enumerate allotype-specific NP-binding GC B cells ($B220^+NP^+IgD^-Fas^+IgG2a^{a+}$ or $IgG2a^{b+}$) from WT (IgH^b): WT(IgH^a) and Mb1-cre/MyD88$^{f/f}$ (IgH^b): WT(IgH^a) BM chimeras two weeks after immunization with nonCpG-NP-CGG and CpG-NP-CGG, left. Right, compiled flow cytometry data showing the frequencies of NP-specific GC B cells that expressed either $IgG2a^{a+}$ or $IgG2a^{b+}$ on their cell surface. (**C**) Summarized flow cytometry data showing the reconstitution efficiencies of Ly5 allotype-expressing $IgD^{hi}Fas^-$ follicular B cells from mixed bone marrow chimeras generated by reconstituting $Ly5.1^+$BoyJ mice with equal parts of either *Mb1-Cre MyD88*$^{fl/fl}$($Ly5.2^+$) and WT($Ly5.1^+$) bone marrows or WT($Ly5.2^+$) and WT($Ly5.1^+$) bone marrows as a control. (**D**) Flow cytometry gating scheme to distinguish Fas^+B220^+ GC precursor B cells that expressed either IgD^a or IgD^b (IgD^{a-}). Graph, percentage of Fas-positive IgD^{a+} (open circles) or IgD^{b+} (filled circles) $B220^+$ GC precursor B cells in draining iLNs 14 days after immunization of chimeric mice. (**E**) Flow cytometry plots showing gating strategy to distinguish IgD^+Fas^+ GC percursor B cells that expressed either Ly5.1 or Ly5.2, left.

Right, summary of percentage of GC precursor B cells expressing either Ly5.1 (open circles) or Ly5.2 (filled circles) from draining iLNs (open bars) or mLNs (grey bars) of chimeric mice 14 days after immunization with CpG- and nonCpG-NP-CGG conjugates. (**F**) The number of FoxP3$^+$T$_{FR}$ as a percentage of total follicular CD4$^+$T cells (CD62L^{lo}CD44^{hi}CXCR5$^+$PD-1$^+$) in draining LNs from the same mixed bone marrow chimeras described in ***A*** and Fig. 5. Data are from one of two replicate experiments with similar results.

Figure 2.11 TLR9 signaling in DCs and B cells preferentially enhances development and maintenance of T$_{FH}$ over FoxP3$^+$T follicular regulatory cells (T$_{FR}$). Wild type mice or mice deleted for Myd88 selectively in DCs, B cells, or both DCs and B cells were either immunized with nonCpG-NP-CGG (open symbols) or CpG-NP-CGG (closed symbols). Preimmune T$_{FR}$ numbers are also shown (grey circles). (**A**) Analysis by flow cytometry of FoxP3$^+$follicular T cells (gated as CD4$^+$CD62L$^-$B220$^-$CD44$^+$PD-1$^+$CXCR5$^+$FoxP3$^+$). The percentage of follicular CD4$^+$T cells that are FoxP3$^+$ in individual lymph nodes are indicated on the representative plots. (**B**) Percentage of T$_{FR}$ cells in the follicular CD4$^+$ T cell pool, gated as in ***A***. (**C**) Total number of T$_{FR}$ per draining lymph node. Symbols represent individual mice. One-way ANOVA followed by Bonferroni's *post hoc* analysis for comparison of groups immunized with CpG-NP-CGG; Student's *t*-test for comparison of two-different types of antigen for wild type mice as in **Fig. 2.5**, *$p<0.05$, **$p<0.005$, ***$p<0.0001$. Figure represents pooled data from two of two replicate experiments in which similar results were obtained.

Figure 2.12 TLR9/MyD88 signaling modulates the frequency of follicular but not extrafollicular FoxP3$^+$CD4$^+$T cells. (**A**) The number of FoxP3$^+$ T$_{FR}$ as a percentage of follicular CD4$^+$T cells at days 5 and 14 after immunization of WT littermate control, DC$^{-/-}$, and B$^{-/-}$ mice with nonCpG- and CpG-NP-CGG. (**B**) Relative expression of FoxP3 mRNA in follicular T cells sorted as CD4$^+$CD62L^{lo}B220^{lo}CD44^{hi}PD-1$^+$CXCR5$^+$ from WT mice that were immunized 14 days prior with either nonCpG- or CpG-NP-CGG. (**C**) Number of FoxP3$^+$ T$_{REG}$ cells as a percentage of activated extrafollicular T cells (CD4$^+$CD62L^{lo}CXCR5$^-$CD44^{hi}CXCR5$^-$).

Figure 2.13 TLR signaling in DCs and B cells controls GC magnitude and quality, respectively. The experiments presented in chapter two add to previous knowledge represented in **Fig.1.2.** Deletion of MyD88 in DCs and B cells revealed a division of labor in the GC response where DCs set the magnitude of the GC reaction by significantly augmenting T$_{FH}$ cell development in response to TLR stimuli. Separately, TLR signaling in B cells controlled qualitative aspects of the GC by enhancing affinity maturation, B cell memory, and class switch to IgG2a^b (IgG2c). Still signaling in DCs and B cells both modulated the qualitative aspects of the T$_{FH}$ compartment by modulating ICOS and PD-1 levels as well as the composition of FoxP3$^+$T$_{FR}$ cells in the follicular CD4$^+$T cell pool, likely impacting selection.

Figure 2.1

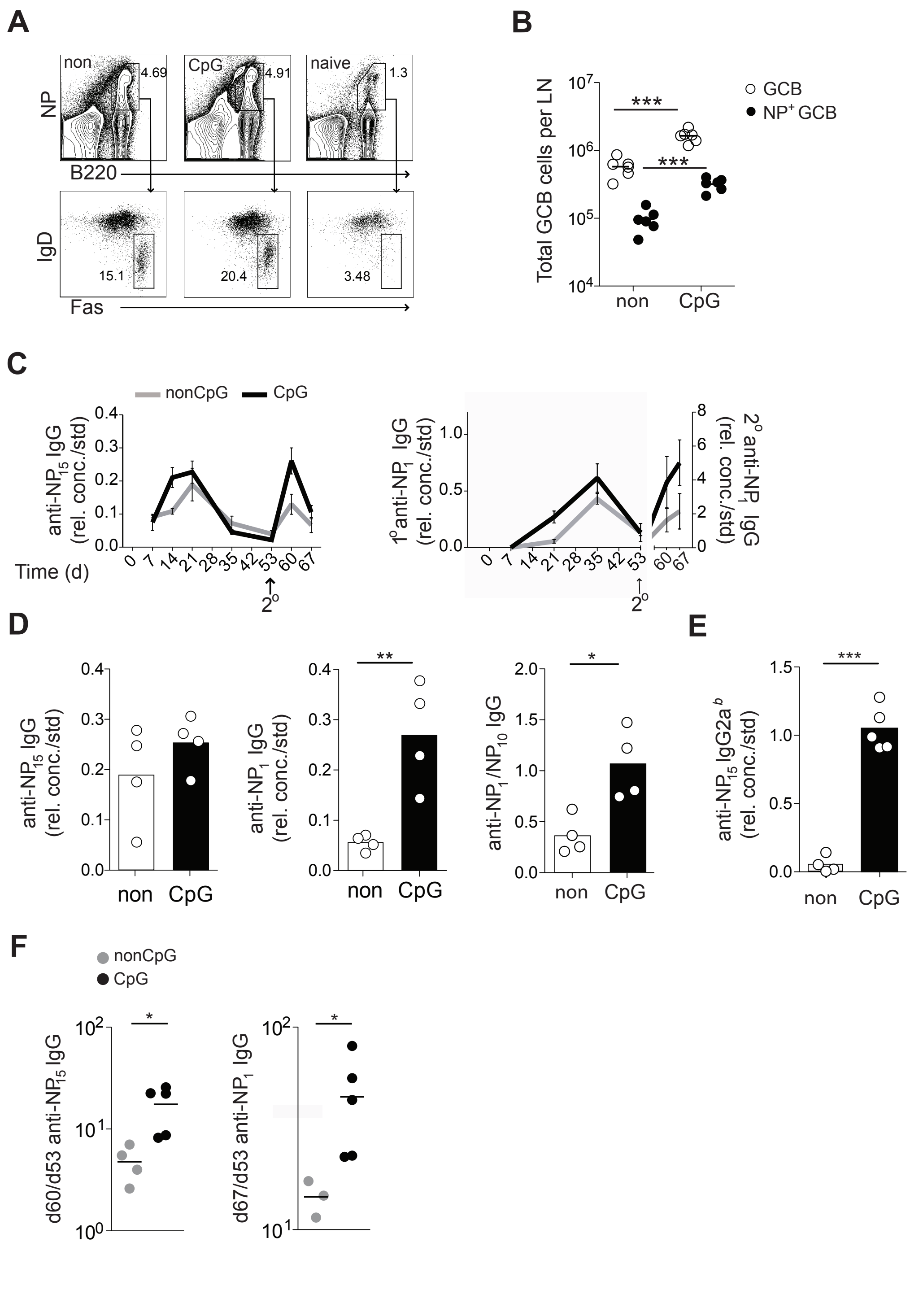
A
non
CpG
naive
4.69
4.91
1.3
NP
B220
IgD
Fas
15.1
20.4
3.48
B
Total GCB cells per LN
GCB
NP+ GCB
***
***
non
CpG
C
nonCpG
CpG
anti-NP15 IgG (rel. conc./std)
Time (d)
1° anti-NP1 IgG (rel. conc./std)
2° anti-NP1 IgG (rel. conc./std)
D
anti-NP15 IgG (rel. conc./std)
anti-NP1 IgG (rel. conc./std)
anti-NP1/NP10 IgG
E
anti-NP15 IgG2a^b (rel. conc./std)
F
nonCpG
CpG
d60/d53 anti-NP15 IgG
d67/d53 anti-NP1 IgG

Figure 2.2

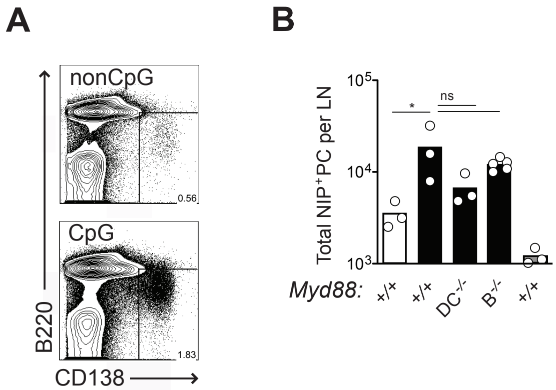
A
B
nonCpG
0.56
CpG
1.83
B220
CD138
Total NIP+PC per LN
10^5
10^4
10^3
*
ns
Myd88:
+/+
+/+
DC-/-
B-/-
+/+

Figure 2.3

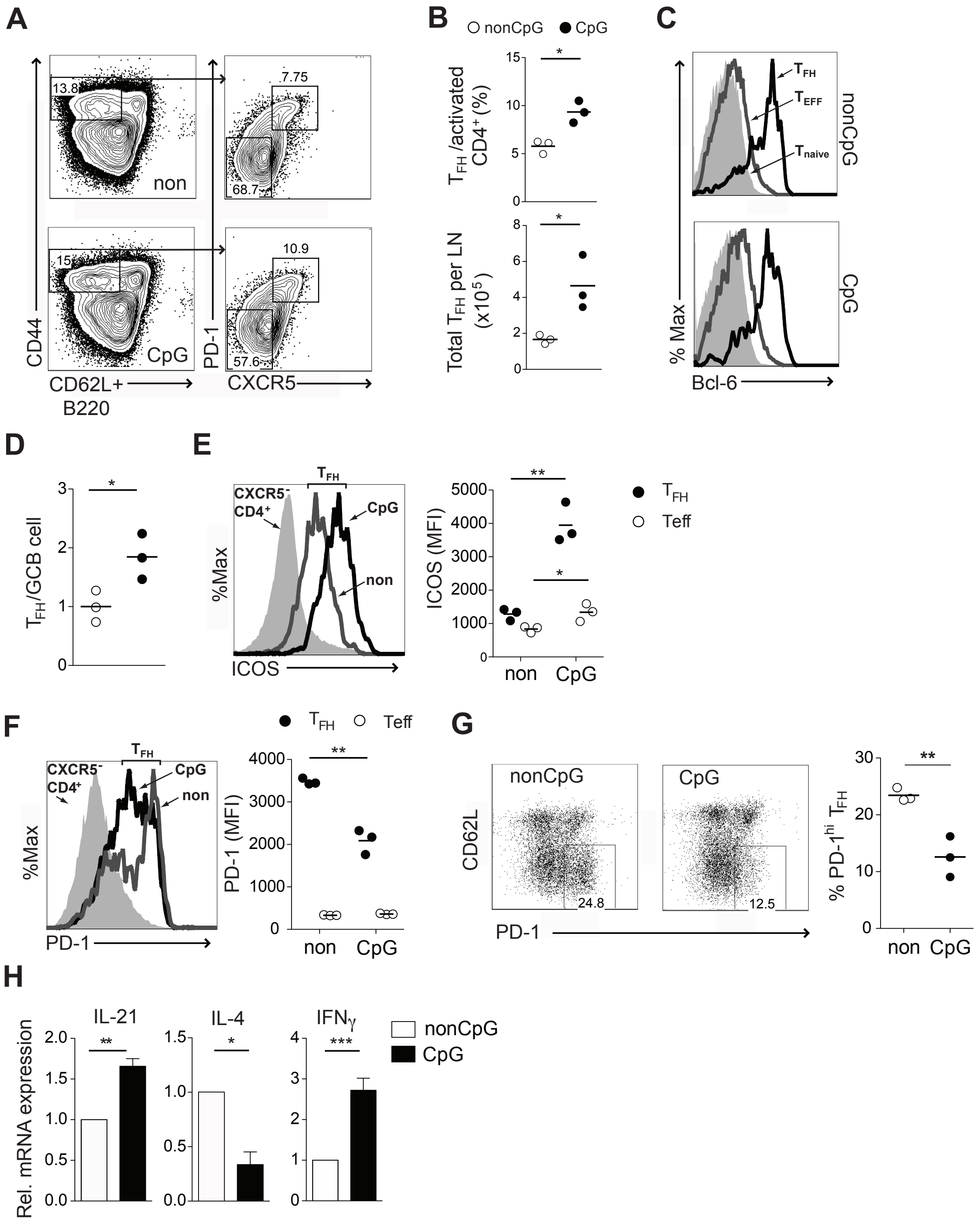
A
CD44
CD62L+
B220
PD-1
CXCR5
13.8
15
7.75
68.7
10.9
57.6
non
CpG
B
nonCpG
CpG
T_{FH} /activated CD4+ (%)
Total T_{FH} per LN (x10^5)
C
% Max
Bcl-6
T_{FH}
T_{EFF}
T_{naive}
nonCpG
CpG
D
T_{FH}/GCB cell
E
CXCR5- CD4+
%Max
ICOS
ICOS (MFI)
T_{FH}
Teff
non
CpG
F
PD-1
PD-1 (MFI)
G
nonCpG
CpG
CD62L
PD-1
24.8
12.5
% PD-1^{hi} T_{FH}
H
IL-21
IL-4
IFNγ
Rel. mRNA expression
nonCpG
CpG

Figure 2.4

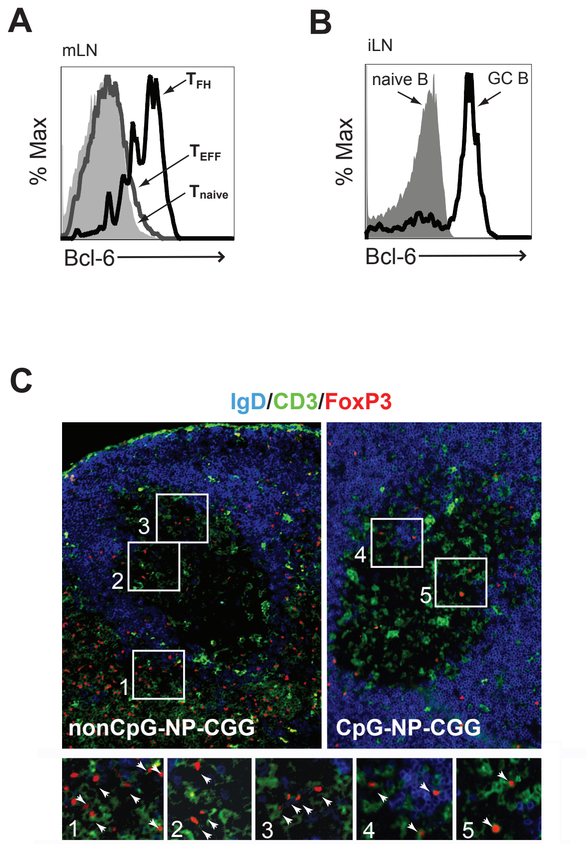
A
mLN
% Max
T_{FH}
T_{EFF}
T_{naive}
Bcl-6
B
iLN
naive B
GC B
% Max
Bcl-6
C
IgD/CD3/FoxP3
3
2
1
nonCpG-NP-CGG
4
5
CpG-NP-CGG
1
2
3
4
5

Figure 2.5

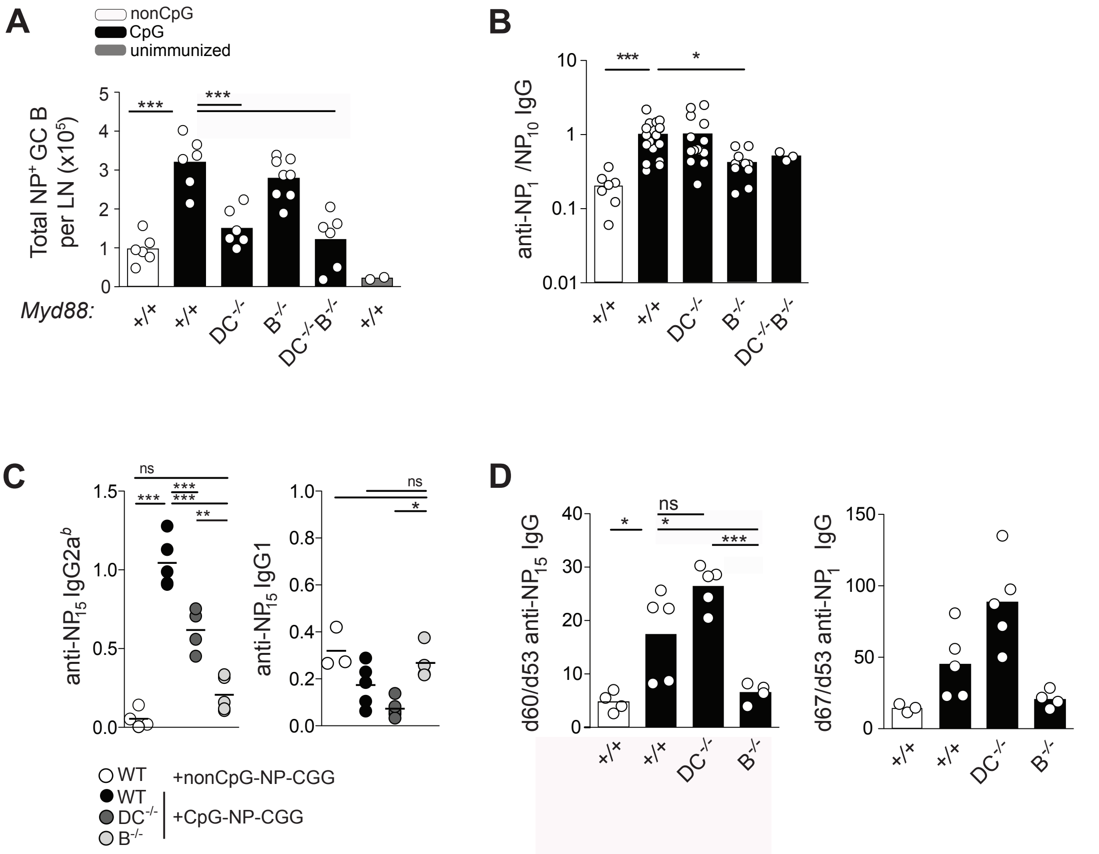
A
nonCpG
CpG
unimmunized
Total NP+ GC B per LN (x10^5)
Myd88:
+/+
+/+
DC-/-
B-/-
DC-/-B-/-
+/+
B
anti-NP1 /NP10 IgG
C
anti-NP15 IgG2a^b
anti-NP15 IgG1
ns
WT
WT
DC-/-
B-/-
+nonCpG-NP-CGG
+CpG-NP-CGG
D
d60/d53 anti-NP15 IgG
d67/d53 anti-NP1 IgG

Figure 2.6

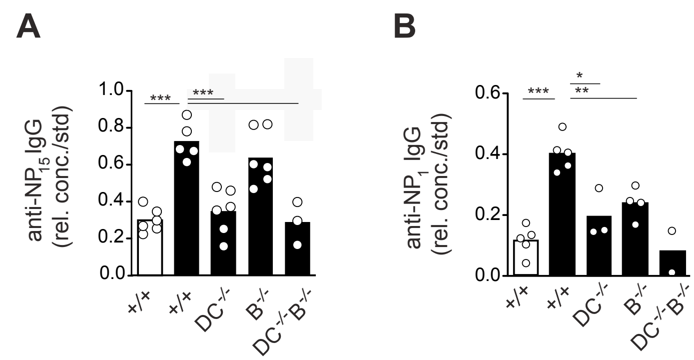
A
anti-NP15 IgG (rel. conc./std)
1.0
0.8
0.6
0.4
0.2
0.0
***
***
+/+
+/+
DC-/-
B-/-
DC-/-B-/-
B
anti-NP1 IgG (rel. conc./std)
0.6
0.4
0.2
0.0
***
*
**
+/+
+/+
DC-/-
B-/-
DC-/-B-/-

Figure 2.7

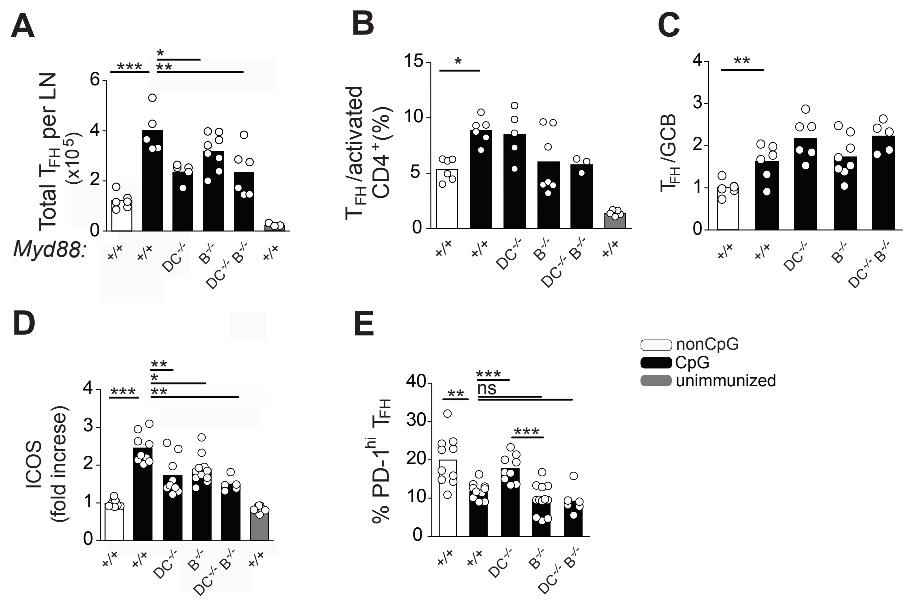
A
Total T_{FH} per LN (x10^5)
Myd88:
+/+
DC-/-
B-/-
DC-/- B-/-
B
T_{FH} /activated CD4+(%)
C
T_{FH} /GCB
D
ICOS (fold increse)
E
% PD-1hi T_{FH}
ns
nonCpG
CpG
unimmunized

Figure 2.8

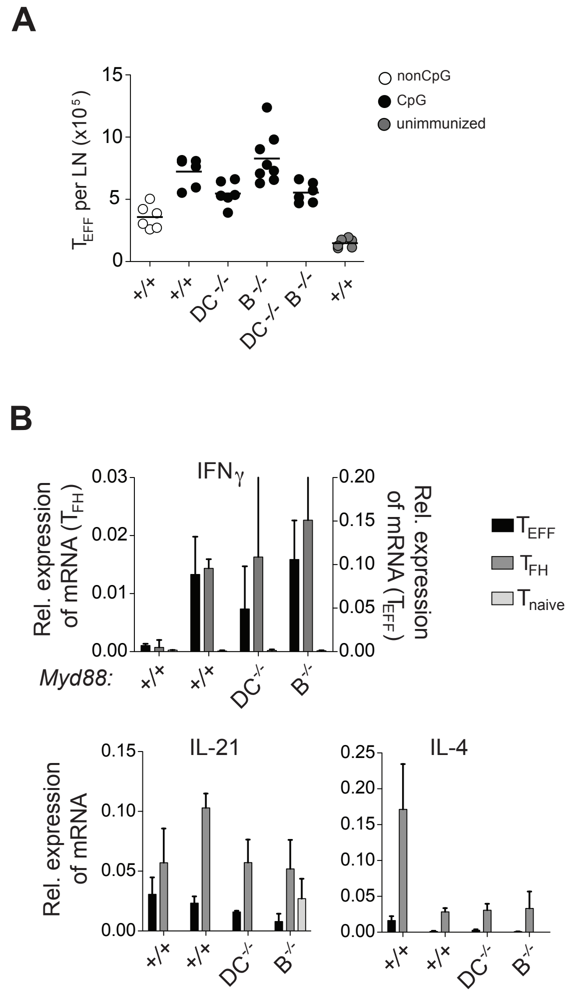
A
15
10
5
0
T EFF per LN (x10 5)
nonCpG
CpG
unimmunized
+/+
+/+
DC -/-
B -/-
DC -/- B -/-
+/+
B
IFNγ
0.03
0.02
0.01
0.00
Rel. expression of mRNA (T FH)
0.20
0.15
0.10
0.05
0.00
Rel. expression of mRNA (T EFF)
T EFF
T FH
T naive
Myd88:
+/+
+/+
DC -/-
B -/-
IL-21
0.15
0.10
0.05
0.00
Rel. expression of mRNA
IL-4
0.25
0.20
0.15
0.10
0.05
0.00

Figure 2.9

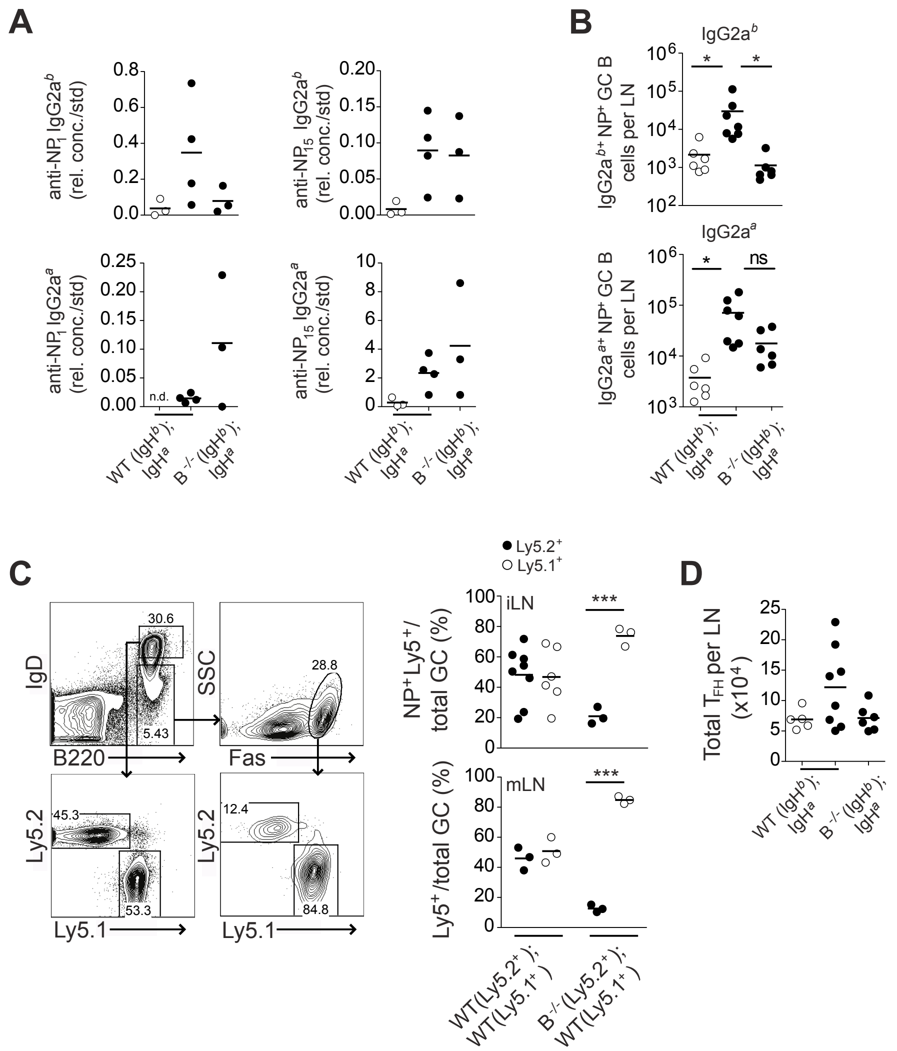
A
B
IgG2a^b
IgG2a^a
C
D
Ly5.2$^+$
Ly5.1$^+$
iLN
mLN
IgD
B220
SSC
Fas
Ly5.2
Ly5.1
NP$^+$Ly5$^+$/ total GC (%)
Ly5$^+$/total GC (%)
Total T_{FH} per LN ($\times 10^4$)
WT (IgH^b); IgH^a
B$^{-/-}$ (IgH^b); IgH^a
WT(Ly5.2$^+$); WT(Ly5.1$^+$)
B$^{-/-}$(Ly5.2$^+$); WT(Ly5.1$^+$)

Figure 2.10

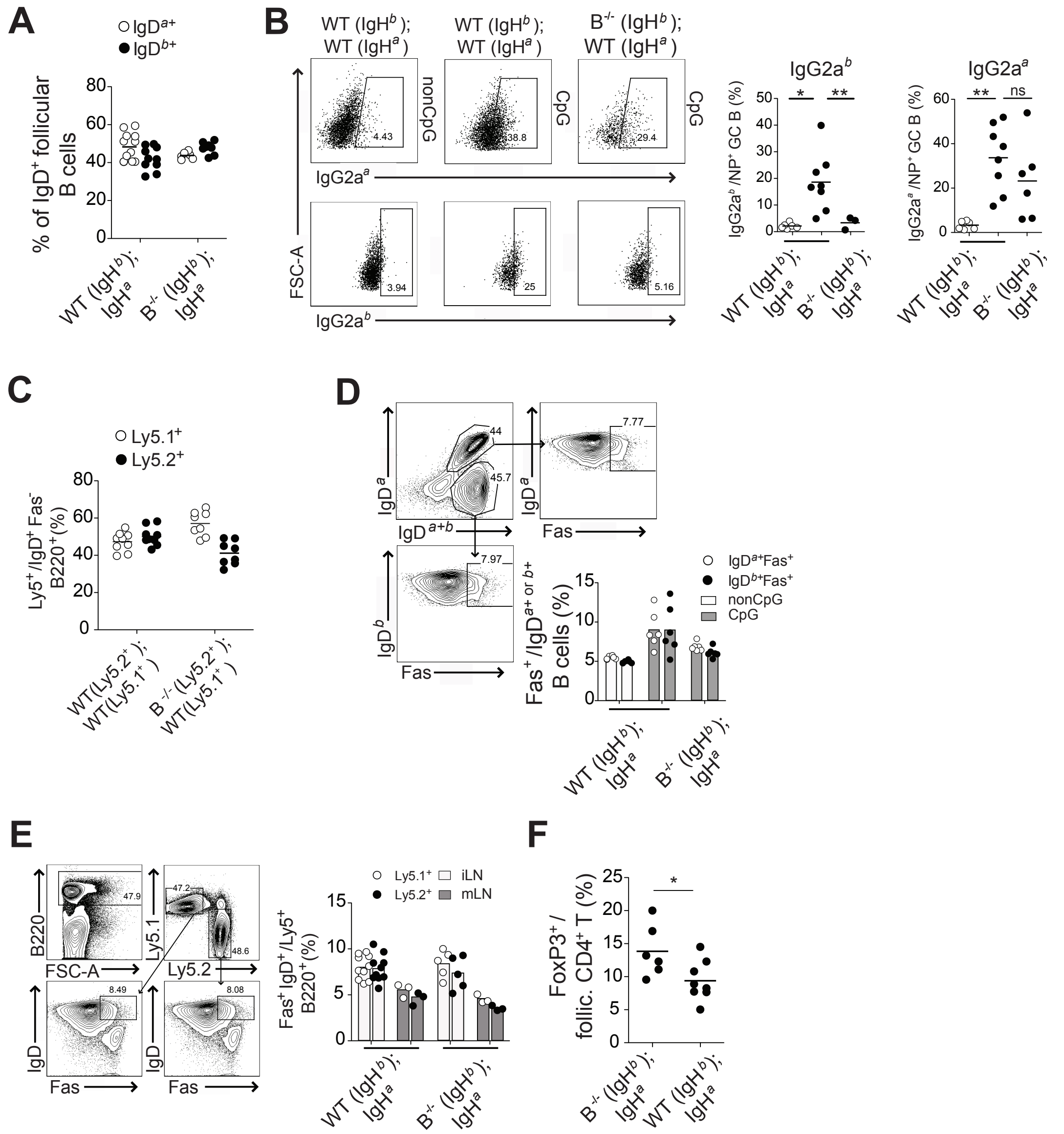

Figure 2.11

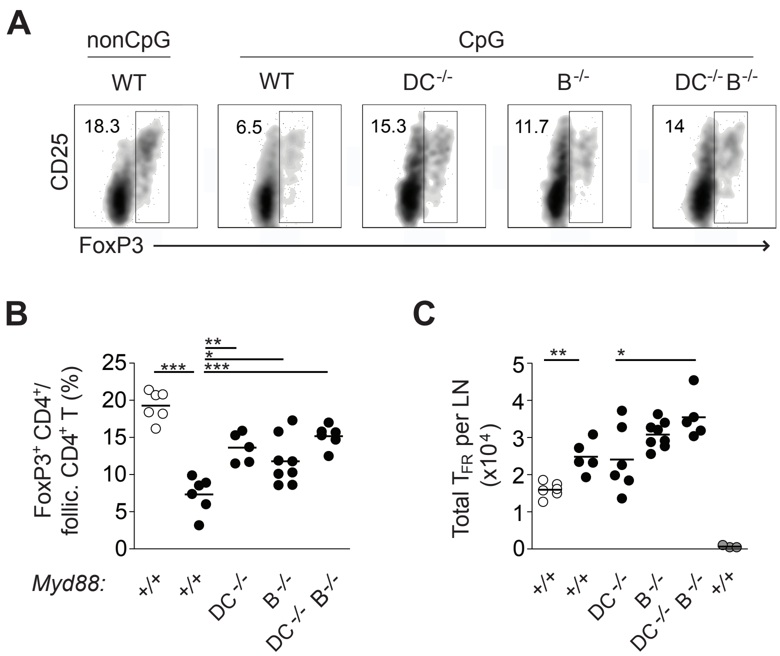
A
nonCpG
CpG
WT
WT
DC-/-
B-/-
DC-/- B-/-
18.3
6.5
15.3
11.7
14
CD25
FoxP3
B
FoxP3+ CD4+/ follic. CD4+ T (%)
Myd88:
+/+
+/+
DC-/-
B-/-
DC-/- B-/-
C
Total TFR per LN (x10^4)
+/+
+/+
DC-/-
B-/-
DC-/- B-/-
+/+

Figure 2.12

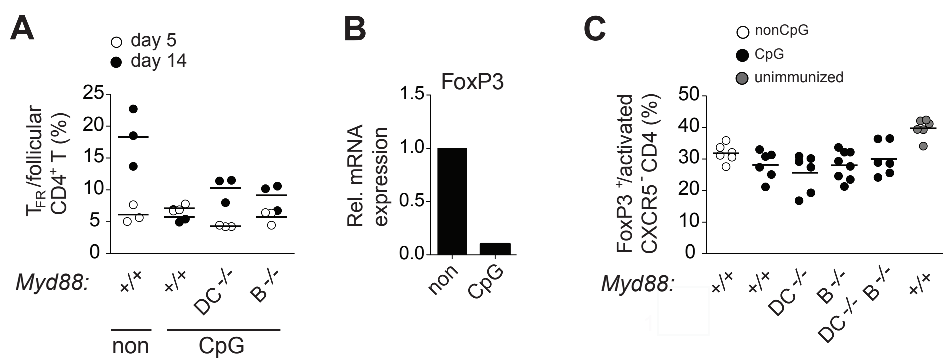
A
day 5
day 14
T_FR/follicular CD4+ T (%)
25
20
15
10
5
0
Myd88:
+/+
+/+
DC -/-
B -/-
non
CpG
B
FoxP3
Rel. mRNA expression
1.5
1.0
0.5
0.0
non
CpG
C
nonCpG
CpG
unimmunized
FoxP3+/activated CXCR5- CD4 (%)
50
40
30
20
10
0
Myd88:
+/+
+/+
DC -/-
B -/-
DC -/- B -/-
+/+

Figure 2.13

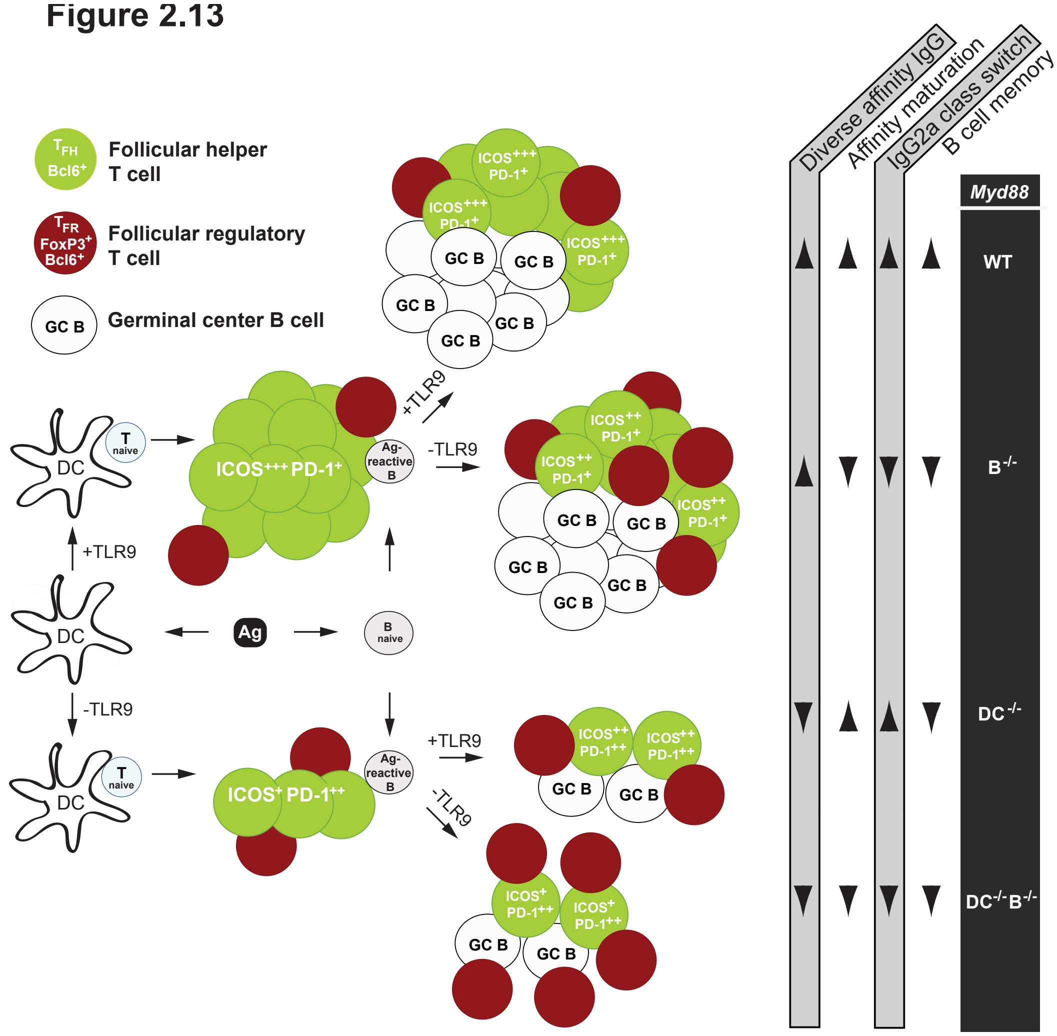
Follicular helper T cell
Follicular regulatory T cell
GC B
Germinal center B cell
DC
+TLR9
-TLR9
Ag
ICOS+++ PD-1+
ICOS+ PD-1++
Ag-reactive B
Diverse affinity IgG
Affinity maturation
IgG2a class switch
B cell memory
Myd88
WT
B-/-
DC-/-
DC-/-B-/-

Chapter Three

Requirement for ICOS/ICOSL costimulation in TLR-enhanced GC reactions and affinity maturation

B cell-extrinsic and -intrinsic roles for ICOSL during affinity maturation

ABSTRACT

TLR signaling informs adaptive responses such as germinal center (GC) responses that critically require ICOS/ICOSL costimulation for reciprocal maintenance between cognate follicular helper CD4$^+$T cells and GC B cells. How TLRs enhance GC output such as affinity maturation is not well understood. To investigate the regulation of ICOS/ICOSL costimulation by TLR signaling during a GC response, I linked a T-dependent antigen to oligonucleotides containing (CpG) or lacking (nonCpG) a TLR9 ligand. TLR9 signaling boosted the GC response by expanding T_{FH} as well as GC B cell numbers and by increasing production of diverse and high affinity IgG. Experiments using *Icosl*$^{-/-}$ mice as well as a series of mixed bone marrow chimeras demonstrated that TLR9 required ICOSL expression on B cells to promote production of diverse affinity IgG and to expand the T_{FH} cell compartment in a B cell-extrinsic way. Surprisingly, TLR9 required ICOSL expression specifically on responding B cells to enhance affinity maturation, revealing that ICOSL plays a previously unknown B cell-intrinsic role in GC selection processes.

INTRODUCTION

Antibody quality and serological memory are refined in germinal centers (GCs), transient structures that form in B cell follicles in response to antigen and that are exceptionally well-suited for B cells to affinity mature their B cell receptors as they compete for survival and selection cues from a transcriptionally distinct subset of $CD4^{+}T$ helper cells that express $CXCR5^{+}$, follicular T helper cells (T_{FH})[32, 49]. The costimulatory receptor ICOS and its ligand ICOSL belong to the larger CD28/B7 family of costimulatory receptor-ligand pairs and their expression is critical for germinal center formation and persistence, most likely due to their ability to support T_{FH} cell development and maintenance[48, 97-99, 129].

T_{FH} and GC B cell development are codependent. Early reports described the presence of $CD4^{+}T_{H}$ cells in humans that expressed high levels of both CXCR5 and ICOS, localized to the light zone of germinal centers where selection occurs, and were superior to $CXCR5^{-}CD4^{+}T$ cells in their provision of B cell help[53-55]. Subsequently, it was observed that ICOS-deficient patients as well as *Icos*$^{-/-}$ mice had a reduction or absence of $CXCR5^{+}CD4^{+}T_{FH}$ cells[112, 129]. It is now apparent that T_{FH} cells and ultimately GCs develop through two key checkpoints: a first checkpoint in which antigen-presenting DCs induce clonal expansion of naive $CD4^{+}T$ cells, which then adopt either an effector T (T_{EFF}) or a T_{FH} cell fate, and a second checkpoint in which cognate GC B cells interact with T_{FH} cells to induce their full maturation or stabilization as T_{FH} cells. The first checkpoint requires ICOSL expression on DCs for T_{FH} cell development and GC formation[108, 130]. The second checkpoint depends on the homophilic interaction of Ly108, a member of the signal lymphocyte activation molecule (SLAM) family of cell adhesion molecules that signals through SLAM associated protein (SAP) and on ICOSL[73, 107, 108, 111, 122, 123, 131]. During the second phase, ICOSL on B cells stimulates production of IL-4 and IL-21 cytokines from T_{FH} cells[73, 131] which promote T_{FH} and GC B cell survival, affinity maturation, plasma cell formation and B cell memory[43, 69, 70].

ICOSL expression on B cells is dynamically regulated by multiple mechanisms. For example, BAFF-R and CD40 transcriptionally upregulate expression of ICOSL on B cells through noncanonical NF-κB signaling[132]. Conversely, another TNFR family member on B cells, TACI appears to negatively regulate ICOSL levels on B cells[133]. ICOSL expression on B cells is reduced upon interaction with T cells expressing ICOS by shedding from the cell surface, and TLR7 or TLR9 signaling in B cells can prevent this shedding[42, 134]. In several of these studies, changes in ICOSL levels on B cells correlated with the size of the GC reaction.

Several groups have shown that TLR signaling in B cells can impact the size and quality of a GC reaction[82, 83, 135], but how this might interface with ICOSL/ICOS costimulation is not known. To address this issue, I studied the GC antibody response to conjugates made by linking the T-dependent antigen NP-CGG to oligonucleotides that either contained (CpG) or lacked (nonCpG) a TLR9 ligand. Interestingly, attachment of a TLR9 ligand to NP-CGG induced a stronger GC response that resulted in more anti-NP IgG and enhanced affinity maturation, compared to immunization with a control conjugate lacking a CpG motif. Strikingly, T_{FH} cells expressed 3-fold higher levels of

ICOS when the antigen contained a TLR9 ligand. The CpG enhancement of the GC response was not seen in *Icosl*$^{-/-}$ mice or in mixed bone marrow chimeric mice in which B cells were selectively deficient in ICOSL expression, demonstrating that ICOS costimulation was required during the phase of the GC response when cognate B cells interact with T_{FH} cells. ICOSL expression on B cells appeared to contribute to the enhanced GC response by stabilizing T_{FH} cell function and also by a cell-intrinsic enhancement of the ability of ICOS-expressing GC B cells to be selected for higher affinity.

RESULTS

Attachment of a TLR9 ligand to a haptenated protein antigen enhances the germinal center response

To address how TLR signaling can enhance a T cell-dependent antibody response, I linked nitrophenol-haptenated chicken gamma globulin (NP-CGG) with a biotinylated oligonucleotide either containing (CpG) or lacking (nonCpG) a TLR9 ligand motif. In *Icosl*$^{+/+}$ (C57BL/6) mice, the IgG anti-NP response was enhanced 2-5-fold by conjugation of a TLR9 ligand to the antigen and this enhancement was greater when only high affinity IgG was assessed with an ELISA using NP_1-BSA on the plate than when diverse (high plus low) affinity IgG was measured using NP_{15}-BSA (**Fig. 3.1A**). This enhancement was lost when *Icosl*$^{-/-}$ mice were immunized, even though the response to the nonCpG conjugate was only decreased by 2-fold (**Fig. 3.1A**). The enhanced high affinity IgG response seen when a TLR9 ligand was conjugated to NP-CGG was accompanied by a several-fold increase in the number of PD-1$^+$CXCR5$^+$ T_{FH} cells per draining LN (Fig. 1B) and an increase in the fraction of GC phenotype B cells (**Fig. 3.1C**). The 2-fold increased number of GC B cells was absent in immunized *Icosl*$^{-/-}$ mice. Interestingly, the conjugation of a TLR9 ligand to NP-CGG increased the expression of ICOS on the T_{FH} by approximately 3-fold (**Fig. 3.1D**). Since the enhanced IgG response and GC B cell expansion were dependent on ICOSL, this increase in ICOS expression on T_{FH} is likely to be a contributor to the enhanced response. Interesting in this regard, ICOSL expression on GC B cells was unaffected by TLR9 stimulation (**Fig. 3.1E**).

ICOSL on DCs is sufficient for GC formation but not for antibody abundance or quality in mice lacking ICOSL selectively in B cells

The requirement of ICOSL for TLR9 to enhance the GC response to CpG-NP-CGG could originate during the early phase of GC development when costimulatory interactions between DCs and T cells activate CD4$^+$T helper cells, during which ICOS stimulation can enhance adoption of the T_{FH} cell fate by some of these cells[108, 110, 129, 131], or it could reflect a role for ICOSL later during the ongoing GC reaction when T_{FH} cell maintenance relies mainly on antigen presentation and costimulatory signals from cognate GC B cells[108, 111, 114, 136, 137]. To address this question, I generated mixed bone marrow chimeras in which the B cells were selectively defective in ICOSL. Lethally-irradiated Ly5.1$^+$ mice were reconstituted with a 4:1 mixture of bone marrows from μMT

(B cell-deficient) and *Icosl*$^{-/-}$ mice, respectively, or, as a control, with a 4:1 mixture of bone marrow from μMT and *Icosl*$^{+/+}$ (C57BL/6) mice. In the former, bone marrow chimeric mice, 80% of hematopoietic-derived cells other than B cells express ICOSL normally, whereas all donor-derived B cells are ICOSL-deficient. These mice were immunized as above with CpG-NP-CGG or with nonCpG-NP-CGG. At day 7, diverse affinity anti-NP IgG titers were significantly expanded following immunization of the *Icosl*$^{+/+}$; μMT chimeras with CpG-NP-CGG compared to those similar mice that received nonCpG-NP-CGG (**Fig. 3.2A**). Deletion of ICOSL on B cells significantly reduced the titers of anti-NP IgG to similar levels seen upon immunization with nonCpG-NP-CGG (Fig. 2A). Similarly, mice lacking ICOSL on donor B cells produced much less high affinity anti-NP IgG on day 14 (**Fig. 3.2B**). This correlated with a decrease in the number of T_{FH} cells in the lymph node (**Fig. 3.2C**). A complication of these experiments was that recipient B cells, which were wild type for the ICOSL gene, were not totally depleted by the procedure used (**Fig. 3.2D**). This may explain why the differences in diverse affinity anti-NP IgG were less different between the experimental groups on day 14 after immunization with CpG-NP-CGG (data not shown), as by this time the wild type recipient B cells may have made a greater contribution to the overall IgG response. Despite this complication, it was clear from these experiments that ICOSL expression on DC and cells other than B cells was not sufficient to enable a TLR9 ligand to enhance the IgG response to NP-CGG, and therefore ICOSL expression on B cells was an important contributor to the response.

B cells lacking ICOSL fail to be selected for high affinity antibody production normally in response to an antigen containing a TLR9 ligand

As ICOSL on B cells was found to be important for the magnitude of the anti-NP IgG response, and for generation of high affinity anti-NP IgG, I next created mice in which wild type and ICOSL-deficient B cells were equally prevalent and were IgH allotype marked to make it possible to determine the ability of each type of B cell to contribute to the anti-NP IgG response. For this purpose, I generated mixed bone marrow chimeras by reconstituting lethally-irradiated Ly5.1^{+} mice with equal portions of bone marrow from *Icosl*$^{-/-}$(IgH^{b}) and from *Icosl*$^{+/+}$(IgH^{a}) mice, or as a control equal portions of bone marrow from *Icosl*$^{+/+}$(IgH^{b}) and *Icosl*$^{+/+}$(IgH^{a}) mice. Immunization of these two types of chimeric mice with CpG-NP-CGG induced robust production of diverse affinity and high affinity anti-NP IgG2a^{a} from the wild type B cells in both types of mice, measured 14 days after immunization. Diverse affinity anti-NP IgG2a^{b} antibody was also produced at similar levels in both types of chimeric mice. In contrast, the *Icosl*$^{-/-}$ B cells produced several-fold less high affinity anti-NP IgG2a^{b} than their wild type counterparts on day 14 (**Fig. 3.3A**). Correspondingly, the fraction of anti-NP IgG2a^{b} antibody that had attained a high affinity, as reflected by anti-NP$_{1}$/NP$_{15}$ ratio, was approximately 5-fold reduced in the mice where the IgH^{b} B cells were ICOSL-deficient compared to the control chimeric mice, whereas there was only a small downward trend in the corresponding ratio for IgG2a^{a} (**Fig. 3.3B**). These results demonstrate that the requirement for B cell expression of ICOSL for affinity maturation was mediated via a cell intrinsic effect, and *Icosl*$^{+/+}$ B cells in the same mice had only a slight decrease in their ability to undergo affinity maturation. Interestingly, the presence of 50% *Icosl*$^{+/+}$B cells in the *Icosl*$^{-/-}$(IgH^{b}); *Icosl*$^{+/+}$(IgH^{a}) chimeric animals restored the magnitude of diverse affinity anti-NP IgG2a^{b} production by *Icosl*$^{-/-}$ B cells (**Fig. 3.3A**). Taken together with the results described above, this result indicates that the overall magnitude of the anti-NP IgG2a component of the response requires ICOSL expression on some B cells, but not necessarily on the responding B cells themselves. Thus, ICOSL expression on B cells contributed to the response to a TLR9 ligand-containing haptenated antigen in at least two ways, one mechanism that only operated to enhance the response in ICOSL expressing B cells and that was important for affinity maturation and another mechanism that operated in a more general fashion to enhance the magnitude of the antibody response, perhaps by enhancing the numbers and/or function of T_{FH} cells.

In these experiments, it appeared that ICOSL-expressing B cells had some advantage in expansion and/or survival in the GC. The chimeric mice that had 50% ICOSL$^{-/-}$ B cells had a lower percentage of GC B cells that had switched to IgG2b than did the control chimeric mice. This analysis includes both the ICOS-deficient and the ICOS-expressing B cells. In contrast, no decrease was seen in the percentage of GC B cells that had switched to IgG2a^{a}, which only detects the wild type B cells in both types of chimeric mice (**Fig. 3.3E**), suggesting that the decreased percentage of IgG2b GC B cells represented primarily the ICOS-deficient B cells. In these experiments, I did not directly follow the IgG2a^{b}-expressing B cells due to technical challenges; however, both the reduced frequency of IgG2b^{+}GC B as well as reduced titers of high affinity anti-NP IgG2a^{b} were likely conservative measurements as *Icosl*$^{-/-}$ hematopoietic cells demonstrated a slight advantage after reconstitution (**Fig. 3.4**).

There was a substantial decrease in diverse affinity anti-NP IgG production in the CpG/NP-CGG immunized bone marrow chimeric mice that had a high percentage (80-90%) of ICOSL-deficient B cells in the context of 80% ICOSL-expressing DCs and other hematopoietic cells (**Fig. 3.2A**), whereas there was no detectable decrease in these antibodies in immunized mice containing approximately 50% *Icosl*$^{-/-}$ hematopoietic cells and 50% *Icosl*$^{+/+}$ hematopoietic cells (**Fig. 3.3A**). Therefore, I examined the number of T_{FH} and their expression of ICOS in the latter mice. Interestingly, CpG-NP-CGG immunized mice containing 50% *Icosl*$^{-/-}$ hematopoietic cells had approximately 2-fold fewer T_{FH} cells than did the immunized control chimeric mice (**Fig. 3.5A**), whereas there was no difference in T_{FH} cell numbers following immunization with nonCpG-NP-CGG. Thus, in the context of TLR9 stimulation, ICOSL expression was limiting for T_{FH} cell expansion or maintenance. Interestingly, TLR9 stimulation increased ICOS levels on T_{FH} cells similarly in the immunized chimeric mice containing 50% *Icosl*$^{-/-}$ bone marrow-derived cells and in the control chimeric mice (**Fig. 3.5B**), indicating that TLR9 stimulation of DCs can lead to an upregulation of ICOS expression on T_{FH} cells in a manner that is less dependent on ICOSL expression than is T_{FH} cell number. In addition, TLR9 signaling selectively triggered T_{FH} cell expansion, as there was no difference in the total number of T_{EFF} cells between these groups of mice (data not shown).

DISCUSSION

Recently, others have found that TLR ligands can enhance the magnitude of the germinal center antibody response and can promote increased affinity matur-ation[82, 83, 135]. Mice immunized with the T cell-dependent antigen NP-CGG conjugated to an oligonucleotide containing a TLR9 ligand made more anti-NP IgG by day 14 and especially made more high affinity anti-NP IgG, compared to mice immunized with a NP-CGG conjugate containing a control oligonucleotide. This response also exhibited increased numbers of T_{FH} cells, indicating that TLR9 signaling enhanced T_{FH} cell differentiation, proliferation, and/or survival. Interestingly, T_{FH} cell ICOS levels were upregulated about 3-fold more when the immunogen included a TLR9 ligand. As the ICOS/ICOSL costimulatory pathway is critical for the GC response, I conducted a series of experiments designed to characterize the role of this costimulatory pathway in the TLR9-enhanced germinal center response. These experiments demonstrate that ICOSL expression on B cells was important to the enhanced GC response seen upon immunization with NP-CGG conjugated to a CpG-containing oligonucleotide and contributed to the response both by boosting the GC in a general way and by strengthening affinity maturation selectively of B cells expressing ICOSL.

When *Icosl*$^{-/-}$ mice were immunized with the NP-CGG conjugates, the anti-NP IgG response to the conjugate containing a nonCpG oligonucleotide was only slightly decreased, whereas the response to the CpG-containing conjugate was much weaker and was no longer greater than the response to the nonCpG conjugate. Thus, the response to CpG-NP-CGG conjugates was highly dependent on ICOS costimulation. This is consistent with the hypothesis that the upregulation of ICOS expression on T_{FH} cells was important for promoting the GC response to this antigen. High ICOS levels on T_{FH} may contribute to their increased survival due to enhanced costimulation by ICOSL-expressing GC B cells that were also expanded in response to CpG-NP-CGG. Important in this regard, ICOS signaling through PI3-kinase and c-Maf has been shown to increase production of the hallmark T_{FH} cyokine IL-21, which is important for both T_{FH} and GC B cell persistence[43, 69, 70, 73, 131, 138].

A variety of studies have indicated that full maturation and maintenance of T_{FH} cells in the GC response involves at least two checkpoints: early priming of T_{FH} cells by antigen presenting DCs during the first several days post immunization, and a later phase requiring antigen-presentation by cognate GC B cells, which are reciprocally maintained by T_{FH} cell help [107, 108, 111, 130]. ICOSL is constitutively expressed by DCs and B cells, and its expression can be further modulated by TLR ligands[134, 139, 140]. Thus, to investigate the relative role of ICOSL during these two checkpoints, I generated mixed bone marrow chimeras by reconstituting lethally-irradiated Ly5.1^{+}BoyJ mice with a 4:1 mixture of bone marrows from μMT and *Icosl*$^{-/-}$ mice, respectively, or a 4:1 mixture of bone marrows from μMT and *Icosl*$^{+/+}$ (C57BL/6) mice as a control. In the first scenario, all donor B cells lacked ICOSL while 80% of DCs expressed it, and in the second scenario, all B cells and DCs were *Icosl*$^{+/+}$. Immunization of *Icosl*$^{+/+}$; μMT chimeric mice with CpG-NP-CGG boosted total anti-NP IgG , expanded the numbers of T_{FH} and GC B cells, and enhanced affinity maturation, consistent with data from *Icosl*$^{+/+}$ animals. When

ICOSL was selectively deleted on B cells in *Icosl*$^{-/-}$; μMT chimeric mice, increased numbers of both T_{FH} and GC B cells were evident; however, fewer T_{FH} cells were maintained, consistent with another report[108]. Interestingly, ICOSL deficiency of B cells blocked the increase in both total anti-NP IgG as well as affinity maturation, indicating that ICOSL expression on B cells was required for TLR9 enhancement of these elements of the response.

To dissect in more detail the role of ICOSL on B cells for affinity maturation, I generated mixed bone marrow chimeras containing equal numbers of *Icosl*$^{+/+}$ and *Icosl*$^{-/-}$ B cells with distinct IgH allotypes (IgH^{a} and IgH^{b}, respectively), allowing us to determine the extent to which B cell participation in the GC reaction and in affinity maturation required expression of ICOSL on the responding B cell. Immunization with CpG-NP-CGG resulted in roughly equivalent diverse affinity anti-NP IgG2a^{b} responses in mice containing 50% ICOSL-deficient IgH^{b} B cells combined with 50% *Icosl*$^{+/+}$ IgH^{a} B cells and in chimeric mice in which both IgH allotype B cells were *Icosl*$^{+/+}$. Strikingly, *Icosl*$^{-/-}$ B cells produced much less high affinity anti-NP IgG2a^{b} than did *Icosl*$^{+/+}$GC B cells in the immunized control chimeras. Thus, there was a selective defect in affinity maturation of ICOSL-deficient B cells, even though these B cells were making a normal amount of lower affinity IgG. While the exact mechanism of this cell-intrinsic defect in affinity maturation of ICOSL-deficient B cells was not determined, it appeared that ICOSL deficiency on B cells decreased their fitness in the germinal center, even in the context of 50% ICOSL-expressing B cells. This was suggested by the drop in the number of IgG2b^{+}(IgH$^{a+\text{and }b+}$) GC B cell in the mice containing both *Icosl*$^{+/+}$ and *Icosl*$^{-/-}$ B cells compared to the control mice with all *Icosl*$^{+/+}$ B cells (Fig. 3E). This was likely due to a selective decrease in ICOSL-deficient B cells, as *Icosl*$^{+/+}$ (IgG2a^{a+}) GC B cells developed equivalently between the two sets of chimeras. The number of antigen binding (NIP^{+}) B cells in the GC of these mice also trended downward, which would be consistent with poorer fitness of *Icosl*$^{-/-}$ GC B cells, although it did not reach statistical significance (**Fig. 2.3D**). These results extend previous findings showing that ablation of ICOS signaling using an ICOS blocking antibody during GC onset at days 5, 6 and 7 post immunization with NP-CGG in alum reduced high affinity antibody titers that was most evident in the memory B cell compartment[141]; however, the reduction seen by those investigators could simply reflect reduced GC output from smaller GC reactions as a consequence of ICOS blockade. Importantly, our data reveal that TLR9-enhanced affinity maturation following immunization with CpG-NP-CGG required ICOSL directly on the responding B cell to enhance GC selection in a way that was not transferrable to neighboring B cells, and primarily affected high affinity IgG titers.

Thus, our findings demonstrate that ICOSL expression on B cells acts beyond the extrinsic maintenance of T_{FH} cells that was previously reported[108, 112, 129, 131] and in addition, functions intrinsically to promote GC B cell selection and affinity maturation. The ability of GC B cells to capture and present antigen is thought to drive competition for selection and survival cues from T_{FH} cells[48, 60, 121], and conversely, prolonged TCR stimulation through antigen presentation preferentially stimulates/maintains T_{FH} cells[111, 115]. This hypothesis predicts that GC B cells with the highest affinity BCRs will capture, and thus present, more antigen than GC B cells with BCRs of weaker affinity, allowing them to monopolize help from T_{FH} cells and undergo positive selection. During collaboration with T_{FH} cells, GC B cells also provide costimulatory signals through ICOSL that stimulate production of cytokines such as IL-21[43, 131]. IL-21 acts on B cells to promote proliferation, memory B cell formation, and affinity maturation[69, 70]. Therefore, in our system, the ability of *Icosl*$^{+/+}$ B cells to stimulate ICOS on T_{FH} cells likely permitted those B cells to receive more or better help from T_{FH} cells, resulting in better affinity maturation. In addition, ICOSL/ICOS costimulation in the GC improved the availability of T cell help for *Icosl*$^{-/-}$GC B cells in the *Icosl*$^{-/-}$(IgH^{b});*Icosl*$^{+/+}$(IgH^{a}) mice, since lower affinity anti-NP IgG2a^{b} titers were improved to a level close to that seen in the control chimeric mice.

As mentioned above, expression of ICOSL on B cells was necessary for a robust germinal center response, including maintenance of T_{FH} cell numbers. This effect was also evident to some extent in *Icosl*$^{-/-}$(IgH^{b});*Icosl*$^{+/+}$(IgH^{a}) mice, which had reduced numbers of T_{FH} cells following immunization with CpG-NP-CGG compared to the control chimeric mice. These results agree with recent findings demonstrating that the amount of ICOSL expressed by B cells can adjust the size of the T_{FH} cell compartment [132, 133].

As mentioned above, the conjugation of a TLR9 ligand to NP-CGG increased the magnitude and the degree of affinity maturation of the anti-NP IgG response in a manner that was dependent on ICOSL. Interestingly, recent studies have demonstrated that enhanced ICOS signaling through increased ICOSL expression on B cells can augment the GC reaction [132, 142], raising the possibility that part of the mechanism by which TLR9 signaling in GC B cells enhanced the GC response may have been through enhancement of ICOSL expression. However, at the time points examined, ICOSL expression levels on GC B cells were identical in wild type mice immunized with CpG-NP-CGG or with nonCpG-NP-CGG. This was surprising to us because ICOS on T_{FH} cells was increased about 3-fold, and in vitro experiments have demonstrated that association of ICOS with ICOSL can cause shedding of ICOSL from the surface of B cells[134]. In vivo data suggest that this is an important mechanism of regulating ICOSL expression. For example, ICOS-deficient patients diagnosed with common variable immune deficiency (CVID) show increased expression of ICOSL on B cells[143] and transgenic overexpression of ICOS on CD4^{+}T cells in mice was found to downmodulate ICOSL expression on APCs through a post-transcriptional mechanism[144]. Interestingly, in vitro experiments demonstrated that ICOS-induced shedding could be prevented by TLR9 signaling in B cells[134]. Thus, it is possible that part of the mechanism by which TLR9 signaling enhanced the response of GC B cells was by stabilizing their expression of ICOSL, for example, by reducing shedding. This hypothesis would explain why ICOSL levels were maintained on GC B cells despite 3-fold higher ICOS levels on T_{FH} cells. However, I did not see direct evidence for regulation ICOSL expression on GC B cells, so this hypothesis remains speculative at this time.

The ability of innate immunity to sculpt adaptive responses and program immunological memory is an area of intense focus for its implications in rational vaccine design as well as human diseases[28, 145]. CVID which is an umbrella diagnosis that describes a broad spectrum of defects in B cell function that manifest as low serum titers of switched immunoglobulin, reduced frequencies of CD27^{+}memory B cells, and poor response to certain types of vaccination among a host of other phenotypes[146]. The data presented in this study have particular relevance to understanding CVID as homozygous deletion of ICOS was the first genetic defect identified in CVID patients[143]. Although mutations in the gene encoding ICOSL, *ICOSLG,* have not yet been identified, other mutations have come to light including members of the TNF receptor superfamily, *TNFRSF13B* and *TNFRSF13C,* that encode TACI and BAFF-R, respectively[147, 148] and have demonstrated roles in B cell survival as well as the regulation of ICOSL expression[132, 142, 144]. Finally, the use of nucleic acids as vaccine adjuvants has received considerable attention and the experiments in this study shed light on the mechanism of nucleic acid adjuvanticity, revealing potent expansion of a T_{FH} cell compartment with robust ICOS expression that improves GC output of high affinity antibody, a central aim of vaccine development.

MATERIALS AND METHODS

Mice

WT (C57BL/6J), *Icosl*$^{-/-}$ (B6.129P2-*Icoslg*^{tm1Mak}/J), IgH^a (B6.Cg-*Igh*^{a} *Thy1*^{a} *Gpi1*^{a}/*J*), and Ly5.1$^+$WT (B6.SJL-*Ptprc*^{a} *Pepc*^{b}/BoyJ) mice were purchased from the Jackson Laboratory and housed in specific pathogen free facilities at the University of California San Francisco. Mouse procedures were performed according to the National Institutes of Health guidelines and with approval from the UCSF institutional animal care and use committee (IACUC). Mice were immunized by subcutaneous flank injection with CpG- or nonCpG-containing oligos linked to NP-CGG in 50μl of PBS, and 7 or 14 days later, blood was collected by submandibular bleeding or cardiac puncture for quantification of relative anti-NP IgG concentrations by ELISA and the LNs harvested for analysis of lymphocyte populations by flow cytometry.

Generation of CpG- and nonCpG-NP-CGG oligonucleotide conjugates

Lyophilized 4-Hydroxy-3-nitrophenyl-haptenated chicken gamma globulin (10 mg, NP_{15-17}, Biomol was reconstituted in 1mL of a 0.1M solution of sodium bicarbonate buffer (pH 8.3) and was conjugated with biotin by adding 112 μl of a solution containing 1.12 mg of biotin-sulfosuccinimidyl ester (Invitrogen, B6352) in dimethylformamide, followed by constant stirring at room temperature in the dark. After three hours, biotin-NP-CGG was washed three times in Dulbecco’s PBS by 30-fold dilution and centrifugation in an Amicon Ultra Centrifugal Filter (Millipore) with a 50kD molecular weight cut-off according to the manufacturer’s guidelines. Biotinylated oligonucleotides with a phosphorothioate backbone (Integrative DNA Technologies) containing CpG (CpG1826, TCCATGACGTTCCTGACGTT) or lacking CpG-motifs (nonCpG1982, TCCAGGACTTCTCTCAGGTT) were combined with biotin-NP-CGG in PBS (pH 7.4) at a molar ratio of 2.6 to 1, respectively, and linked by the addition of 4 moles of streptavidin (Invitrogen, 434302) for each mole of biotin-NP-CGG in an equal volume of PBS. Conjugation was carried out for 3hrs on a rocker at 4°C, followed by four washes as described for biotin-NP-CGG, and the final concentration adjusted to 0.5-0.66mg of biotin-NP-CGG/ml for subcutaneous injection of 50μl per flank. The total amount of CpG or nonCpG-containing oligonucleotide was estimated at 25-30μg/injection.

Construction of mixed bone marrow chimeric mice

To generate *Icosl*$^{-/-}$;μMT and *Icosl*$^{+/+}$;μMT mixed bone marrow chimeric mice, lethally-irradiated Ly5.1^{+}WT (B6.SJL-*Ptprc*^{a} *Pepc*^{b}/BoyJ) mice were reconstituted with a 4:1 mixture of bone marrows from either μMT and *Icosl*$^{-/-}$ mice or μMT and *Icosl*$^{+/+}$ mice as a control. Thus, in the *Icosl*$^{-/-}$;μMT chimeric mice, all B cells lacked ICOSL and 80% of other types of hematopoietic cells including DCs expressed it, whereas in *Icosl*$^{+/+}$;μMT mice, all B cells and DCs were *Icosl*$^{+/+}$. For the generation of *Icosl*$^{-/-}$(IgH^{b}); *Icosl*$^{+/+}$(IgH^{a}) and *Icosl*$^{+/+}$(IgH^{b}); *Icosl*$^{+/+}$(IgH^{a}) mixed bone marrow chimeric mice, lethally-irradiated Ly5.1^{+}WT (B6.SJL-*Ptprc*^{a} *Pepc*^{b}/BoyJ) mice were reconstituted with equal portions of bone marrow from either *Icosl*$^{-/-}$(IgH^{b}) and *Icosl*$^{+/+}$(IgH^{a}) mice or from *Icosl*$^{+/+}$(IgH^{b}) and *Icosl*$^{+/+}$(IgH^{a}) mice as a WT control. All chimeric mice were reconstituted for 10 weeks before immunization with nonCpG- or CpG-NP-CGG conjugates.

Analysis of lymphocyte populations by flow cytometry

Draining inguinal lymph nodes from immunized mice were harvested and passaged through a 40μm cell strainer (Fisher Scientific) to separate cells for labeling in flow cytometry buffer (Hank's Balanced Salt Solution (Cellgro) supplemented with 2% heat-inactivated FBS (GIBCO), 1mM EDTA, and 0.02% NaN_3). Antibodies with specificities to the following antigens were used to distinguish lymphocyte populations: CXCR5-biotin, IgG2a^{a}-biotin, IgG2a^{b}-biotin, CD45.1-biotin, CD4-PECy7, PD-1-PE, IgD-FITC, CD44-FITC, CD44-APC, B220-PacBlu, B220-Alexa647, CD25-APC (BD Biosciences), IgD-PerCPCy-5.5, ICOS-PerCPCy-5.5, ICOS-PECy7, B220-APC-Cy7, CD62L-APC-Cy7, B7h/ICOSL-PE (clone HK5.3), CD45.2-Pacific Blue, CD45.2-Alexa700 (Biolegend) IgD-APC, and GL7-APC (eBioscience). Biotinylated antibodies were labeled with streptavidin-Qdot605 (Invitrogen) –PE (Jackson). To reveal antigen specific NP-binding B cell populations, NP (4-Hydroxy-3-nitrophenyl)- or NIP (4-Hydroxy-3-iodo-5-nitrophenyl)-labeled (Biosearch Technologies) R-phycoerythrin (PE; P801, Invitrogen) or allophycocyanin (A803, Invitrogen) were prepared as previously described[128]. All labeling procedures were performed on ice except CXCR5 for identification of T_{FH} cells which was performed at room temperature for 30 minutes, followed by secondary coating with streptavidin during a 20 minute incubation on ice. Flow cytometry data were generated on an LSRII (Becton Dickinson) and analyzed using FlowJo (TreeStar) software, version 9.5.

Enzyme-linked immunosorbent assay (ELISA)

NP_{15}-BSA and NP_{1}-BSA in PBS (pH7.4) were used to coat 96-half-well high binding polystyrene plates (Costar 3690) overnight at 4°C to capture diverse and high affinity anti-NP antibodies, respectively. Antigen-coated plates were blocked with 2% FBS in PBS for 1hr at room temperature, incubated with two-fold serial dilutions of serum (1/6400 starting concentration) over night at 4°C and washed four times in PBS (pH 7.4) containing 0.02% Tween-20 detergent. Bound anti-NP IgG was detected with anti-IgG antibodies conjugated to horseradish peroxidase (Southern Biotech) at a concentration of 1/6000 for 1 hour at room temperature. For quantification of allotype-specific titers, biotin-anti-IgG1^{a}, starting concentration, 1/100; biotin-anti-IgG1^{b}, 1/200; biotin-anti-IgG2a^{a}, 1/100; biotin anti-IgG2a^{b}, 1/200 antibodies were used to label serum-bound plates before washing as above and application of horseradish peroxidase-linked streptavidin (1/5000, Southern Biotech) for one additional hour at room temperature. Serum-bound and Ig-labeled plates were washed four more times and the relative amounts of anti-NP IgG visualized by colorimetric change following addition of the HRP substrate 3,3',5,5'-tetramethylbenzidine (TMB) (Vector Labs). TMB development was quenched by the addition of 25µl 2N sulfuric acid and the optical densities at 450 and 570 were measured on a VERSAmax microplate reader (Molecular Devices). The difference in optical densities (O.D.450-570) was then plotted to compare slopes and calculate relative titers.

Statistical analyses

One-way analyses of variance (ANOVA), Newman-Keuls tests for comparison of multiple groups, and Student's *t*-tests were performed with a 95% confidence interval using Graphpad's Prism software, version 5.0b.

Figure 3.1 Immunization with antigen linked to CpG-containing oligonucleotides programs a T_{FH} cell compartment with robust ICOS expression and augments germinal center antibody production. (**A-C**) C57BL/6 mice were immunized either in the footpad or flank with NP-CGG linked to either CpG- or nonCpG-containing oligonucleotides and T_{FH} and GC B cell populations analyzed by flow cytometry14 days later. (**A**) Anti-NP IgG response at day 14 post immunization, measured as total anti-NP IgG, using ELISA of binding of IgG to NP_{15}-BSA-coated plates (anti-NP_{15}, left) and high affinity anti-NP IgG, using ELISA of binding of IgG to NP1-BSA-coated plates (anti-NP_{1}, right). (**B**) The gating strategy for characterization of $CD4^{+}CD44^{+}CD62L^{-}PD\text{-}1^{+}CXCR5^{+}$ T_{FH} cell populations is shown (left) and compiled data from groups of mice enumerate the total number of T_{FH} cell in draining lymph nodes (right). (**C**) Flow cytometry gating strategy for characterization of $IgD^{-}B220^{+}Fas^{+}$ GC B cells from the same mice depicted in panel *A* (left), and enumeration of GC B cells from individual mice immunized as in panel *A* (right). (**D**) Expression profiles of ICOS on T_{FH} cells as defined in panel *A* are shown along with the median fluorescent intensity of ICOS expression for individual mice immunized with the two types of antigen. Open circles, $CD62L^{+}CD44^{-}CD4^{+}$ naive T cells; grey circles, $CD4^{+}CD44^{+}CD62L^{-}PD\text{-}1^{-}CXCR5^{-}$ T_{EFF} cells; filled circles, T_{FH} cells gated as in panel ***A***. (**E**) Flow cytometry histograms of ICOSL expression on naive B cells (grey, $B220^{+}IgD^{+}Fas^{-}$) and GC B cells gated as in panel ***C*** (left), and compiled data showing ICOSL mean fluorescence intensities of GC B cells from C57BL/6 mice immunized with nonCpG- and CpG-NP-CGG (right). (**A-D**) Unpaired Student's *t* test *$p<0.05$, **$p<0.001$, ***$p<0.0001$.*

Figure 3.2 Requirement for ICOSL expression on B cells for the germinal center response to an antigen linked to a TLR9 ligand. (**A**) Total diverse affinity anti-NP (anti-NP_{15}) IgG levels in serum 7 days after immunization of mixed bone marrow chimeric mice in which the B cells are selectively deficient in ICOSL ($Icosl^{-/-}$;μMT) or control bone marrow chimeric mice ($Icosl^{+/+}$;μMT) or of mice deficient in ICOSL in all bone marrow-derived cells ($Icosl^{-/-}$>BoyJ) or in control bone marrow chimeric mice ($Icosl^{+/+}$>BoyJ). Mice were immunized with NP-CGG conjugated to either nonCpG oligonucleotide (open circles) or to CpG oligonucleotide (closed circles). (**B**) High affinity (anti-NP_1) anti-NP IgG titers from mice 14 days after subcutaneous immunization as in ***A***. (**C**) Total number of T_{FH} cells from chimeric mice immunized as in *A* and enumerated as in Fig 2.1B. (**D**) presence of recipient-derived CD45.1$^+$ B cells in mixed bone marrow chimeras. Percent of antigen-specific naive B cells (B220$^+$IgD$^+$Fas$^+$) that were CD45.1$^+$ recipient cells 14 days after immunization as in ***A*** (left), and percent of antigen-specific GC B cells (NIP$^+$B220$^+$IgD$^+$Fas$^+$) that were CD45.1$^+$ recipient cells 14 days after immunization as in ***A*** (right). (**A**, **B**) A one-way analysis of variance (ANOVA) followed by Newman-Keuls *ad hoc* test for comparison of individual groups was employed to determine statistical significance. *$p<0.05$, **$p<0.001$, ***$p<0.0001$.*

Figure 3.3 Expression of ICOSL on B cells enhances GC selection and affinity maturation in a cell intrinsic manner. Lethally-irradiated WT Ly5.1$^+$BoyJ mice were reconstituted with equivalent portions of either ICOSL$^{-/-}$(IgH^b) and WT (IgH^a) bone marrows or with C57BL/6 (IgH^b) and WT (IgH^a) bone marrows as a control. (**A**) Diverse affinity and high affinity anti-NP IgG2a^b (top) and IgG2a^a (bottom) titers at day 14 post immunization with nonCpG-NP-CGG (open circles) or with CpG-NP-CGG (closed circles). (**B**) Degree of affinity maturation of allotype-marked IgG2a antibody as assessed by the fraction of anti-NP IgG that was high affinity (anti-NP_1/NP_{15} ratio) of mice immunized as in panel ***A***, IgG2a^b (top) and IgG2a^a (bottom). (**C**) Degree of affinity maturation of all anti-NP IgG antibody from immunized bone marrow chimeric mice at day 14 post immunization. (**D**) Total number of antigen-binding (NIP$^+$) GC B cells per draining LN, enumerated as in Fig. 2.1 except also gated for binding to the hapten NIP conjugated to APC. (**E**) Frequencies of IgG2a^a or IgG2b (IgH$^{a+\text{and }b+}$) isotype-switched GC B cells, gated as shown (left) from mixed bone marrow chimeric mice immunized as in panel *A*. Summary of frequencies of IgG2a^{a+} and IgG2b^{a+b+}GC B cells as a percentage of B220$^+$IgD$^-$Fas$^+$GC B cells (right). (***A***-***D***) Open bars, C57BL/6 (IgH^b);WT(IgH^a); grey bars, ICOSL$^{-/-}$(IgH^b);WT(IgH^a). (*E*) Closed circles, IgG2b$^+$(IgH$^{a+or\ b+}$) GC B cells; open circles, IgG2a^{a+}(IgH^a) GC B cells. (***A, D, E***) A one-way analysis of variance (ANOVA) followed by Newman-Keuls *ad hoc* test for comparison of individual groups was employed to determine statistical significance. (***B***, ***C***) An unpaired Student's *t* test was performed to compare two individual groups. *$p<0.05$, **$p<0.001$, ***$p<0.0001$.*

Figure 3.4 Reconstitution of Ly5.1$^+$BoyJ mice with equal portions of *Icosl*$^{-/-}$(IgH^b) and *Icosl*$^{+/+}$(IgH^a) bone marrow or of *Icosl*$^{+/+}$(IgH^b) and *Icosl*$^{+/+}$(IgH^a) bone marrow. (**A**) Percentage of B220$^+$B cells among peripheral blood mononuclear cells. (**B**) Fraction of peripheral blood B220$^+$ cells that expressed IgM^a. (**C**) Fraction of peripheral blood B220$^+$ cells that expressed IgM^b. (**D**) Ratio of B220$^+$ B cells to CD4$^+$ T cells in peripheral blood. Unpaired student's *t*-test was used to determine statistical significance, ***$p<0.0001$. Data in **Fig. 3.4** show reconstitution efficiencies of mixed bone marrow chimeric mice used in the experiments displayed in **Fig. 3.3** and **3.5**.

Figure 3.5 Decreased magnitude of the T_{FH} cell compartment in mice containing 50% ICOSL-deficient B cells. The numbers of T_{FH} and their expression of ICOS was determined in the ICOSL$^{-/-}$(IgH^b);WT (IgH^a) and C57BL/6 (IgH^b);WT (IgH^a) bone marrow chimeric mice analyzed in Fig. 2.3. (**A**) The numbers of T_{FH} in draining LNs 14 days after immunization with either nonCpG-NP-CGG or CpG-NP-CGG were determined by flow cytometry as in Fig. 2.1A. Open circles, nonCpG-NP-CGG; closed circles, CpG-NP-CGG. (**B**) ICOS expression on T cells 14 days after the indicated immunization; T_{FH} cells (black line) and T_{naive} CD4$^+$ cells (filled histogram). Representative flow cytometry profiles of ICOS expression (left) and ICOS median fluorescent intensity (MFI) (right); open circles, nonCpG-NP-CGG immunization; closed circles, CpG-NP-CGG immunization, naive T cells (open bars) and T_{FH} cells (black bars). Statistical significance was determined using the student's *t*-test. **$p<0.001$, ***$p<0.0001$.

Figure 3.6 Direct requirement for ICOSL on the responding B cell during TLR9-enhanced affinity maturation. Following immunization with an oligovalent antigen linked to a CpG-containing oligo (+TLR9), a robust GC reaction produces high affinity antibody and this is blocked when mice are deficient for ICOSL (ICOSL$^{-/-}$). However, the presence of roughly 50% ICOSL$^{+/+}$B cells can partially restore affinity maturation in ICOSL$^{-/-}$B cells, revealing the expected B cell-extrinsic effect of ICOSL and also an unexpected B cell-intrinsic role for ICOSL in GC B cell selection.

Figure 3.1

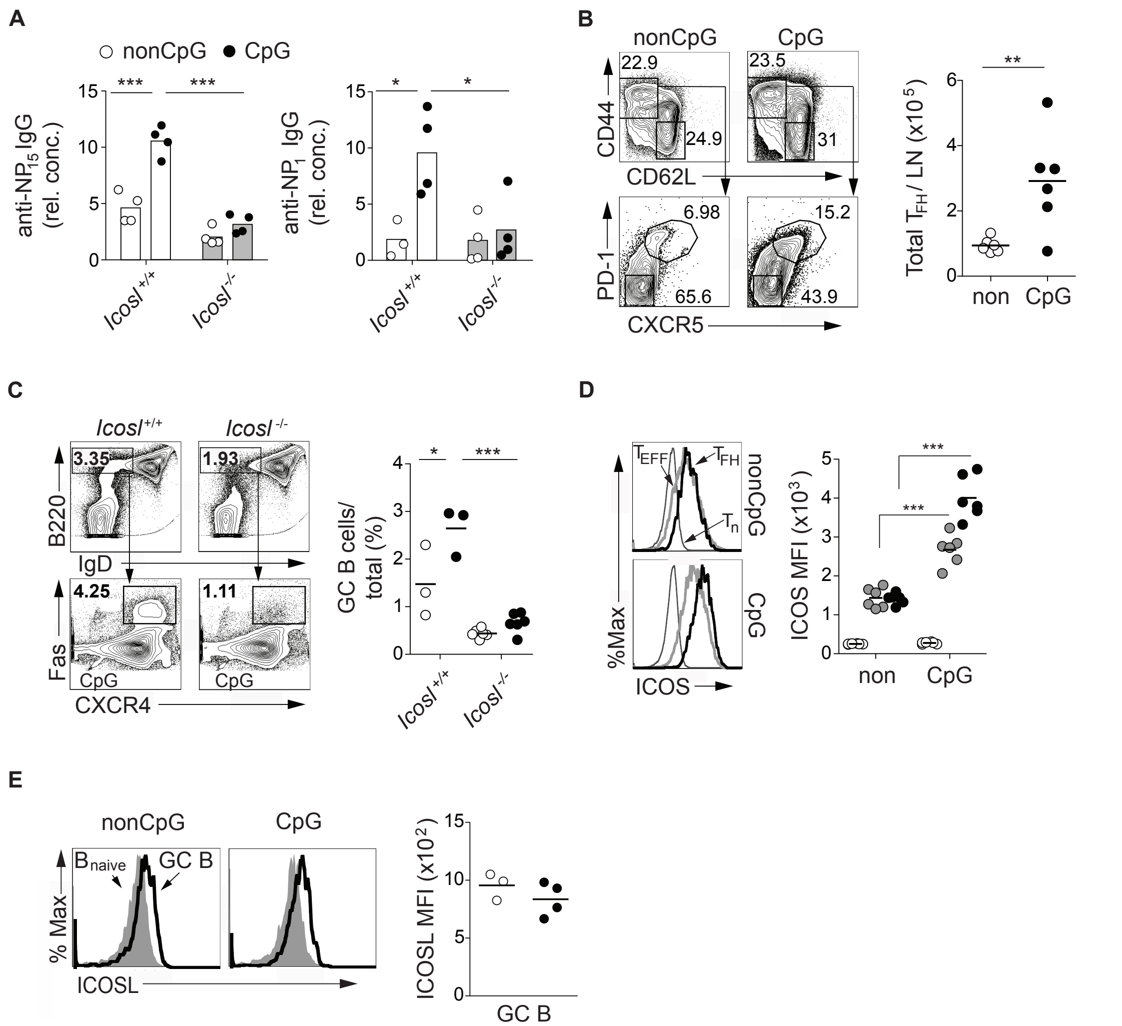
A
○ nonCpG ● CpG
anti-NP15 IgG (rel. conc.)
anti-NP1 IgG (rel. conc.)
Icosl+/+
Icosl-/-
B
nonCpG
CpG
CD44
CD62L
PD-1
CXCR5
22.9
24.9
23.5
31
6.98
65.6
15.2
43.9
Total TFH / LN (x10^5)
non
CpG
C
Icosl+/+
Icosl-/-
B220
IgD
Fas
CXCR4
3.35
1.93
4.25
1.11
GC B cells/ total (%)
D
TEFF
TFH
Tn
nonCpG
CpG
%Max
ICOS
ICOS MFI (x10^3)
non
CpG
E
nonCpG
CpG
Bnaive
GC B
% Max
ICOSL
ICOSL MFI (x10^2)
GC B

Figure 3.2

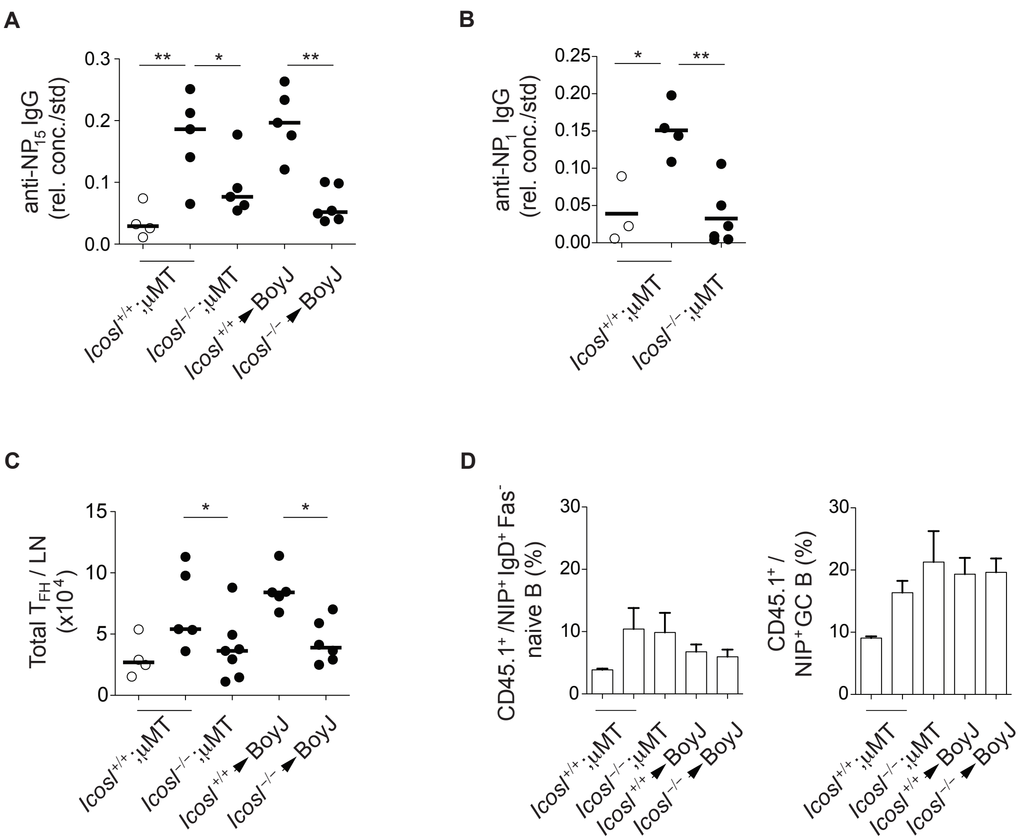
A
anti-NP_{15} IgG (rel. conc./std)
0.0
0.1
0.2
0.3
**
*
**
$Icosl^{+/+}$;µMT
$Icosl^{-/-}$;µMT
$Icosl^{+/+}$→BoyJ
$Icosl^{-/-}$→BoyJ
B
anti-NP_{1} IgG (rel. conc./std)
0.00
0.05
0.10
0.15
0.20
0.25
*
**
$Icosl^{+/+}$;µMT
$Icosl^{-/-}$;µMT
C
Total T_{FH} / LN ($x10^4$)
0
5
10
15
*
*
$Icosl^{+/+}$;µMT
$Icosl^{-/-}$;µMT
$Icosl^{+/+}$→BoyJ
$Icosl^{-/-}$→BoyJ
D
$CD45.1^+$/NIP^+ IgD^+ Fas^- naive B (%)
0
10
20
30
$CD45.1^+$/ NIP^+GC B (%)
0
10
20
30
$Icosl^{+/+}$;µMT
$Icosl^{-/-}$;µMT
$Icosl^{+/+}$→BoyJ
$Icosl^{-/-}$→BoyJ

Figure 3.3

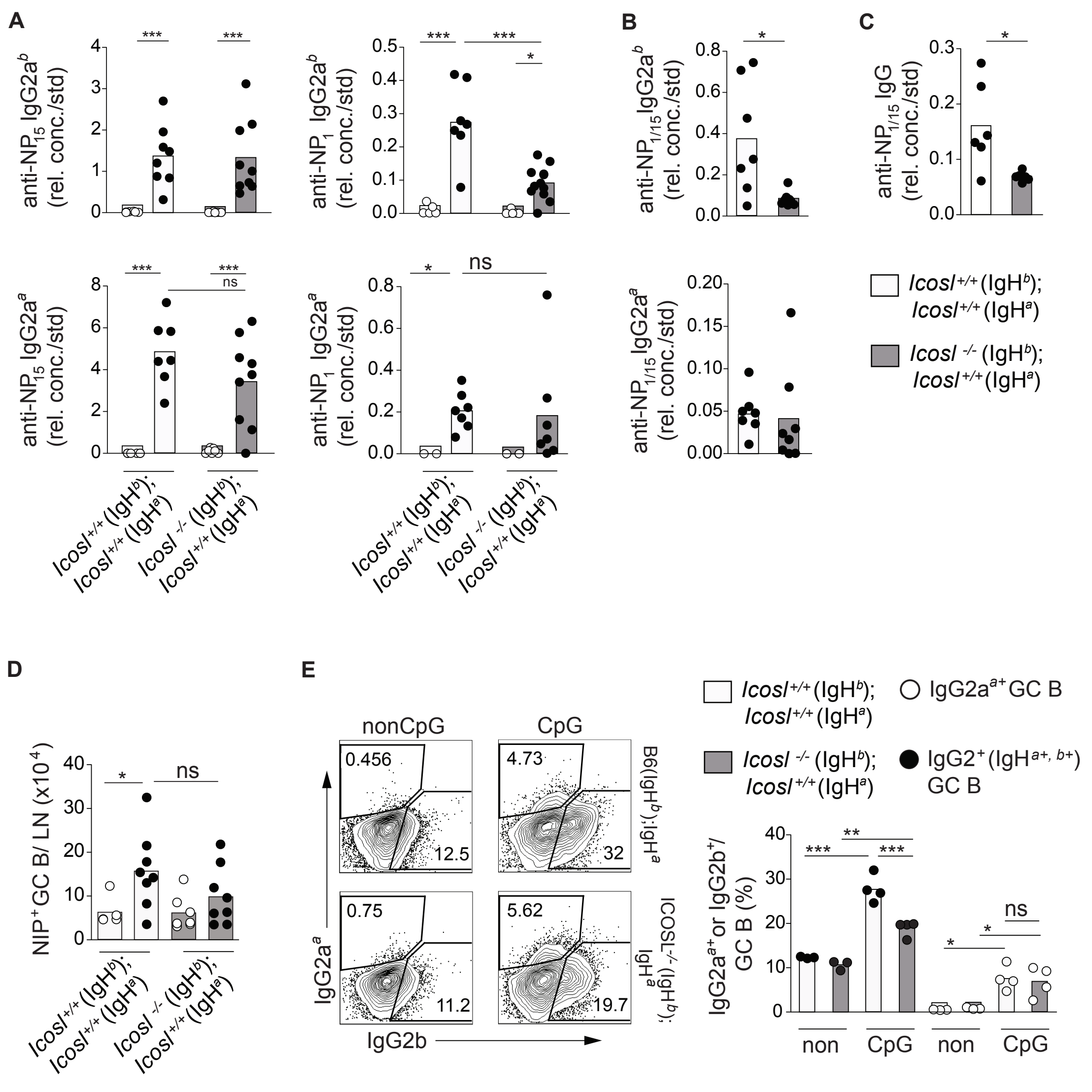
A
B
C
D
E
anti-NP15 IgG2a^b (rel. conc./std)
anti-NP1 IgG2a^b (rel. conc./std)
anti-NP1/15 IgG2a^b (rel. conc./std)
anti-NP1/15 IgG (rel. conc./std)
anti-NP15 IgG2a^a (rel. conc./std)
anti-NP1 IgG2a^a (rel. conc./std)
anti-NP1/15 IgG2a^a (rel. conc./std)
Icosl+/+ (IgH^b); Icosl+/+ (IgH^a)
Icosl -/- (IgH^b); Icosl+/+ (IgH^a)
ns
NIP+GC B/ LN (x10^4)
nonCpG
CpG
B6(IgH^b);IgH^a
ICOSL-/- (IgH^b); IgH^a
IgG2a^a
IgG2b
IgG2a^a+ GC B
IgG2+ (IgH^a+, b+) GC B
IgG2a^a+ or IgG2b+/ GC B (%)
non
CpG

Figure 3.4

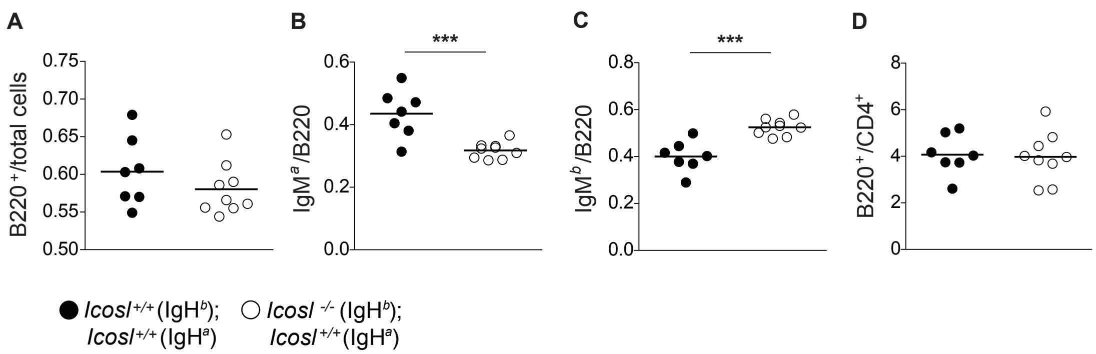
A
B
***
C
***
D
B220+/total cells
IgMa/B220
IgMb/B220
B220+/CD4+
Icosl+/+ (IgHb); Icosl+/+ (IgHa)
Icosl -/- (IgHb); Icosl+/+ (IgHa)

Figure 3.5

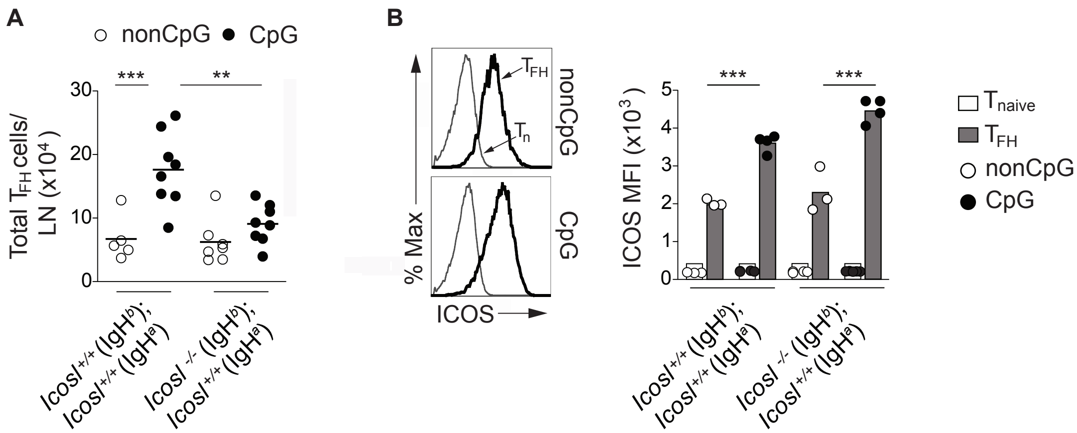
A
nonCpG
CpG
Total TFH cells/ LN (x10^4)
***
**
Icosl+/+ (IgHb); Icosl+/+ (IgHa)
Icosl-/- (IgHb); Icosl+/+ (IgHa)
B
TFH
Tn
nonCpG
CpG
% Max
ICOS
ICOS MFI (x10^3)
Tnaive
TFH

Figure 3.6

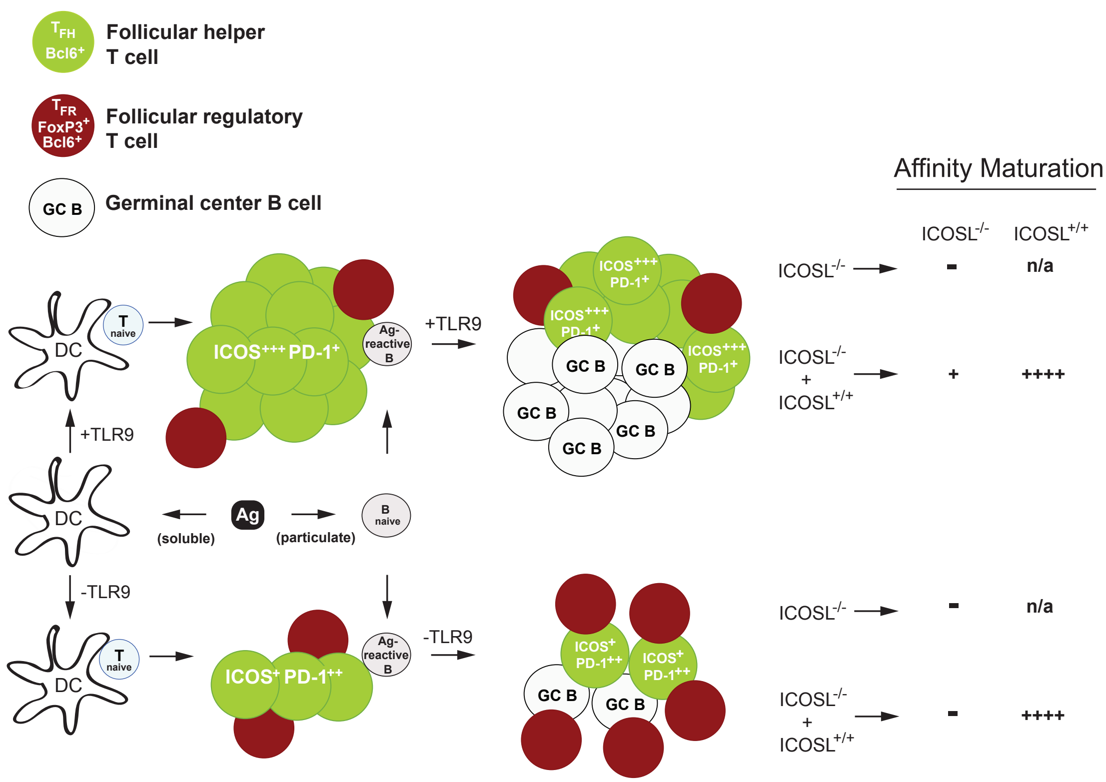

TFH Bcl6+
Follicular helper T cell
TFR FoxP3+ Bcl6+
Follicular regulatory T cell
GC B
Germinal center B cell
Affinity Maturation
ICOSL-/-
ICOSL+/+
DC
T naive
ICOS+++ PD-1+
Ag-reactive B
+TLR9
-TLR9
Ag
(soluble)
(particulate)
B naive
ICOS+ PD-1++
GC B
ICOSL-/- + ICOSL+/+
-
n/a
+
++++

Chapter Four

Thesis Summary

Suggestions and Implications

THESIS SUMMARY

The body of work presented here expands our understanding of the relationship between innate and adaptive signaling by extending the findings of others that demonstrated the ability of TLR signaling to impact the size of a GC reaction and T-dependent antibody responses. It was previously known that TLR signaling in both DCs and B cells augmented T-dependent antibody responses specifically to soluble versus multivalent particulate antigens[82, 85], respectively, and that TLR signaling in B cells could enhance development of antigen-specific GC B cells to particulate antigen[83, 85] as well as to LCMV infection[84], and also improve affinity maturation[83]. The work presented in this thesis extends these observations by elucidating the cell-specific requirements for TLR signaling in DCs and B cells to regulate the magnitude and quality of a GC reaction, respectively. Furthermore, aside from one observation that a TLR ligand supported T_{FH} cell formation[78], the effects of specific TLR signaling on T_{FH} cell quality and number had not been addressed even though it is a key component for understanding the ability of TLRs to choreograph GC reactions. In addition, I addressed the cellular requirements for ICOS/ICOSL signaling, which is crucial to T_{FH} cell development and persistence in TLR-enhanced GC responses. Surprisingly, the ability of TLR9 to enhance the GC response required ICOSL expression specifically on responding B cell to fully enhance affinity maturation, revealing a previously unappreciated B cell-intrinsic role for ICOSL.

The experiments presented here open more avenues of investigation. For instance whether TLR signaling programs B cell memory in a B cell-intrinsic or -extrinsic fashion is not clear. The specific DC and B cell signals that modulate the T_{FH} and T_{FR} cell composition in the follicular $CD4^+$ T cell compartment is also of interest as the ability to limit T_{FH} cell expansion and helper ability is crucial for immune homeostasis as shown by the phenotype of mice lacking a negative regulator of ICOS expression, roquin. A mutation in this RING-type ubiquitin ligase exacerbated autoimmunity in mice characterized by increased T_{FH} and GC B cells, elevated IL-21 levels, and hypergammaglobulinaemia[40, 41].

The signals that promote selection of GC B cells into the memory compartment are not entirely understood, and multiple factors may influence whether B cells are selected to become quiescent memory B cells or Ig-secreting long-lived plasma cells that reside in the bone marrow[149]. Important in this regard, experiments using mice that are specifically deleted for MyD88 in B cells revealed that TLR signaling in B cells promoted memory B cell formation (Chapter 2). However, it remains to be answered whether this is a B cell-intrinsic or -extrinsic event as memory B cells require T cell help for expansion upon secondary antigen exposure[150]. My data indicate that TLR/MyD88 signaling in B cells boosts collaboration between T_{FH} and GC B cells. Thus, it could be that the memory defect observed in mice with *Myd88*-deficient B cells resulted from extrinsic properties of TLR signaling in B cells that helped mature the T_{FH} cell population to acquire a memory phenotype. Memory T_{FH} cells were previously reported to develop in response to immunization with a protein antigen[151]. These putative memory T_{FH} cells exhibited a quiescent state characterized by reduced ICOS protein and cytokine mRNA expression and were retained it the draining LN, potentially to strategically position them near memory B cells which reside near retracted GCs in draining LNs[150, 151].

Although much progress has been made to understand T_{FH} cell function, the signals delivered by APCs during T cell priming that promote T_{FH} cell development remain less well characterized. I have demonstrated that TLR signaling in DCs triggered robust T_{FH} cell development (Chapter 2). This may be expected given that cytokines downstream of TLR stimulation in DCs such as IL-6 and IL-12 are able to drive T_{FH} formation[152-154]. Alternatively, it was previously demonstrated that TCR receptor avidity for peptide-MHC complexes promoted T_{FH} cell development[115], and it is plausible that TLR signaling in DCs partially controlled TCR signal strength my modulating MHC-peptide topography[155]. Furthermore, while T_{FH} cells exhibit a unique transcriptional program governed by the transcriptional repressor Bcl6[71, 72], they frequently adopt characteristics shared by other T cell subsets such Th17 (IL-17 production) and Th2 (IL-4 production) cells, making their etiology unclear. For instance, it is possible that T_{FH} cells develop from previously differentiated helper T cells or that the specific priming events during activation of naive T cells prime them to adopt a T_{FH} cell fate[32]. In our system, TLR signaling in DCs selectively promoted T_{FH} cell expansion while in B cells it had no effect on T_{FH} cell numbers, suggesting that events more proximal to T cell activation determined T_{FH} cell development, consistent with an origin independent of other T cell subsets.

The ability of different adjuvants as well as microbes to imprint T_{FH} cell character is gaining appreciation for what it reveals about T_{FH} development as well as for how it could potentially inform vaccine design[48]. Interestingly, TLR signaling in both B cells and DCs shaped T_{FH} cell quality at the levels of costimulatory receptor expression and the composition of T_{FH} and FoxP3$^+$$T_{FR}$ cells in the follicular CD4$^+$T cell pool. Regarding modulation of costimulatory receptors, it was interesting that the TLR-boost in ICOS expression was attenuated by deletion of MyD88 in both DCs and B cells but that the presence of ICOSL on DCs or B cells apparently did not affect ICOS levels. Furthermore, expression of the RING-type ubiquitin ligase roquin that restricts ICOS expression in T cells[40] was not affected by TLR signaling in our system (data not shown). In a more speculative light, it is plausible that upregulation of the transcription factor T-bet which regulates the Th1/IFNγ^+ T cell phenotype may positively regulate ICOS in our system[156]. Conversely, T-bet negatively regulates PD-1 levels in some circumstances[157]. The decreased ICOS levels on T_{FH} cells from mice with *Myd88*-deficient B cells suggests there may be a reduced interaction between GC B and T_{FH} cells as SAP signaling downstream of SLAM interactions between B and T cells boosts ICOS expression[158].

The percentage of follicular CD4$^+$T cells that were FoxP3$^+$ T_{FR} cells increased in mice with *Myd88*-deficient DCs even though their total numbers did not change relative to WT. T_{FR} cells have the capacity to limit T_{FH} cell expansion[92-94], and it may be that TLR9 signaling in DCs leads to T_{FH} cell expansion in part through inhibition of T_{FR} cells.

Multiple studies have unveiled the ability of TLR2, TLR4 and TLR9 to restrict T_{REG} suppressive capacity and to boost expansion of T_{EFF} cells relative to T_{REG} cells by triggering DCs to produce IL-6, a potent inducer of T_{FH} cell development[78, 152, 159-161]. Furthermore, it was recently demonstrated that ICOS costimulation was selectively required when unlinked TLR ligands were administered with protein antigen to trigger vigorous T_{EFF} cell expansion that potently skewed the T_{EFF}/T_{REG} balance[161]. Thus, the ability of T_{FH} cells to expand robustly in the presence of restrictive T_{FR} cells following CpG-NP-CGG immunization may be linked to either an IL-6-mediated reduction in suppressive capacity of T_{FR} cells or to enhanced ICOS expression by T_{FH} cells.

In contrast to mice with *Myd88*-deficient DCs, mice with *Myd88*-deficient B cells had an increase in the total number of T_{FR} cells. Furthermore, when ICOSL was specifically deleted on B cells, the number of T_{FR} cells decreased (data not shown). Together, these data suggest that TLR9 signaling in B cells regulated T_{FR} cell numbers through a mechanism involving cell contact and ICOS costimulation. Since cell contact is required for B cells to maintain follicular T cells, it is possible that B cells interacted more efficiently with T_{FR} and provided to them proliferation and/or survival signals when TLR9 signaling was compromised. Cell contact-dependent repression of both T_{FH} and B cells by T_{FR} cells has been demonstrated in vitro[95, 96]. Whether TLR signaling in DCs and B cells affected T_{FR} cell quality and/or suppressive capacity will require further investigation in our system.

The level of selection stringency determines the quality of antibody and humoral memory generated by GC reactions. When stringency is highest, GC B cell clones expressing BCRs with the strongest affinity will capture antigen and present it to T cells more efficiently than lower affinity clones. Through this process, the memory compartment becomes enriched for cells expressing high affinity BCRs[49]. During the GC reaction, multiple factors modulate selection stringency including the availability and quality of help from T_{FH} cells, manifested, for example, by the provision of cytokines and costimulatory signals[48]. In our system, TLR signaling appeared to reduce GC selection stringency by increasing production of IL-21 and expression of ICOS as well as reducing the relative number of T_{FR} cells in the follicular $CD4^{+}$T cell pool. Surprisingly then, TLR signaling still increased affinity maturation as well as the number of antigen-specific GC B cells despite what appeared to be less stringent selection. These observations are somewhat surprising given that more stringent selection is thought to enrich the pool of antigen-specific GC B cells and lead to better antibody affinity[49, 60, 93]. Recent reports suggest that the availability of help from T_{FH} cells drives competition and affinity maturation[59, 60]. Given that T_{FH} numbers are boosted by TLR9 signaling, the enhancement of affinity maturation suggests that there is a qualitative difference in the ability of the T_{FH} cells to help GC B cells. Although the frequency of T_{FR} cells relative to the number of T_{FH} cells decreased following immunization with an antigen linked to TLR9 ligand, their suppressive qualities could be enhanced, increasing selection stringency. It is also tempting to speculate that an alternative cell type with suppressive function such as the so-called regulatory B cell (B_{reg}) imparts selection stringency. Regulatory B cells express high amounts of IL-10 and suppress autoimmunity and excessive inflammation[162]. Intriguingly, B cell-deficient μMT mice and mice with B cells that lack MyD88 develop more severe EAE[162]. Moreover, TLR9 stimulation in B cells increases IL-10 production[163], and a recent report demonstrated a requirement for IL-21 in B_{reg} development, suggesting that T_{FH} cells in GCs or Th17 cells might create an environment conducive to B_{reg} formation[164]. Accordingly, further investigation into the mechanism of TLR-established selection stringency is warranted.

The work here represents a small piece of understanding in the increasingly complex array of innate signaling pathways. Since the discovery of TLRs, a variety of other receptors belonging to the RLR, NLR, CLR and ALR families of PRRs[3] have also been discovered that can interact with each other and with TLRs, revealing a highly regulated, labyrinthine system of innate sensing for containing infection and refining adaptive responses. This is good news for vaccine development. Since its discovery as an effective adjuvant for antibody responses in 1926[165], alum has been preferentially used in vaccines worldwide[166]. However, its usefulness is limited in that it does not stimulate broad T cell responses which are required in the case of intracellular pathogens such as *Mycobacterium tuberculosis*, for example, and can complement antibody responses to viruses that are present in both intra- and extracellular spaces. Thus, a more precise understanding of how individual PRR signaling pathways affect adaptive responses will facilitate the rational design of vaccine adjuvants to tailor a desired outcome. For this reason, the possibility of an HIV vaccine is finally foreseeable[167]. The HIV envelope (Env) spike is a heterodimer of glycoproteins gp120 and gp41 that facilitates binding of CD4 and either CCR5 or CXCR4 on target cells, and examination of broadly neutralizing antibodies generated in a fraction of HIV-infected individuals has revealed multiple epitopes in this region[167], identifying the targets for a successful vaccine. Indeed, passive immunization with broadly neutralizing antibodies (bnAbs) protected against HIV infection and reduced viral loads to below detectable levels in nonhuman primates and in humanized mice[168-170]. Detailed studies of innate signaling networks will undoubtedly help generate the blueprint for the specification of bnAbs with key attributes for protection against HIV infection in humans. The innate instructions for development of T_{FH} cells will need to be included in this blueprint for their integral role in the production of highly neutralizing antibodies as indicated by the observation that T_{FH} cell frequency correlates with serum anti-HIV IgG quantity and quality in nonhuman primates[171]. Thus, studies in fruit flies and Charles Janeway's receptor recognition hypothesis, which roughly coincide with the discovery of HIV over 3 decades ago, triggered a conflagration of investigation that is still accelerating and, as it turns out, providing a lot of hope.

REFERENCES

1. Sousa, F.O.a.C.R.e. Myeloid C-type Lectin Receptors in Pathogen Recognition and Host Defense. *Immunity* **34**, 651-664 (2011).
2. Blasius AL, B.B. Intracellular toll-like receptors. *Immunity* **32**, 305-315 (2010).
3. Kawai, T. & Akira, S. Toll-like receptors and their crosstalk with other innate receptors in infection and immunity. *Immunity* **27**, 637-650 (2011).
4. Loo YM, G.M. Immune signaling by RIG-I-like receptors. *Immunity* **34**, 680-692 (2011).
5. Kylsten P, S.C., Hultmark D. The cecropin locus in Drosophila; a compact gene cluster involved in the response to infection. *EMBO* **9**, 217-224 (1990).
6. Samakovlis C, K.D., Kylsten P, Engström A, Hultmark D. The immune response in Drosophila: pattern of cecropin expression and biological activity. *EMBO* **9**, 2969-2976 (1990).
7. Wicker C, R.J., Hoffmann D, Hultmark D, Samakovlis C, Hoffmann JA. Insect immunity. Characterization of a Drosophila cDNA encoding a novel member of the diptericin family of immune peptides. *Journal of Biological Chemistry* **265**, 22493-22498 (1990).
8. Hashimoto C, H.K., Anderson KV. The Toll gene of Drosophila, required for dorsal-ventral embryonic polarity, appears to encode a transmembrane protein. *Cell* **52**, 269-279 (1988).
9. Lemaitre B, N.E., Michaut L, Reichhart JM, Hoffmann JA. The dorsoventral regulatory gene cassette spätzle/Toll/cactus controls the potent antifungal response in Drosophila adults. *Cell* **86**, 973-983 (1996).
10. Gay NJ, K.F. Drosophila Toll and IL-1 receptor. *Nature* **351**, 355-356 (1991).
11. Schneider DS, H.K., Lin TY, Anderson KV. Dominant and recessive mutations define functional domains of Toll, a transmembrane protein required for dorsal-ventral polarity in the Drosophila embryo. *Genes Dev* **5**, 797-807 (1991).
12. Heguy A, B.C., Macchia G, Telford JL, Melli M. Amino acids conserved in interleukin-1 receptors (IL-1Rs) and the Drosophila toll protein are essential for IL-1R signal transduction. *Journal of Biological Chemistry* **267**, 2605-2609 (1992).
13. Janeway, C. Approaching the Asymptote? Evolution and Revolution in Immunology. *Cold Spring Harb Symp Quant Biol* **54**, 1-13 (1989).
14. Rich, T. *Toll and Toll-Like Receptors: An Immunologic Perspective*. (Kluwer Academic/Plenum Publishers, 2005).
15. Medzhitov R, P.-H.P., Janeway CA Jr. A human homologue of the Drosophila Toll protein signals activation of adaptive immunity. *Nature* **388**, 394-397 (1997).
16. Botos I, S.D., Davies DR. The structural biology of Toll-like receptors. *Structure* **19**, 447-459 (2011).
17. Kawai T, A.S. The role of pattern-recognition receptors in innate immunity: update on Toll-like receptors. *Nature immunology* **11**, 373-384 (2010).

18. Barbalat R, L.L., Locksley RM, Barton GM. Toll-like receptor 2 on inflammatory monocytes induces type I interferon in response to viral but not bacterial ligands. *Nature immunology* **10**, 1200-1207 (2009).
19. Wilson RH, M.S., Whitehead GS, Foley JF, Flake GP, Sever ML, Zeldin DC, Kraft M, Garantziotis S, Nakano H, Cook DN. The Toll-like receptor 5 ligand flagellin promotes asthma by priming allergic responses to indoor allergens. *Nature medicine* **18**, 1705-1710 (2012).
20. Barton, G.M. & Kagan, J.C. A cell biological view of Toll-like receptor function: regulation through compartmentalization. *Nature reviews. Immunology* **9**, 535-542 (2009).
21. Barton GM, K.J., Medzhitov R. Intracellular localization of Toll-like receptor 9 prevents recognition of self DNA but facilitates access to viral DNA. *Nature immunology* **7**, 49-56 (2006).
22. Coban C, I.Y., Yagi M, Reimer T, Koyama S, Aoshi T, Ohata K, Tsukui T, Takeshita F, Sakurai K, Ikegami T, Nakagawa A, Horii T, Nuñez G, Ishii KJ, Akira S. Immunogenicity of whole-parasite vaccines against Plasmodium falciparum involves malarial hemozoin and host TLR9. *Cell host & microbe* **7**, 50-61 (2010).
23. Mathur R, O.H., Zhang D, Park SG, Seo J, Koblansky A, Hayden MS, Ghosh S. A mouse model of salmonella typhi infection. *Cell* **151**, 590-602 (2012).
24. Watters TM, K.E., O'Neill LA. Structure, function and regulation of the Toll/IL-1 receptor adaptor proteins. *Immunology and cell biology* **85**, 411-419 (2007).
25. Lin SC, L.Y., Wu H. Helical assembly in the MyD88-IRAK4-IRAK2 complex in TLR/IL-1R signalling. *Nature* **465**, 885-890 (2010).
26. Netea MG, W.C., O'Neill LA. Genetic variation in Toll-like receptors and disease susceptibility. *Nature immunology* **13**, 535-542 (2012).
27. Takeuchi O, H.K., Akira S. Cutting edge: TLR2-deficient and MyD88-deficient mice are highly susceptible to Staphylococcus aureus infection. *Journal of immunology* **165**, 5392-5396 (2000).
28. Casanova JL, A.L., Quintana-Murci L. Human TLRs and IL-1Rs in host defense: natural insights from evolutionary, epidemiological, and clinical genetics. *Annual Review of Immunology* **29**, 447-491 (2011).
29. Meresse B, M.G., Cerf-Bensussan N Celiac disease: an immunological jigsaw. *Immunity* **36**, 907-919 (2012).
30. Bretscher P, C.M. A theory of self-nonself discrimination. *Science* **169**, 1042-1049 (1970).
31. PA., B. A two-step, two-signal model for the primary activation of precursor helper T cells. *Proceedings of the National Academy of Sciences of the United States of America* **96**, 185-190 (1999).
32. Crotty, S. Follicular helper CD4 T cells (TFH). *Annu Rev Immunol* **29**, 621-663 (2011).
33. Markus Schnare1, * Gregory M. Barton1,2,*,Agnieszka Czopik Holt1, Kiyoshi Takeda3, Shizuo & Akira3 and Ruslan Medzhitov1 Toll-like receptors control activation of adaptive immune responses. *Nature immunology* **2**, 947-950 (2001).

34. Kasper Hoebe1, E.M.J., Sung O Kim1, Lena Alexopoulou3, Richard A Flavell3, Jiahuai Han1 & Bruce Beutler1 Upregulation of costimulatory molecules induced by lipopolysaccharide and double-stranded RNA occurs by Trif-dependent and Trif-independent pathways. *Nature immunology* **4**, 1223-1229 (2003).

35. Takeda‡, S.A.a.K. TOLL-LIKE RECEPTOR SIGNALLING. *Nature Reviews Immunology* **4**, 499-511 (2004).

36. Beutler, B. Innate immunity: an overview. *Molecular Immunology* **40**, 845-859 (2004).

37. Rebecca J. Greenwald, G.J.F. & Sharpe, a.A.H. THE B7 FAMILY REVISITED. *Annual Review of Immunology* **23**, 515-548 (2005).

38. Hutloff A, D.A., Beier KC, Eljaschewitsch B, Kraft R, Anagnostopoulos I, Kroczek RA. ICOS is an inducible T-cell co-stimulator structurally and functionally related to CD28. *Nature* **397** (1999).

39. Yoshinaga SK, W.J., Khare SD, Sarmiento U, Guo J, Horan T, Shih G, Zhang M, Coccia MA, Kohno T, Tafuri-Bladt A, Brankow D, Campbell P, Chang D, Chiu L, Dai T, Duncan G, Elliott GS, Hui A, McCabe SM, Scully S, Shahinian A, Shaklee CL, Van G, Mak TW, Senaldi G. T-cell co-stimulation through B7RP-1 and ICOS. *Nature* **402**, 827-832 (1999).

40. Vinuesa CG, C.M., Angelucci C, Athanasopoulos V, Rui L, Hill KM, Yu D, Domaschenz H, Whittle B, Lambe T, Roberts IS, Copley RR, Bell JI, Cornall RJ, Goodnow CC. A RING-type ubiquitin ligase family member required to repress follicular helper T cells and autoimmunity. *Nature* **435**, 452-458 (2005).

41. Yu D, T.A., Hu X, Athanasopoulos V, Simpson N, Silva DG, Hutloff A, Giles KM, Leedman PJ, Lam KP, Goodnow CC, Vinuesa CG. Roquin represses autoimmunity by limiting inducible T-cell co-stimulator messenger RNA. *Nature* **450**, 299-303 (2007).

42. Liang L, P.E., Sha WC Constitutive expression of the B7h ligand for inducible costimulator on naive B cells is extinguished after activation by distinct B cell receptor and interleukin 4 receptor-mediated pathways and can be rescued by CD40 signaling. *Journal of Experimental Medicine* **196**, 97-108 (2002).

43. Gigoux M, S.J., Pak Y, Xu M, Choe J, Mak TW, Suh WK. Inducible costimulator promotes helper T-cell differentiation through phosphoinositide 3-kinase. *PNAS* **106**, 20371-20376 (2009).

44. Sharpe, A. Mechanisms of Costimulation. *Immunological reviews* **229**, 5-11 (2009).

45. Croft, M., So, T., Duan, W. & Soroosh, P. The significance of OX40 and OX40L to T-cell biology and immune disease. *Immunological reviews* **229**, 173-191 (2009).

46. Cerutti A, P.I., Cols M. Innate control of B cell responses. *Trends Immunol* **32**, 202-211 (2011).

47. MacLennan, I.C.M. *et al*. Extrafollicular antibody responses. *Immunol. Rev*. **194**, 8-18 (2003).
48. Linterman MA, L.A., Vinuesa CG T-follicular helper cell differentiation and the co-option of this pathway by non-helper cells. *Immunological reviews* **247**, 143-159 (2012).
49. Victora, G.D., Nussenzweig M. C. Germinal centers. *Annual Review of Immunology* **30**, 429-457 (2012).
50. Opstelten, P.N.a.D. Functional Anatomy of Germinal Centers. *The American Journal of Anatomy* **170**, 421-435 (1984).
51. Elsner RA, E.D., Baumgarth N. Single and coexpression of CXCR4 and CXCR5 identifies CD4 T helper cells in distinct lymph node niches during influenza virus infection. *J Virol* **86**, 146-157 (2012).
52. Allen CD, A.K., Low C, Lesley R, Tamamura H, Fujii N, Cyster JG. Germinal center dark and light zone organization is mediated by CXCR4 and CXCR5. *Nature immunology* **5**, 943-952 (2004).
53. Schaerli P, W.K., Lang AB, Lipp M, Loetscher P, Moser B. CXC chemokine receptor 5 expression defines follicular homing T cells with B cell helper function. *The Journal of experimental medicine* **192**, 1553-1562 (2000).
54. Breitfeld D, O.L., Kremmer E, Ellwart J, Sallusto F, Lipp M, Förster R. Follicular B helper T cells express CXC chemokine receptor 5, localize to B cell follicles, and support immunoglobulin production. *The Journal of experimental medicine* **192**, 1545-1552 (2000).
55. Kim CH, R.L., Clark-Lewis I, Campbell DJ, Wu L, Butcher EC. Subspecialization of CXCR5+ T cells: B helper activity is focused in a germinal center-localized subset of CXCR5+ T cells. *The Journal of experimental medicine* **193**, 1373-1381 (2001).
56. Burton GF, K.M., Szakal AK, Tew JG. Iccosomes and the secondary antibody response. *Immunology* **73**, 271-276 (1991).
57. Chan TD, B.R. Affinity-based selection and the germinal center response. *Immunological reviews* **247**, 11-23 (2012).
58. Fleire SJ, G.J., Carrasco YR, Weber M, Bray D, Batista FD. B cell ligand discrimination through a spreading and contraction response. *Science* **312** (2006).
59. Christopher D. C. Allen, T.O., *† H. Lucy Tang,‡ Jason G. Cyster† Imaging of Germinal Center Selection Events During Affinity Maturation. *Science* **315,**, 528-531 (2007).

60. Victora GD, S.T., Fooksman DR, Kamphorst AO, Meyer-Hermann M, Dustin ML, Nussenzweig MC. Germinal center dynamics revealed by multiphoton microscopy with a photoactivatable fluorescent reporter. *Cell* **143**, 592-605 (2010).
61. Phan TG, P.D., Chan TD, Turner ML, Nutt SL, Basten A, Brink R. High affinity germinal center B cells are actively selected into the plasma cell compartment. *J Exp Med* **203**, 2419-2424 (2006).

62. Kouyama E, N.Y., Okazawa T, Magari M, Ohmori H, Kanayama N. Analysis of antigen-stimulated B cell migration into germinal centers during the early stage of a T-dependent immune response. *Immunol Lett* **109**, 28-35 (2007).
63. Shih TA, M.E., Roederer M, Nussenzweig MC. Role of BCR affinity in T cell dependent antibody responses in vivo. *Nature immunology* **3**, 570-575 (2002).
64. Schwickert TA, V.G., Fooksman DR, Kamphorst AO, Mugnier MR, Gitlin AD, Dustin ML, Nussenzweig MC. A dynamic T cell-limited checkpoint regulates affinity-dependent B cell entry into the germinal center. *The Journal of experimental medicine* **208**, 1243-1252 (2011).
65. Tarlinton, D.M. Evolution in miniature: selection, survival and distribution of antigen reactive cells in the germinal center. *Immunol. Cell Biol.* **86**, 133-138 (2008).
66. Taylor JJ, P.K., Jenkins MK. A germinal center-independent pathway generates unswitched memory B cells early in the primary response. *The Journal of experimental medicine* **209**, 597-606 (2012).
67. Kaji T, I.A., Hikida M, Taka J, Hijikata A, Kubo M, Nagashima T, Takahashi Y, Kurosaki T, Okada M, Ohara O, Rajewsky K, Takemori T. Distinct cellular pathways select germline-encoded and somatically mutated antibodies into immunological memory. *The Journal of experimental medicine* **209**, 2079-2097 (2012).
68. Dogan, I. *et al*. Multiple layers of B cell memory with different effector functions. *Nat. Immunol.* **10**, 1292-1299 (2009).
69. Linterman MA, B.L., Yu D, Ramiscal RR, Srivastava M, Hogan JJ, Verma NK, Smyth MJ, Rigby RJ, Vinuesa CG. IL-21 acts directly on B cells to regulate Bcl-6 expression and germinal center responses. *Journal of Experimental Medicine* **207**, 353-363 (2010).
70. Zotos D, C.J., Zhang Y, Light A, D'Costa K, Kallies A, Corcoran LM, Godfrey DI, Toellner KM, Smyth MJ, Nutt SL, Tarlinton DM. IL-21 regulates germinal center B cell differentiation and proliferation through a B cell-intrinsic mechanism. *Journal of Experimental Medicine* **207**, 365-378 (2010).
71. Johnston RJ, P.A., DiToro D, Yusuf I, Eto D, Barnett B, Dent AL, Craft J, Crotty S. Bcl6 and Blimp-1 are reciprocal and antagonistic regulators of T follicular helper cell differentiation. *Science* **325**, 1006-1010 (2009).
72. Nurieva RI, C.Y., Martinez GJ, Yang XO, Tanaka S, Matskevitch TD, Wang YH, Dong C. Bcl6 mediates the development of T follicular helper cells. *Science* **325**, 1001-1005 (2009).
73. Bauquet AT, J.H., Paterson AM, Mitsdoerffer M, Ho IC, Sharpe AH, Kuchroo VK. The costimulatory molecule ICOS regulates the expression of c-Maf and IL-21 in the development of follicular T helper cells and TH-17 cells. *Nature immunology* **10**, 167-175 (2009).
74. Lüthje K, K.A., Shimohakamada Y, TBelz GT, Light A, Tarlinton DM, Nutt SL. The development and fate of follicular helper T cells defined by an IL-21 reporter mouse. *Nature immunology* **13**, 491-498 (2012).

75. King IL, M.M. IL-4-producing CD4+ T cells in reactive lymph nodes during helminth infection are T follicular helper cells. *Journal of Experimental Medicine* **206**, 1001-1007 (2009).
76. Yusuf I, K.R., Monticelli L, Johnston RJ, Ditoro D, Hansen K, Barnett B, Crotty S. Germinal center T follicular helper cell IL-4 production is dependent on signaling lymphocytic activation molecule receptor (CD150). *J Immunol* **185**, 190-202 (2010).
77. Reinhardt RL, L.H., Locksley RM. Cytokine-secreting follicular T cells shape the antibody repertoire. *Nature immunology* **10**, 385-393 (2009).
78. Cucak H, Y.U., Reizis B, Kalinke U, Johansson-Lindbom B. Type I interferon signaling in dendritic cells stimulates the development of lymph-node-resident T follicular helper cells. *Immunity* **31**, 491-501 (2009).
79. Gavin, A.L. *et al*. Adjuvant-enhanced antibody responses in the absence of toll-like receptor signaling. *Science* **314**, 1936-1938 (2006).
80. Pasare, C. & Medzhitov, R. Control of B-cell responses by Toll-like receptors. *Nature* **438**, 364-368 (2005).
81. Palm, N.W. & Medzhitov, R. Immunostimulatory activity of haptenated proteins. *Proceedings of the National Academy of Sciences of the United States of America* **106**, 4782-4787 (2009).
82. Hou, B. *et al*. Selective utilization of Toll-like receptor and MyD88 signaling in B cells for enhancement of the antiviral germinal center response. *Immunity* **34**, 375-384 (2011).
83. Kasturi, S.P. *et al*. Programming the magnitude and persistence of antibody responses with innate immunity. *Nature* **470**, 543-547 (2011).
84. Walsh KB, T.J., Zuniga EI, Welch MJ, Fremgen DM, Blackburn SD, von Tiehl KF, Wherry EJ, Flavell RA, Oldstone MB. Toll-like receptor 7 is required for effective adaptive immune responses that prevent persistent virus infection. *Cell Host Microbe*. **146**, 980-991 (2012).
85. Hou, B., Reizis, B. & DeFranco, A.L. Toll-like receptors activate innate and adaptive immunity by using dendritic cell-intrinsic and -extrinsic mechanisms. *Immunity* **29**, 272-282 (2008).
86. Pasare, C. & Medzhitov, R. Toll-dependent control mechanisms of CD4 T cell activation. *Immunity* **21**, 733-741 (2004).
87. Sporri, R. & Reis e Sousa, C. Inflammatory mediators are insufficient for full dendritic cell activation and promote expansion of CD4+ T cell populations lacking helper function. *Nature immunology* **6**, 163-170 (2005).
88. Rawlings DJ, S.M., Jackson SW, Meyer-Bahlburg A. Integration of B cell responses through Toll-like receptors and antigen receptors. *Nature Reviews Immunology* **12**, 282-294 (2012).
89. Ecki-Dorna, J. & Batista, F.D. BCR-mediated uptake of antigen linked to TLR9 ligand stimulates B-cell proliferation and antigen-specific plasma cell formation. *Blood* **113**, 3969-3977 (2009).
90. Browne, E.P. Toll-like receptor 7 controls the anti-retroviral germinal center response. *PLoS pathogens* **7**, e1002293 (2011).

91. Alexander CM, T.L., Boyden AW, Wolniak KL, Legge KL, Waldschmidt TJ. T regulatory cells participate in the control of germinal centre reactions. *Immunology* **133**, 452-468 (2011).

92. Wollenberg I, A.-D.A., Hernández A, Almeida C, Oliveira VG, Faro J, Graca L. Regulation of the germinal center reaction by Foxp3+ follicular regulatory T cells. *Journal of Immunology* **187**, 4553-4560 (2011).

93. Linterman, M.A. *et al*. Foxp3+ follicular regulatory T cells control the germinal center response. *Nature medicine* **17**, 975-982 (2011).

94. Chung Y, T.S., Chu F, Nurieva RI, Martinez GJ, Rawal S, Wang YH, Lim H, Reynolds JM, Zhou XH, Fan HM, Liu ZM, Neelapu SS, Dong C. Follicular regulatory T cells expressing Foxp3 and Bcl-6 suppress germinal center reactions. *Nature medicine* **17**, 983-988 (2011).

95. Lim HW, H.P., Banham AH, Kim CH. Cutting edge: direct suppression of B cells by CD4+ CD25+ regulatory T cells. *Journal of Immunology* **175**, 4180-4183 (2005).

96. Lim HW, H.P., Kim CH. Regulatory T cells can migrate to follicles upon T cell activation and suppress GC-Th cells and GC-Th cell-driven B cell responses. *Journal of Clinical Investigation* **115**, 1640-1649 (2004).

97. Tafuri A, S.A., Bladt F, Yoshinaga SK, Jordana M, Wakeham A, Boucher LM, Bouchard D, Chan VS, Duncan G, Odermatt B, Ho A, Itie A, Horan T, Whoriskey JS, Pawson T, Penninger JM, Ohashi PS, Mak TW. ICOS is essential for effective T-helper-cell responses. *Nature* **409**, 105-109 (2001).

98. McAdam AJ, G.R., Levin MA, Chernova T, Malenkovich N, Ling V, Freeman GJ, Sharpe AH. ICOS is critical for CD40-mediated antibody class switching. *Nature* **409**, 102-105 (2001).

99. Dong C, T.U., Flavell RA. Cutting edge: critical role of inducible costimulator in germinal center reactions. *Journal of Immunology* **166**, 3659-3662 (2001).

100. Bennett, F. *et al*. Program death-1 engagement upon TCR activation has distinct effects on costimulation and cytokine-driven proliferation: attenuation of ICOS, IL-4, and IL-21, but not CD28, IL-7, and IL-15 responses. *J Immunol* **170**, 711-718 (2003).

101. Good-Jacobson, K.L. & Shlomchik, M.J. Plasticity and heterogeneity in the generation of memory B cells and long-lived plasma cells: the influence of germinal center interactions and dynamics. *J. Immunol*. **185**, 3117-3125 (2010).

102. Kawamoto, S. *et al*. The inhibitory receptor PD-1 regulates IgA selection and bacterial composition in the gut. *Science* **336**, 485-489 (2012).

103. Peng SL, S.S., Glimcher LH. T-bet regulates IgG class switching and pathogenic autoantibody production. *PNAS* **99**, 5545-5550 (2002).

104. Linterman MA, R.R., Wong RK, Yu D, Brink R, Cannons JL, Schwartzberg PL, Cook MC, Walters GD, Vinuesa CG. Follicular helper T cells are required for systemic autoimmunity. *Journal of Experimental Medicine* **206**, 561-576 (2009).

105. Harker JA, L.G., Mack L, Zuniga EI. Late interleukin-6 escalates T follicular helper cell responses and controls a chronic viral infection. *Science* **334**, 825-829 (2011).
106. Link A, Z.F., Schnetzler Y, Titz A, Brombacher F, Bachmann MF. Innate immunity mediates follicular transport of particulate but not soluble protein antigen. *Journal of Immunology* **188**, 3724-3733 (2012).
107. Goenka R, B.L., Silver JS, O'Neill PJ, Hunter CA, Cancro MP, Laufer TM. Cutting edge: dendritic cell-restricted antigen presentation initiates the follicular helper T cell program but cannot complete ultimate effector differentiation. *Journal of Immunology* **187**, 1091-1095 (2011).

108. Choi, Y.S., Kageyama R., Eto D., Escobar T.C., Johnston R.J., Monticelli L., Loa C., Crotty S. ICOS receptor instructs T follicular helper cell versus effector cell differentiation via induction of the transcriptional repressor Bcl6. *Immunity* **34**, 932-946 (2011).
109. Kitano M, M.S., Ando Y, Hikida M, Mori Y, Kurosaki T, Okada T. Bcl6 protein expression shapes pre-germinal center B cell dynamics and follicular helper T cell heterogeneity. *Immunity* **34**, 961-972 (2011).

110. Kerfoot SM, Y.G., Patel JR, Johnson KL, Gonzalez DG, Kleinstein SH, Haberman AM. Germinal center B cell and T follicular helper cell development initiates in the interfollicular zone. *Immunity* **34**, 947-960 (2011).
111. Deenick EK, C.A., Ma CS, Gatto D, Schwartzberg PL, Brink R, Tangye SG. Follicular helper T cell differentiation requires continuous antigen presentation that is independent of unique B cell signaling. *Immunity* **33**, 241-253 (2010).

112. Akiba H, T.K., Kojima Y, Usui Y, Harada N, Yamazaki T, Ma J, Tezuka K, Yagita H, Okumura K. The role of ICOS in the CXCR5+ follicular B helper T cell maintenance in vivo. *Journal of Immunology* **175**, 2340-2348 (2005).
113. Fahey LM, W.E., Elsaesser H, Fistonich CD, McGavern DB, Brooks DG. Viral persistence redirects CD4 T cell differentiation toward T follicular helper cells. *Journal of Experimental Medicine* **208**, 987-999 (2011).
114. Zaretsky AG, T.J., King IL, Marshall FA, Mohrs M, Pearce EJ. T follicular helper cells differentiate from Th2 cells in response to helminth antigens. *Journal of Experimental Medicine* **206**, 991-999 (2009).
115. Fazilleau N, M.-W.L., Rosen H, McHeyzer-Williams MG. The function of follicular helper T cells is regulated by the strength of T cell antigen receptor binding. *Nature immunology* **10**, 375-384 (2009).
116. Chung, Y. *et al*. Follicular regulatory T cells expressing Foxp3 and Bcl-6 suppress germinal center reactions. *Nature medicine* **17**, 983-988 (2011).
117. Wollenberg, I. *et al*. Regulation of the germinal center reaction by Foxp3+ follicular regulatory T cells. *J Immunol* **187**, 4553-4560 (2011).
118. Alexander, C.M. *et al*. T regulatory cells participate in the control of germinal centre reactions. *Immunology* **133**, 452-468 (2011).

119. Lim, H.W., Hillsamer, P. & Kim, C.H. Regulatory T cells can migrate to follicles upon T cell activation and suppress GC-Th cells and GC-Th cell-driven B cell responses. *The Journal of clinical investigation* **114**, 1640-1649 (2004).
120. Lim, H.W., Hillsamer, P., Banham, A.H. & Kim, C.H. Cutting edge: direct suppression of B cells by CD4+ CD25+ regulatory T cells. *J Immunol* **175**, 4180-4183 (2005).
121. Allen CD, O.T., Cyster JG. Germinal-center organization and cellular dynamics. *Immunity* **27**, 190-202 (2007).
122. Cannons JL, Q.H., Lu KT, Dutta M, Gomez-Rodriguez J, Cheng J, Wakeland EK, Germain RN, Schwartzberg PL. Optimal germinal center responses require a multistage T cell:B cell adhesion process involving integrins, SLAM-associated protein, and CD84. *Immunity* **32**, 253-265 (2010).
123. Qi H, C.J., Klauschen F, Schwartzberg PL, Germain RN. SAP-controlled T-B cell interactions underlie germinal centre formation. *Nature* **455** (2008).
124. Jegerlehner A, M.P., Bessa J, Hinton HJ, Kopf M, Bachmann MF. TLR9 signaling in B cells determines class switch recombination to IgG2a. *Journal of Immunology* **178**, 2415-2420 (2007).
125. Finkelman FD, H.J., Katona IM, Urban JF Jr, Beckmann MP, Park LS, Schooley KA, Coffman RL, Mosmann TR, Paul WE. Lymphokine control of in vivo immunoglobulin isotype selection. *Annual Review of Immunology* **8**, 303-333 (1990).
126. Hobeika, E. *et al*. Testing gene function early in the B cell lineage in mb1-cre mice. *Proceedings of the National Academy of Sciences of the United States of America* **103**, 13789-13794 (2006).
127. Caton ML, S.-R.M., Reizis B Notch-RBP-J signaling controls the homeostasis of CD8- dendritic cells in the spleen. *The Journal of experimental medicine* **204**, 1653-1664 (2007).
128. Lalor PA, N.G., Sanderson RD, McHeyzer-Williams MG Functional and molecular characterization of single, (4-hydroxy-3-nitrophenyl)acetyl (NP)-specific, IgG1+ B cells from antibody-secreting and memory B cell pathways in the C57BL/6 immune response to NP. *European journal of immunology* **22**, 3001-3011 (1992).
129. Bossaller L, B.J., Draeger R, Grimbacher B, Knoth R, Plebani A, Durandy A, Baumann U, Schlesier M, Welcher AA, Peter HH, Warnatz K. ICOS deficiency is associated with a severe reduction of CXCR5+CD4 germinal center Th cells. *Journal of Immunology* **177**, 4927-4932 (2006).
130. Larimore K, L.L., Bakkour S, Sha WC B7h-expressing dendritic cells and plasma B cells mediate distinct outcomes of ICOS costimulation in T cell-dependent antibody responses. *BMC Immunol*. **13**, 29 doi:10.1186/1471-2172-1113-1129 (2012).
131. Nurieva RI, C.Y., Hwang D, Yang XO, Kang HS, Ma L, Wang YH, Watowich SS, Jetten AM, Tian Q, Dong C. Generation of T follicular helper cells is mediated by interleukin-21 but independent of T helper 1, 2, or 17 cell lineages. *Immunity* **29**, 138-149 (2008).

132. Hu H, W.X., Jin W, Chang M, Cheng X, Sun SC. Noncanonical NF-kappaB regulates inducible costimulator (ICOS) ligand expression and T follicular helper cell development. *Proceedings of the National Academy of Sciences of the United States of America* **108**, 12827-12832 (2011).
133. Ou X, X.S., Lam KP Deficiency in TNFRSF13B (TACI) expands T-follicular helper and germinal center B cells via increased ICOS-ligand expression but impairs plasma cell survival. *PNAS* www.pnas.org/cgi/doi/10.1073/pnas.1200386109 (2012).
134. Logue EC, B.S., Murphy MM, Nolla H, Sha WC. ICOS-Induced B7h Shedding on B Cells Is Inhibited by TLR7/8 and TLR9. *Journal of Immunology* **177**, 2356-2364 (2006).
135. EP., B. Toll-like receptor 7 controls the anti-retroviral germinal center response. *PLoS pathogens* **7**, e1002293 (2011).
136. Haynes NM, A.C., Lesley R, Ansel KM, Killeen N, Cyster JG. Role of CXCR5 and CCR7 in follicular Th cell positioning and appearance of a programmed cell death gene-1high germinal center-associated subpopulation. *Journal of Immunology* **179**, 5099-5108 (2007).
137. Baumjohann D, O.T., Ansel KM. Cutting Edge: Distinct waves of BCL6 expression during T follicular helper cell development. *Journal of Immunology* **186**, 2792-2799 (2011).
138. Vogelzang A, M.H., Yu D, Sprent J, Mackay CR, King C. A fundamental role for interleukin-21 in the generation of T follicular helper cells. *Immunity* **29** (2008).
139. Zhou Z, H.K., Du X, Jiang Z, Shamel L, Beutler B. Antagonism between MyD88- and TRIF-dependent signals in B7RP-1 up-regulation. *European journal of immunology* **35**, 1918-1927 (2005).
140. Ogata M, I.T., Shimamoto K, Nakanishi T, Satsutani N, Miyamoto R, Nomura S. Plasmacytoid dendritic cells have a cytokine-producing capacity to enhance ICOS ligand-mediated IL-10 production during T-cell priming. *International immunology* (2012).
141. Inamine, A. *et al*. Two waves of memory B-cell generation in the primary immune response. *Int. Immunol.* **17**, 581-589 (2005).
142. Ou X, X.S., Lam KP. Deficiency in TNFRSF13B (TACI) expands T-follicular helper and germinal center B cells via increased ICOS-ligand expression but impairs plasma cell survival. *Proceedings of the National Academy of Sciences of the United States of America* **109**, 15401-15406 (2012).
143. Grimbacher B, H.A., Schlesier M, Glocker E, Warnatz K, Dräger R, Eibel H, Fischer B, Schäffer Homozygous loss of ICOS is associated with adult-onset common variable immunodeficiency. *Nature immunology* **4**, 261-268 (2003).
144. Watanabe M, T.Y., Kotani M, Hara Y, Inamine A, Hayashi K, Ogawa S, Takeda K, Tanabe K, Abe R. Down-Regulation of ICOS Ligand by Interaction with ICOS Functions as a Regulatory Mechanism for Immune Responses. *Journal of Immunology* **180**, 5222-5234 (2008).
145. Ishii, C.J.D.K.J. Nucleic acid sensing at the interface between innate and adaptive immunity in vaccination. *Nature reviews. Immunology* **12**, 479-491 (2012).

146. Park JH, R.E., Cunningham-Rundles C. Perspectives on common variable immune deficiency. *annals New York academny of sciences* **1246**, 41-49 (2011).
147. Warnatz K, S.U., Rizzi M, Fischer B, Gutenberger S, Böhm J, Kienzler AK, Pan-Hammarström Q, Hammarström L, Rakhmanov M, Schlesier M, Grimbacher B, Peter HH, Eibel H. B-cell activating factor receptor deficiency is associated with an adult-onset antibody deficiency syndrome in humans. *Proceedings of the National Academy of Sciences of the United States of America* **106**, 13945-13950 (2009).
148. Losi CG, S.A., Fiorini C, Soresina A, Meini A, Ferrari S, Notarangelo LD, Lougaris V, Plebani A. Mutational analysis of human BAFF receptor TNFRSF13C (BAFF-R) in patients with common variable immunodeficiency. *Journal of clinical immunology* **25**, 496-502 (2005).
149. McHeyzer-Williams M, O.S., Wang N, McHeyzer-Williams L. Molecular programming of B cell memory. *Nature Reviews Immunology* **12**, 24-34 (2012).
150. Aiba Y, K.K., Hamadate M, Moriyama S, Sakaue-Sawano A, Tomura M, Luche H, Fehling HJ, Casellas R, Kanagawa O, Miyawaki A, Kurosaki T. Preferential localization of IgG memory B cells adjacent to contracted germinal centers. *Proceedings of the National Academy of Sciences of the United States of America* **107**, 12192-12197 (2010).
151. Fazilleau N, E.M., Malherbe L, Ebright JN, Pogue-Caley RR, McHeyzer-Williams LJ, McHeyzer-Williams MG. Lymphoid reservoirs of antigen-specific memory T helper cells. *Nature immunology* **8**, 753-761 (2007).
152. Eto, D. *et al*. IL-21 and IL-6 are critical for different aspects of B cell immunity and redundantly induce optimal follicular helper CD4 T cell (Tfh) differentiation. *PloS one* **6**, e17739 (2011).
153. Ma CS, S.S., Avery DT, Chan A, Nanan R, Santner-Nanan B, Deenick EK, Tangye SG. Early commitment of naïve human CD4(+) T cells to the T follicular helper (T(FH)) cell lineage is induced by IL-12. *Immunology and cell biology* **87**, 590-600 (2009).
154. Schmitt N, M.R., Bourdery L, Bentebibel SE, Zurawski SM, Banchereau J, Ueno H. Human dendritic cells induce the differentiation of interleukin-21-producing T follicular helper-like cells through interleukin-12. *Immunity* **31**, 158-169 (2009).
155. Jarrett J. Adams1 *et al*. T Cell Receptor Signaling Is Limited by Docking Geometry to Peptide-Major Histocompatibility Complex. *Immunity* **35**, 681-693 (2011).
156. Simpson TR, Q.S., Allison JP. Regulation of CD4 T cell activation and effector function by inducible costimulator (ICOS). *Current Opinion in Immunology* **22**, 326-332 (2010).
157. Kao C, O.K., Paley MA, Crawford A, Angelosanto JM, Ali MA, Intlekofer AM, Boss JM, Reiner SL, Weinmann AS, Wherry EJ. Transcription factor T-bet represses expression of the inhibitory receptor PD-1 and sustains virus-specific CD8+ T cell responses during chronic infection. *Nature immunology* **12**, 663-671 (2011).

158. Cannons JL, Y.L., Jankovic D, Crotty S, Horai R, Kirby M, Anderson S, Cheever AW, Sher A, Schwartzberg PL. SAP regulates T cell-mediated help for humoral immunity by a mechanism distinct from cytokine regulation. *The Journal of experimental medicine* **203**, 1551-1565 (2006).
159. Pasare C, M.R. Toll pathway-dependent blockade of CD4+CD25+ T cell-mediated suppression by dendritic cells. *Science* **299**, 1033-1036 (2003).
160. Hall JA, B.N., Sun CM, Wohlfert EA, Blank RB, Zhu Q, Grigg ME, Berzofsky JA, Belkaid Y. Commensal DNA limits regulatory T cell conversion and is a natural adjuvant of intestinal immune responses. *Immunity* **29**, 637-649 (2008).
161. Lischke T, H.A., Gurka S, Vu Van D, Burmeister Y, Lam KP, Kershaw O, Mollenkopf HJ, Mages HW, Hutloff A, Kroczek RA. Comprehensive analysis of CD4+ T cells in the decision between tolerance and immunity in vivo reveals a pivotal role for ICOS. *Journal of Immunology* **189**, 234-244 (2012).
162. Bosma, C.M.a.A. Immune Regulatory Function of B Cells. *Annual Review of Immunology* **30**, 221-241 (2012).
163. Barr TA, B.S., Ryan G, Zhao J, Gray D. 2007. TLR-mediated stimulation of APC: distinct cytokine responses of B cells and dendritic cells. *European journal of immunology* **37**, 3040-3053 (2007).
164. Yoshizaki A, M.T., DiLillo DJ, Matsushita T, Horikawa M, Kountikov EI, Spolski R, Poe JC, Leonard WJ, Tedder TF. Regulatory B cells control T-cell autoimmunity through IL-21-dependent cognate interactions. *Nature* **491**, 264-268 (2012).
165. Glenny, A.T., Poop, C. G., Waddington, H. and Wallace, U. Immunological Notes: XVII-XXIV. *J. Pathol. Bacteriol.* **29**, 31-40 (1926).
166. Marrack P, M.A., Munks MW. Towards an understanding of the adjuvant action of aluminium. *Nature reviews. Immunology* **9**, 287-293 (2009).
167. Burton DR, A.R., Barouch DH, Butera ST, Crotty S, Godzik A, Kaufmann DE, McElrath MJ, Nussenzweig MC, Pulendran B, Scanlan CN, Schief WR, Silvestri G, Streeck H, Walker BD, Walker LM, Ward AB, Wilson IA, Wyatt R. A Blueprint for HIV Vaccine Discovery. *Cell host & microbe* **18**, 396-407 (2012).
168. Klein F, H.-S.A., Horwitz JA, Gruell H, Scheid JF, Bournazos S, Mouquet H, Spatz LA, Diskin R, Abadir A, Zang T, Dorner M, Billerbeck E, Labitt RN, Gaebler C, Marcovecchio PM, Incesu RB, Eisenreich TR, Bieniasz PD, Seaman MS, Bjorkman PJ, Ravetch JV, Ploss A, Nussenzweig MC. HIV therapy by a combination of broadly neutralizing antibodies in humanized mice. *Nature* (2012).
169. Hessell AJ, P.P., Hunter M, Hangartner L, Tehrani DM, Bleeker WK, Parren PW, Marx PA, Burton DR. Effective, low-titer antibody protection against low-dose repeated mucosal SHIV challenge in macaques. *Nat Med* **15**, 951-954 (2009).

170. Mascola JR, L.M., Stiegler G, Harris D, VanCott TC, Hayes D, Louder MK, Brown CR, Sapan CV, Frankel SS, Lu Y, Robb ML, Katinger H, Birx DL. Protection of Macaques against pathogenic simian/human immunodeficiency virus 89.6PD by passive transfer of neutralizing antibodies. *J Virol* **73**, 4009-4018 (1999).

171. Petrovas C, Y.T., Gerner MY, Boswell KL, Wloka K, Smith EC, Ambrozak DR, Sandler NG, Timmer KJ, Sun X, Pan L, Poholek A, Rao SS, Brenchley JM, Alam SM, Tomaras GD, Roederer M, Douek DC, Seder RA, Germain RN, Haddad EK, Koup RA. CD4 T follicular helper cell dynamics during SIV infection. *The Journal of clinical investigation* **122**, 3281-3294 (2012).